Nuclear Energy University Programs (NEUP)

Final Report on

Systematic Enterprise Risk Management by Integrating the RISMC Toolkit and Cost-Benefit Analysis

Project ID: 17-12614

Prepared by:

Zahra Mohaghegh (Principal Investigator), Tatsuya Sakurahara, John Beal, Wen-Chi Cheng, Pegah Farshadmanesh, Seyed Reihani, Ernie Kee

Socio-Technical Risk Analysis (SoTeRiA) Research Laboratory
Department of Nuclear, Plasma, and Radiological Engineering
Grainger College of Engineering, University of Illinois at Urbana-Champaign

Arden Rowell

College of Law, University of Illinois at Urbana-Champaign

Fatma Yilmaz

South Texas Project Nuclear Operating Company

Prepared for

U.S. Department of Energy
Office of Nuclear Energy





Urbana, Illinois
August 2021

Page intentionally left blank

EXECUTIVE SUMMARY

The goal of this research is to theorize and quantify the relationships between safety and the financial performance of nuclear power plants (NPPs). The Socio-Technical Risk Analysis (SoTeRiA) theoretical framework, which connects the social aspects (e.g., safety culture) and structural features (e.g., safety practices) of an organization with organizational safety and financial risks, is used to theorize the direct and indirect relationships between safety and the financial performance of NPPs. An Integrated Enterprise Risk Management (I-ERM) methodological framework is developed to operationalize SoTeRiA to quantify NPP safety and financial performance in a unified platform where their underlying physical degradation mechanisms, coupled with maintenance performance (considering human and organizational factors), are explicitly incorporated to depict the interconnections and dependencies between safety and financial performance. In this study, NPP safety refers to both occupational safety and system safety (estimated from Probabilistic Risk Assessment, PRA), and financial performance refers to the monetary values associated with NPP operation and maintenance (O&M) strategies. This report covers a case study demonstrating the feasibility of the I-ERM methodological framework. More detailed development of one of the I-ERM modules, i.e., Probabilistic Physics-of-Failure (PPoF) analysis, and its connection with other I-ERM modules is demonstrated in a second case study. The outcome of this research will help NPP decision-makers create cost-saving maintenance strategies while maintaining safety by providing cost- and risk-informed recommendations regarding maintenance work processes and operational strategies.

This report begins with a thorough review and analysis of literature on the interconnections of safety and financial performance. The review highlights that the use of correlation analysis to study the relationships between safety and financial performance may impede accurate evaluation of the interrelationships between these two organizational outcomes; therefore, explicit consideration of the underlying causations is recommended. Previous studies related to the explicit modeling of underlying causations between safety and financial performance are then reviewed and analyzed, focusing on two types of causal paths: (i) direct causal paths, representing costs incurred by accidents and incidents; and (ii) indirect causal paths, where safety and financial performance interact via organizational and regulatory factors. For the indirect paths, this research primarily focuses on the maintenance unit process, which is the sharp end of causation in all indirect causal paths associated with nuclear power plant O&M activities. The insights from the literature review are utilized for two purposes: (a) to justify the contributions of this research, and (b) to identify the causal factors and their paths of influence to support theoretical advancements for modeling the causations between safety and financial performance.

Compared to the previous studies, this research makes the following contributions:

1. Theorizes the financial consequences of system accidents, system incidents, and occupational accidents of NPPs and, for the first time, develops a unified causal model including all three types of financial consequences.

2. Adds realism when modeling (i) the impact of maintenance performance on financial performance, (ii) the impact of maintenance performance on safety, and (iii) the interconnections of safety and financial performance. To achieve these, the research develops an Integrated Enterprise Risk Management (I-ERM) methodological framework that can quantify the causations underlying the impact of maintenance performance on both safety and financial performance of NPPs in a unified, multi-level platform. For the component-level analysis of I-ERM, where maintenance strategies (e.g., preventive maintenance and corrective maintenance) are explicitly incorporated, a multi-state renewal process model is used to compute reliability and availability. Previous studies relied on data-driven approaches and/or expert judgment for quantification of the maintenance parameters as inputs to the renewal process model. The data-driven approaches, however, are challenging if (a) limited or no operational data are available for the system being analyzed; or (b) significant modifications such as redesign and maintenance policy updates have been implemented, causing the empirical data to lack relevance under the current system conditions. The proposed approach in this research addresses this gap by explicitly incorporating the models of maintenance performance and physics-of-failure into the renewal process model. For the explicit modeling of maintenance performance, this research develops a theory-based maintenance organization causal model. The maintenance causal model is quantified using a Human Reliability Analysis (HRA)-based method. This contribution helps avoid reliance on data-driven approaches for the analysis of safety and financial performance. The explicit modeling of maintenance performance can also add resolution to the modeling of the impact of maintenance performance on safety and financial performance; hence, it helps improve the efficiency of maintenance strategies by providing decision-makers with in-depth quantitative insights at the level of maintenance work processes and human performance. Additionally, the coupled effects of physics-of-failure and maintenance performance are explicitly incorporated into the modeling of the interconnections of safety and financial performance. A physics-of-failure model with higher spatial and temporal resolutions (using Finite Element Analysis; FEA) is developed and coupled with the maintenance performance model through the renewal process model. This research incorporates FEA into the PPoF model and advances the interface between the PPoF

analysis and the renewal process model to deal with spatiotemporal FEA outputs and to efficiently estimate the physical transition rates even when the PPoF outputs are dominated by success data. This contribution helps avoid reliance on data-driven approaches and allows for the inclusion of interrelated impacts of underlying physical degradation and maintenance causal factors on the assessment of the relationships and dependencies between the safety and financial performance of NPPs. In I-ERM, the outputs of reliability and availability at the component level are then used as inputs to the system-level safety models. Meanwhile, the financial performance is computed using a cost function, where the direct maintenance cost and the production loss cost are quantified based on the outputs from the renewal process model and where the coupling of maintenance performance and physics-of-failure are explicitly incorporated. The integration of these multiple levels of I-ERM is demonstrated using an NPP case study.

Page intentionally left blank

CONTENTS

EXECUTIVE SUMMARY iii
ACRONYMS xii
1. Introduction 1
2. Categorical Review and Theoretical Bases 6
2.1 Review and Analysis of Literature on Interconnections of Organizational Safety & Financial Performance 6
2.1.1 Existing Studies Examining Correlations Between Safety and Financial Performance (Category I) 8
2.1.2 Previous Studies Related to Explicit Modeling of Underlying Causations between Safety and Financial Performance (Category II) 12
2.2 Theoretical Developments on Interconnections of Safety and the Financial Performance of NPPs 22
2.2.1 Theoretical Causal Model to Formalize the Direct Causal Path from Safety to the Financial Performance of NPPs 23
2.2.2 Theoretical Causal Model for the Performance of the NPP Maintenance Program 29
2.3 Summary 33
3. Methodological Developments and Case Study 35
3.1 Methodological Developments to Quantify Relationships of Safety and the Financial Performance of Nuclear Power Plants 35
3.1.1 Integrated Enterprise Risk Management (I-ERM) Methodological Framework 35
3.1.2 Developments and Integration of the I-ERM Modules 37
3.2 Illustrative Case Study Implementation of the I-ERM Framework 51
3.2.1 Case Study Description 51
3.2.2 Case Study Implementation 53
3.2.3 Case Study Results for Two Maintenance Alternatives 71
3.3 Summary 72
4. Spatiotemporal Probabilistic Physics-of-Failure Analysis and Its Connection to Safety and Financial Performance 74
4.1 Incorporation of Finite Element Analysis into the Probabilistic Physics-of-Failure Analysis module of the I-ERM Framework 75
4.1.1 Development of a Finite Element Analysis (FEA)-based Physics-of-Failure (PoF) model 77
4.1.2 Uncertainty Quantification for the FEA-based PoF Model and Estimation of Physical Transition Rates 80
4.2 Case Study Application 83
4.2.1 Developing a Renewal Process Model for the ERAA Module of the I-ERM Framework 84

4.2.2 Development of the FEA-based PPoF Analysis Module of the I-ERM Framework 87
4.2.3 Estimating Maintenance Transition Rates as Inputs to the ERAA Module of I-ERM Framework 96
4.2.4 Case Study Results 97
4.2.5 Sensitivity Analysis 98
4.3 Summary 100
5. Conclusions 103
5.1 Publication List 106
5.1.1 Technical Reports 106
5.1.2 Journal Articles 107
5.1.3 Conference Papers 107
5.1.4 Relevant Publications 108

FIGURES

Figure 1-1: Socio-Technical Risk Analysis (SoTeRiA) Framework. 1
Figure 1-2. Integrated Enterprise Risk Management (I-ERM) Framework. 3
Figure 2-1: Theoretical Causal Model to Formalize the Direct Causal Path from Safety to the Financial Performance of NPPs (Detailed Model of the Direct Arrow from Node 1 to Node 11 in SoTeRiA). 24
Figure 2-2: Proposed Causal Model for the Quality of the Maintenance Program in NPPs. 30
Figure 3-1. Integrated Enterprise Risk Management (I-ERM) Methodological Framework. 36
Figure 3-2: An Example of the GRA-ERAA Interface Event Tree. 48
Figure 3-3: Illustration of Hypothetical Production System. 51
Figure 3-4: Illustration of Hypothetical Protection System. 53
Figure 3-5: PRA event tree for the protection system, where OK: success and CD: core damage. 54
Figure 3-6: Protection system fault trees for (a) valve train in Block 5, (b) pump train in Block 6, (c) pump train in Block 7, and (d) valve train in Block 8. 55
Figure 3-7: GRA fault tree for the production system. 56
Figure 3-8: Fault trees for GRA systems: (a) Valve Train in Block 1, (b) Pump Train in Block 2, (c) Pump Train in Block 3, and (d) Valve Train in Block 4. 56
Figure 3-9: Multi-Phase Markov Process Model for Each Pump in the Production System. 57
Figure 3-10: Maintenance Event Tree for Production System Pump during Operation as a Result of Condition-based Maintenance. 61
Figure 3-11: Maintenance Event Tree for Normal In-Service Inspections. 62

Figure 3-12: Maintenance Event Tree for Overhaul In-Service Inspections. 63
Figure 3-13: Maintenance Event Tree for Pump in Failure State. 64
Figure 3-14: Maintenance ET during Operation with Component in Success State. 65
Figure 3-15: GRA-ERAA Interface Event Tree for Type A GRA cutsets. 69
Figure 3-16: GRA-ERAA Interface Event Tree for Type B GRA cut sets. Two initiating events are included: (UA, A): A pump is not available, while a non-pump component is available; (A, UA): A pump is available, while a non-pump component is unavailable..... 70
Figure 3-17: Safety and Financial Performance Metrics for two Maintenance Strategy Alternatives: CM + ISI (Subplots A and C), CM + CBPM (Subplots B and D). 72
Figure 4-1. Finite element analysis (FEA)-based Physics-of-Failure (PoF) model for a pipe component subjected to thermal fatigue. 78
Figure 4-2. Uncertainty Quantification (UQ) Procedure in the PPoF Analysis Module of I-ERM. 81
Figure 4-3. CVC system elbow pipe subjected to thermal stratification. 83
Figure 4-4. A Multi-Phase Markov Process (MPMP) model structure..... 86
Figure 4-5: (a) Hoop stress and (b) Temperature distribution along the inner surface of the elbow at the halfway point in the second period (t_f = 100 sec). 93
Figure 4-6: Time profile of hoop stress at Node 1 to Node 8 in Figure 4-5 (a). 94
Figure 4-7: Comparison of maximum hoop stress vs. yield strength for each node in Figure 4-5. 94
Figure 4-8. Annual and Cumulative Probabilities for Leak and Rupture States. 98
Figure 4-9. Annual Leak and Rupture Probabilities at 60 Years for Sensitivity Cases. 100

TABLES

Table 2-1. Classification of literature on the relationships between safety and financial performance. 7
Table 3-1: Failure rate (λ) and repair rate (μ) of GRA equipment in the production system. Ci: components, FM: functional failure modes, FC: fails to close, and FTR: fails to run..... 52
Table 3-2: Failure probability in 24-hour mission time of components in the protection system. FM: functional failure mode, FC: fails to close, FTS: fails to start, and FTR: fails to run. 53
Table 3-3: Transition Rates used for Quantification of the continuous-time Markov Model. 59
Table 3-4: Input parameters used to quantify the maintenance event trees. 64
Table 3-5: Annual Maintenance Cost Equations for Maintenance Scenarios. 66

Table 3-6: Unit Cost Parameters used for Quantification of Maintenance Cost Scenarios. 67
Table 3-7: Quantification of Maintenance Transition Rates in the Multi-phase Markov Process Model. 68
Table 4-1. Parameters of the Thermal Fluid Dynamics Submodel. 89
Table 4-2. Inputs to Finite Element Analysis of Thermomechanical Response Submodel 90
Table 4-3. PPoF-based Estimation of the Physical Transition Rates. 96
Table 4-4. Inspection Strategies and the Corresponding Transition Probabilities. 97
Table 4-5. Sensitivity Cases and Input Parameters 99

Page intentionally left blank

ACRONYMS

CBPM	Condition-based Preventive Maintenance
CDF	Core Damage Frequency
CM	Corrective Maintenance
COD	Crack Opening Displacement
CVCS	Chemical and Volume Control System
DRSEA	Driver Safety Evaluation Area
ERAA	Equipment Reliability and Availability Analysis
ET	Event Tree
FEA	Finite Element Analysis
FL0	Flaw State to Leak0 State
FL1	Flaw State to Leak1 State
FL2	Flaw State to Leak2 State
FLEX	Diverse and Flexible Coping Strategies
FR	Flaw state to Rupture state
FT	Fault Tree
GRA	Generation Risk Assessment
HHE	Human Health Effects
HRA	Human Reliability Analysis
IE	Initiating Event
I-ERM	Integrated Enterprise Risk Management
ISI	In-Service Inspection
JACDEC	Jet Airliner Crash Data Evaluation Center
L0R	Leak0 State to Rupture State
L1R	Leak1 State to Rupture State
L2R	Leak2 State to Rupture State
LERF	Large Early Release Frequency
LMS	Leakage Monitoring System
LWR	Light Water Reactor
MACCS	MELCOR Accident Consequence Code System
MOA	Maintenance Organizational Analysis
MPMP	Multi-phase Markov process
NEI	Nuclear Energy Institute
NEUP	Nuclear Energy University Program
NF	New State to Flaw State
NPP	Nuclear Power Plant
NRC	Nuclear Regulatory Commission
O&M	Operation and Maintenance
OHSRA	Occupational Health and Safety Risk Assessment
OPEX	Operating Experience
OSRA	Organizational Safety Risk Assessment
PM	Preventive Maintenance

POD	Probability of detection
PoF	Physics-of-Failure
PPM	Pre-Defined Preventive Maintenance
PPoF	Probabilistic Physics-of-Failure
PRA	Probabilistic Risk Assessment
PSF	Performance Shaping Factor
PTWC	Partial Through-wall Crack
PV	Probabilistic Validation
PWR	Pressurized Water Reactor
RCS	Reactor coolant system
RDEIM	Regional Disruption Economic Impact Model
ROA	Return on Asset
RTH	Ratio of Wall Thickness to the Hydraulic Diameter
SA	Sensitivity Analysis
SADT	Structured Analysis and Design Technique
SIF	Stress Intensity Factor
SMS	Safety Management System
SoTeRiA	Socio-Technical Risk Analysis
TEPCO	Tokyo Electric Power Company Holdings, Inc.
TWC	Through-wall crack
UF	Usage Factor
UQ	Uncertainty Quantification
UT	Ultrasonic Testing
VHSEA	Vehicle Safety Evaluation Area
VI	Visual Inspection

Page intentionally left blank

1. Introduction

To remain economically competitive in the electric power market, nuclear power plants (NPPs) need to deploy innovative, cost-saving strategies while ensuring continued safe operation, as emphasized in the Nuclear Energy Institute (NEI) "Delivering the Nuclear Promise" initiative [1]. A line of research was initiated by the PI's team to analyze the relationships between safety and the financial performance of NPPs [2-6]. This project is an extension of this line of research, aimed at generating a causation-based approach for modeling interconnections of safety and the financial performance in NPPs.

The Socio-Technical Risk Analysis (SoTeRiA) theoretical framework (Figure 1-1; [7, 8]), which connects the social aspects (e.g., safety culture; Node 8 in Figure 1-1) and structural features (e.g., safety practices; Node 7 in Figure 1-1) of an organization with system risk (Node 1 in Figure 1-1) and financial outcome (Node 11 in Figure 1-1), is used in this research to theorize the relationships between safety and the financial performance of NPPs.

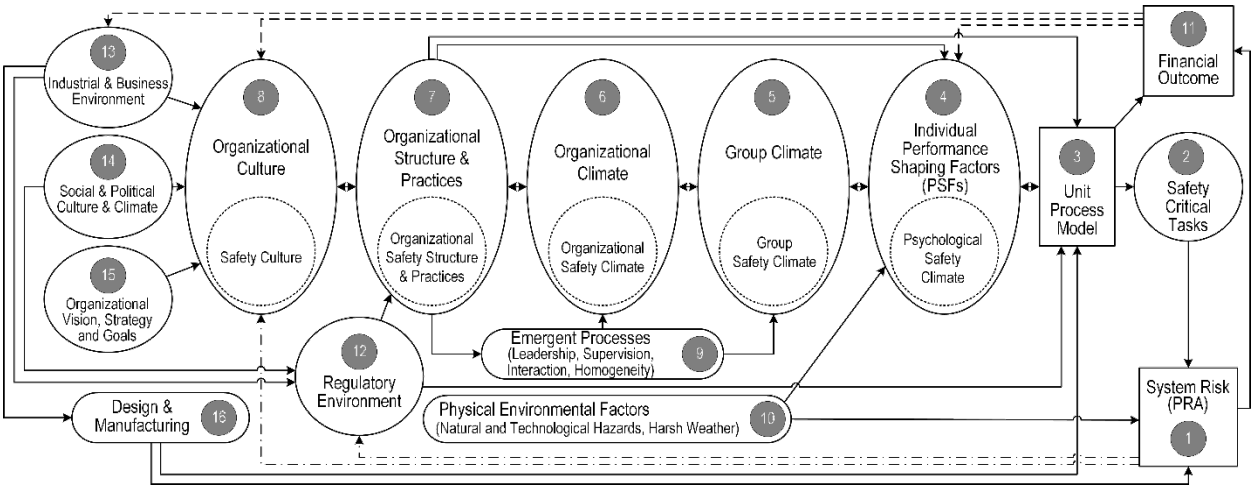


Figure 1-1: Socio-Technical Risk Analysis (SoTeRiA) Framework.

Although regulatory analyses in nuclear power contexts often treat public health and safety as separate from cost [9], a growing volume of scholarly literature suggests that financial outcomes can play an important role in affecting health and safety and that health and safety benefits can generate positive financial outcomes. Chapter 2 of this report provides a categorical review of relevant literature and theoretical bases for this research. Section 2.1 covers a review of related studies and analyzes them with respect to their theoretical bases and methodological quantification techniques. The review highlights that the use of correlation analysis to study the relationships between safety and financial performance may impede accurate evaluation of the interrelationships between these two organizational outcomes; therefore,

explicit consideration of the underlying causations is recommended. In Section 2.1.2.1, the studies related to the direct causal path from safety to financial performance in NPPs (i.e., the direct arrow from Node 1 to Node 11 in SoTeRiA) are reviewed. The focus of the literature review in Section 2.1.2.2 is then centered on the studies associated with the relationships of NPP maintenance unit performance (Node 3 in SoTeRiA) with the financial performance (Node 11 in SoTeRiA) and safety (Node 1 in SoTeRiA), considering that maintenance performance is a common causation influencing both safety and financial performance.

Considering the literature review, Section 2.2 of this report offers theoretical developments to model the causations between safety and financial performance in NPPs. Section 2.2.1 theorizes the direct causal path from NPP safety (Node 1 in SoTeRiA) to financial performance (Node 11 in SoTeRiA), while Section 2.2.2 theorizes the maintenance unit performance (Node 3 in SoTeRiA). In this study, NPP safety refers to both occupational safety and system safety (estimated from Probabilistic Risk Assessment [PRA]), while financial performance refers to the monetary values associated with alternative operation and maintenance (O&M) strategies in NPPs.

Based on the theoretical bases provided in Section 2.2, Chapter 3 of this report develops an Integrated Enterprise Risk Management (I-ERM) methodological framework (Figure 1-2) to operationalize SoTeRiA for quantifying NPP safety and financial performance in a unified platform. In I-ERM, the underlying causations associated with maintenance performance (considering human and organizational factors) coupled with physical degradation mechanisms are explicitly modeled to depict the interconnections and dependencies between safety and financial performance. In Chapter 3, a detailed description is provided on the methodological developments of individual modules and their interfaces. A case study is included in Chapter 3 to demonstrate the feasibility of quantifying the financial and safety impacts of maintenance strategies and performance at NPPs using these new methodological developments. In Chapter 4, detailed development and implementation of one of the I-ERM modules, i.e., the probabilistic physics-of-failure (PPoF) analysis module and its connection to safety and financial performance are reported.

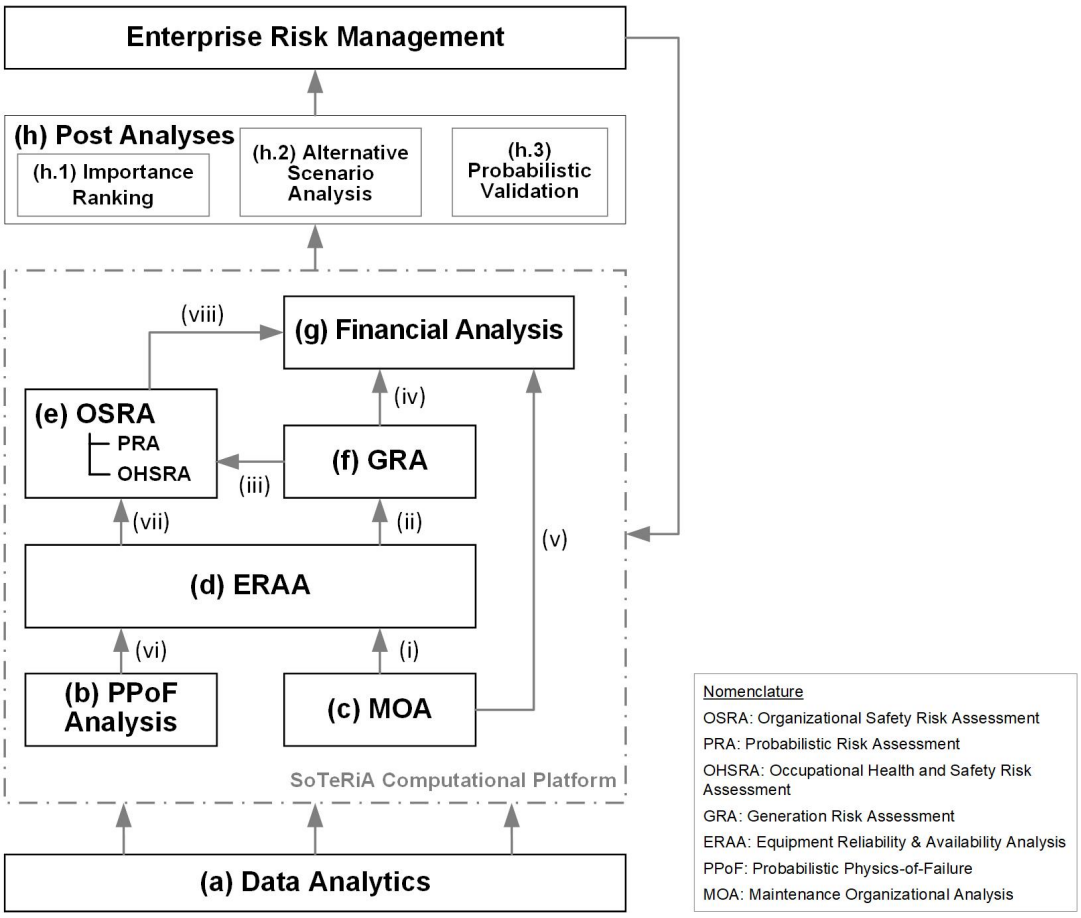


Figure 1-2. Integrated Enterprise Risk Management (I-ERM) Framework.

When compared to the previous studies, the approach developed in this research makes the following key contributions:

- Theorizes the financial consequences of NPP system accidents, system incidents, and occupational accidents in a unified causal model as, previously, there was no such combinatory model. Section 2.2 of this report proposes a "theory-based" causal model, where the inclusion of accident/incident-induced cost factors and their interactions are justified mainly by literature and, for some cases, by NPP expert opinion.

- Adds realism to modeling (i) the influence of maintenance performance on financial performance, (ii) the influence of maintenance performance on safety, and (iii) the interconnections of safety and financial performance by creating an integrated methodological environment – the I-ERM methodological framework – that can quantify the causal effects of maintenance performance on both safety and financial performance in a unified, multi-level platform:

- For the component-level analysis in I-ERM, a multi-phase Markov process model with multiple damage states is developed to compute the component reliability and availability with explicit incorporation of various maintenance strategies. These include preventive maintenance (PM) based on condition monitoring during operation and in-service inspection (ISI) during refueling outages as well as corrective maintenance (CM) following component failure. Previous studies relied on data-driven approaches and/or expert judgment for quantification of the maintenance parameters as inputs to the Markov process model. The data-driven approaches are especially challenging if the system being analyzed is new and has limited or no operational data, or if the system has undergone significant modifications such as redesign and maintenance policy updates and, thus, its historical data are not relevant to the current system conditions. To address this gap, the proposed approach in this research explicitly incorporates models of maintenance performance and physics-of-failure into a multi-phase Markov process model.

  - To support the explicit modeling of maintenance performance, Section 2.2 of this report develops a theory-based maintenance organization causal model. This causal model is quantified in Chapter 3 using a Human Reliability Analysis (HRA)-based technique. This contribution not only helps avoid reliance on data-driven approaches but also helps decision-makers efficiently design maintenance work processes and improve human performance quality in maintenance activities, leading to more efficient maintenance strategies. The model-based approach for maintenance performance analysis in this research contributes to the addition of realism when modeling the connection of maintenance performance to safety and financial performance.

  - The coupled effects of physics-of-failure and maintenance performance are considered when modeling the interconnections of safety and financial performance. Chapter 4 of this report develops an advanced physics-of-failure model with higher spatial and temporal resolutions (using Finite Element Analysis [FEA]) and its interface methodology to couple it with the maintenance performance model. This research incorporates FEA into the PPoF model and advances the interface between the PPoF analysis and the renewal process model to deal with spatiotemporal FEA outputs and to efficiently estimate the physical transition rates even when the PPoF outputs are dominated by success data. This contribution helps avoid reliance on data-driven approaches and allows for the inclusion of interrelated impacts of underlying physical degradation and maintenance causal factors on the assessment of the relationships and dependencies between the safety and financial performance of NPPs.

- In I-ERM, the outputs of component reliability and availability are used as inputs to the system-level safety models, where the production loss and safety risk scenarios are constructed and quantified. The financial performance is computed using a cost function, where the costs of direct maintenance and production loss are quantified based on the outputs from the multi-phase Markov process model, a maintenance performance model coupled with the physics-of-failure, as well as the system-level safety and production loss risk models.

The outcomes of this project have been reported in academic publications. The contents of Chapters 2, 3, and 4 of this report are based on the three-part journal article [10-12] generated as products of this project. In addition to the three-part journal article, the project team published conference papers [13-16] that summarized research progress related to individual elements of the I-ERM framework developed in this project. The methodologies developed in this project have been used in other research studies (e.g., common cause failure analysis) by the research team and so this project was acknowledged in the relevant publications. Section 5.1 provides a comprehensive list of direct publications as well as relevant publications under this project.

2. Categorical Review and Theoretical Bases

This chapter provides the theoretical bases for the I-ERM methodological framework, developed in Chapter 3 to operationalize SoTeRiA in order to quantify NPP safety and financial performance in a unified platform. Section 2.1 provides the review and analysis of literature on the interconnections of safety and financial performance. The insights from the literature review are utilized for two purposes: to justify the contributions of this research and to identify the factors and their connections in the theory-based causal models. Section 2.2 develops theoretical causal models for the interconnections between safety and financial performance of NPPs with the focus on: (i) the direct causal path from safety to financial performance (Subsection 2.2.1); and (ii) the performance of maintenance programs (Subsection 2.2.2). The causal models developed in Section 2.2 are used as theoretical bases for operationalizing SoTeRiA through the I-ERM methodological framework in Chapter 3.

2.1 Review and Analysis of Literature on Interconnections of Organizational Safety & Financial Performance

This section uses the SoTeRiA theoretical framework (Figure 1-1) to analyze the literature related to the interconnections of organizational safety and financial performance. The review includes selected literature from high-consequence industries (e.g., nuclear power, aviation, healthcare, and transportation) to demonstrate the categorization of the studies; meanwhile, the focus of the literature review in Subsections 2.1.2.1.1 and 2.1.2.2.1 is on the nuclear industry, exclusively.

Although Node 1 of the original SoTeRiA represented only system safety (estimated from PRA) [7, 8, 17-24], this research considers both occupational safety and system safety for Node 1. In SoTeRiA, safety critical tasks (Node 2 in Figure 1-1) are identified as those tasks that influence safety scenarios in Node 1, e.g., maintenance performance. The unit process model (Node 3 in Figure 1-1) covers the work processes (e.g., maintenance work processes) that support the quality of safety critical tasks. The organizational aspects, such as safety culture, safety climate, and safety practices (Nodes 5 to 8 in Figure 1-1), influence human performance or the individual Performance Shaping Factors (PSFs) (Node 4 in Figure 1-1) related to the individuals involved in the work processes of the unit process model (Node 3). For example, the training program quality, as part of organizational safety practices, can affect the performance of maintenance technicians involved in maintenance work processes. As shown in Figure 1-1, organizational structure and practices can directly affect individual PSF; for example, a high-quality training program generates a rich safety climate, bolstering individual PSFs [17]. Additionally, organizational structure and practices influence the shared climate through emergent processes (Node 9 in Figure 1-1), such as homogeneity in the organization. Organizational culture, which impacts organizational safety practices, is

affected by the type of industry, social/political culture, and organizational vision (Nodes 13, 14, and 15 in Figure 1-1). The regulatory environment (Node 12 in Figure 1-1) affects organizational safety practices through rules and policies, as well as through the external auditing of organizational practices to ensure compliance with regulation through inspection and enforcement.

Based on SoTeRiA (Figure 1-1), there are direct and indirect connections between safety (Node 1) and financial performance (Node 11). The direct connection relates to the direct causal path from Node 1 to Node 11 in SoTeRiA; for example, accidents and incidents would lead to financial losses. There are also indirect causal paths between safety and financial performance. For example, changes in safety performance (Node 1) may affect organizational safety culture (Node 8) or regulatory environment (Node 12), and these changes can influence organizational structure and practices (Node 7) such as organizational training programs, which impacts the quality of activities within the unit process model (Node 3) (e.g., maintenance work processes), leading to changes in financial outcomes (Node 11). Meanwhile, changes in financial performance may affect management's commitment to safety (under Node 8), which influences the quality of organizational safety practices (Node 7) that have an impact on the quality of activities within the unit process model (Node 3), leading to changes in safety (Node 1) through changes in the quality of safety critical tasks (Node 2). This way, the common causal paths in SoTeRiA can impact both safety and financial performance, generating dependency between these two organizational outcomes.

This section reviews the studies related to the relationships between safety and the financial performance of an organization and categorizes them into two groups, as shown in Table 2-1. Section 2.1.1 reviews and analyzes Category I, focusing on studies evaluating the correlation between safety (system safety and/or occupational safety) and the financial performance of an organization. These studies create a list of indicators to measure safety and financial performance and then evaluate the correlation between these two outcomes. Section 2.1.2 reviews and analyzes Category II focusing on the studies that explicitly model the underlying causations associating safety and financial performance (focusing on the direct and/or indirect causal paths between Node 1 to Node 11 in SoTeRiA).

Table 2-1. Classification of literature on the relationships between safety and financial performance.

Category	Sub-category
I. Correlations between safety and financial performance	I.1 Correlation between system safety and financial performance
	I.2 Correlation between occupational safety and financial performance
II. Explicit modeling of underlying causations associating safety and financial performances	II.1 Direct causal path from safety performance to financial performance
	II.2 Indirect causal paths between safety performance & financial performance

2.1.1 Existing Studies Examining Correlations Between Safety and Financial Performance (Category I)

Selected literature from diverse industries is reviewed to highlight the limitations of correlation analysis for this research topic. The limitations of correlation studies are discussed in Subsection 2.1.1.3, leading to the literature review in Subsection 2.1.2 on studies that analyze safety-financial causations, and justifying the focus of the theoretical model developments (Section 2.2) that support modeling underlying causations between safety and financial performance in NPPs.

2.1.1.1 Previous Studies Examining Correlations Between System Safety and Financial Performance (Category I.1)

Several studies examined the correlation between system safety and financial performance in high-consequence industries, such as aviation (e.g., [25, 26]), health care (e.g., [27]), nuclear (e.g., [28]), and motor carrier (e.g., [29, 30]). In the airline industry, Rose [31] evaluated the relationship between profitability (and other aspects of financial health) and rates of accidents/incidents in the airline industry, identifying a positive correlation between airline profitability and airline safety. Golbe [26], on the other hand, stated that, while theory suggests that the sign of the correlation between safety and profit is indeterminate and depends on risk preference as well as the structure of costs and demands, empirical analysis found no significant correlation between airline profit and safety. Madsen [26] evaluated the influence of the financial performance of an organization relative to its financial goals (aspiration point) on organizational risk-taking in the context of safety. Considering accident rates as a negative indicator of safety, Madsen found a positive relationship between airline profitability and accident rates when profitability is below the profitability aspiration (i.e., the level of performance that decision-makers expect to achieve) and a negative relationship between these two organizational outcomes when the profitability is above the aspiration point. Recently, Kalemba and Campa-Planas [25] evaluated the correlation between airline safety and two organizational economic performance measures, profitability and revenue. The authors utilized a publicly available index – the Jet Airliner Crash Data Evaluation Center (JACDEC) safety index, which consists of eight weighted elements, including fatalities, number of serious incidents, and information regarding International Air Transport Association Operational Safety Audit membership – to represent airline safety. It was found that, while there is no significant correlation between safety and profitability measured by return on investment, safety can significantly impact airline revenue [25].

In the motor carrier industry, Britto et al. [29] identified motor carrier financial performance (based on net profit margin) as having a positive correlation with improved safety performance in a subsequent year. This included the total crashes of a motor carrier as well as two safety indicators – the driver safety evaluation area (DRSEA) score related to the performance of a carrier's drivers and the vehicle safety

evaluation area (VHSEA) score associated with the performance of the carrier's vehicles [29]. Miller and Saldanha [30] used safety indicators (unsafe driving factor, hours-of-service, and vehicle maintenance) and financial indicators (carrier earnings margin before interest, taxes, and depreciation/amortization), finding that both absolute financial performance and changes in financial performance are positive predictors of the motor carrier safety.

In the healthcare industry, Akinleye et al. [27] stated that previous studies evaluating the correlation between financial performance and safety of patient care had generated equivocal results. The lack of clear association may be related to the poor validity of measures of financial and quality/safety performance. They proposed the use of a composite financial performance score, comprising multiple financial measures, to evaluate the correlation between hospital financial performance and safety metrics, concluding that hospitals with more stable financial conditions are able to provide more resources for quality/safety improvements [27].

In the nuclear domain, there are few correlation studies associated with safety and financial performance. Blanco et al. [28], using data from NPPs in the U.S., examined the correlation between the adoption of PRA and the occurrence of safety-related disruptions such as safety system actuation, violation of technical specification, equipment degradation, and equipment inoperability. They illustrated that the adoption of PRA is associated with a decrease in the occurrence of safety-related events. Additionally, they examined the impact of PRA adoption on annual capital costs and generation losses and proved that PRA implementation is associated with an approximate $20.6M decrease in annual production loss (in 2001 values). They also examined the correlation between safety-related disruptions and plant capacity factors, identifying safety-related events as being negatively associated with electricity generation. The IAEA-TECDOC-1209 [32] compared the O&M costs per KWh of NPPs and the Institute of Nuclear Power Operations plant evaluation ratings (associated with nuclear safety) for all U.S. NPPs, finding that plants with the best safety ratings had the lowest O&M costs.

2.1.1.2 Previous Studies Examining Correlations Between Occupational Safety and Financial Performance (Category I.2)

Occupational accidents and workplace injuries may significantly disrupt the work environment and interrupt production processes, leading to financial and lost opportunity costs to an organization. Some studies examined the correlation between occupational accident rates and profitability.

For example, in the construction industry, Feng et al. [33] found that the total workplace accident costs are positively correlated with the project hazard index and accident rates. The hazard index refers to the

overall level of project hazard, including the degree of hazard contributed by roofing work, crane use, or work on contaminated sites. Workplace accident costs consist of "direct costs" associated with the treatment of injuries and any compensation to workers arising from their injuries, and "indirect costs," such as time spent dealing with an accident (e.g., costs of supervisory or staff efforts) and lost productivity due to injured worker. Feng et al. [33] conducted bivariate correlation analysis and identified the ratio of indirect to direct accident costs as being positively correlated with several project characteristics, such as company and project size and the involvement of sub-contractors. As another example, in the mining industry, Asfaw et al. [34] identified an inverse relationship between profitability and the rate of occupational injuries, where three levels of occupational accident severity were evaluated: (i) all fatal and nonfatal injuries, (ii) nonfatal injuries resulting in lost workdays, and (iii) fatal injuries and serious nonfatal injuries.

There are a few cross-industry studies that examined correlations between occupational safety and financial performance. For example, Yakovlev and Sobel [35] examined the pair-wise correlations between capital stock per worker, equipment stock per worker, wage rate, interest rate, and injury rate, identifying a significant correlation between capital and equipment stock per worker and injury rates. The authors evaluated the hypothesis that industries with high injury rates should increase their capital to labor ratios to reduce costs associated with injuries, finding that the injury rate has an economically significant positive affect on capital to labor ratio. Fernández-Muñiz et al. [36] utilized an empirical analysis to evaluate the economic benefits of adopting adequate Safety Management Systems (SMSs) in various industries including the construction, industrial, and service sectors in Spain. It was found that the implementation of SMSs has a significant positive influence on a firm's competitiveness (e.g., productivity, innovation capability, customer satisfaction, and company reputation) as well as on safety performance through reductions in occupational accident rates and fewer injuries and damages. Their study highlighted that SMSs could have a greater influence on an organization's competitiveness and safety performance than on the organization's financial performance.

Following an occupational accident, employees may be required to focus on activities associated with resolving the consequences of the accident while continuing production-supporting activities. For example, managers and supervisors of an organization may be involved in an accident investigation. In this situation, the organization prioritizes activities associated with addressing potential consequences of the accident instead of strategic planning and value-added activities, potentially impacting the long-term financial performance of an organization. This concept is supported by the empirical analysis conducted by Argilés-Bosch et al. [37], who found that the percentage of injured workers in a given year has no significant influence on the short-term financial performance of an organization, measured by Return on Asset (ROA), but has a significant negative impact on the organization's financial performance one year later. Forteza et

al. [38] further explored the findings of Argilés-Bosch et al. [37] using a different dataset in the construction industry, identifying a quadratic relation between workplace accident rates and ROA and found that there may be a tipping point in the relationship between the workplace accident rates and profitability. Their study indicated that, for firms with low workplace accident rates, the workplace accident rates may have a positive correlation with profitability; however, for firms with high workplace accident rates, the workplace accident rates are negatively correlated with profitability.

2.1.1.3 Limitations of Correlation Analysis on the Relationships Between Safety and Financial Performance

As discussed in the preceding sections, several studies (categorized under Category I in Table 2-1) utilized correlation analysis to examine the relationships between safety and the financial performance of an organization. The studies in Category I, however, have two limitations:

a. *Limited support for risk-informed decision-making:* Given that a correlation analysis is valid, it can provide insights on the existence of relationships between safety and financial performance, but it is not informative on the mechanisms of relationships and interconnections between safety and financial performance. Without modeling underlying causations or without modeling "how" safety and financial performance are interconnected, it would be hard to generate management strategies for mitigating undesirable safety and financial consequences and for balancing safety and financial performance.

b. *Validation* deficiencies: When examining the correlation between safety and financial performance, the major issues of the previous studies include data limitations and omitted variables. Several studies utilized cross-sectional data (e.g., [27, 36]) that did not capture the order of occurrence of different observations, which is one of the key components for establishing a causal relationship. To overcome this limitation, some studies utilized longitudinal panel data to explicitly consider the temporal sequence of the observations [25]. The differential timing of safety and financial outcomes (e.g., analysis of immediate and long-term costs incurred by an accident or incident) can also complicate a correlation analysis. Furthermore, challenges associated with identifying and quantifying invisible costs (e.g., time spent by managers after the occurrence of an accident) using available accounting system data may influence the evaluation of the relationship between safety and financial performance. Having a small sample size is also highlighted as a limitation in Category I studies [25, 39]. Another challenge identified in the Category I studies is related to endogenous variables correlated with the error term; if not properly identified and

explicitly accounted for, endogeneity may devoid the correlation results of any meaning [34]. Endogeneity may occur for several reasons, such as omitted control variables [40].

To address the issues of correlation analysis, Section 2.2 offers "theory-based" causal models, where theory supports the validity of the models. To establish the theoretical background for the causal models, Subsection 2.1.2 provides a review of studies related to explicit modeling of the underlying causations between safety and financial performance (Category II in Table 2-1).

2.1.2 Previous Studies Related to Explicit Modeling of Underlying Causations between Safety and Financial Performance (Category II)

Explicit modeling of underlying causations can support decision-makers by capturing shared factors and causal mechanisms influencing both the safety and financial performance of an organization and enabling improved evaluation of the financial implications of safety strategies and of the cost effectiveness of safety investments. Modeling underlying causations supports the simulation of the temporal interactions between safety and financial performance, which is beneficial for management's critical decision-making when balancing safety and profitability.

Based on SoTeRiA (Figure 1-1), there are direct and indirect causal paths between safety (Node 1) and financial performance (Node 11):

- The direct causal path refers to the direct arrow from Node 1 to Node 11 in SoTeRiA, highlighting costs of accidents and incidents (related to technical system safety and occupational safety). Studies related to this direct causal path (Category II.1 in Table 2-1) are reviewed in Subsection 2.1.2.1. This section begins with selected studies from various industries and leads to Subsection 2.1.2.1.1, where the review is narrowed down to the nuclear industry. Subsection 2.1.2.1.1 provides background for the theoretical development in Section 2.2.1.

- The indirect causal paths refer to the cases where safety (or financial performance) affects intra-organizational factors (e.g., organizational culture; Node 8 in SoTeRiA) or external factors (regulatory environment; Node 12 in SoTeRiA), and those factors affect financial performance (or safety) through organizational causal mechanisms (e.g., unit process model; Node 3 in SoTeRiA). Studies related to indirect paths (Category II.2 in Table 2-1) are reviewed in Subsection 2.1.2.2, bringing a few examples from diverse industries and then narrowing the review down to the nuclear industry in Subsection 2.1.2.2.1. Since the unit process model (Node 3 in SoTeRiA) is the sharp end of causation in all indirect causal paths, the review in Subsection 2.1.2.2.1 focuses on modeling one of the units of NPPs, i.e., a maintenance unit, and the connection of the maintenance unit

process to safety and financial performance. Subsection 2.1.2.2.1 provides background for the theoretical development in Subsection 2.2.2.

2.1.2.1 Existing Studies Related to the Direct Causal Path from Safety to Financial Performance (Category II.1)

An accident can damage assets, interrupt production, and lead to additional post-accident activities, such as additional regulatory inspections. Following an accident, an organization's insurance premium may increase. It would usually be easier to assess the potential increase of an insurance premium for minor frequent accidents than for major accidents. An organization's insurance premium may depend on the size of the company, its geographical location, the size of the insurance pool, the pool claim history, and the company's accident claim history [41]. According to Gavious et al. (2009), an organization's annual insurance premium can be determined considering financial damages of equipment, commodities, and facilities; accident leave; number of hospitalization days; accident severity; and potential lawsuits [42].

While many accident costs can be clearly identified (e.g., cost of damaged equipment, immediate medical treatment costs, fines, and increased insurance premiums), there are hidden cost elements that may cause negative long-term impacts on the financial performance of an organization [42]. Previous studies refer to these less identifiable expenses – including increased employee turnover, deterioration of the corporation's public image, and reduction of employee engagement, motivation, and morale – as indirect costs of accidents [42, 43].

There are several studies analyzing indirect costs of accidents. For example, Gavious et al. [42] identified costs associated with the impact of an industrial accident on workers' morale and motivation and damage to a company's reputation as immeasurable costs. Labor costs may also increase following an accident as employees at different organizational levels are tasked with additional required actions to respond to the accident (e.g., investigation costs, costs of increased staffing efforts including overtime hours). Jallon et al. [43] identified four main elements of the indirect cost due to workplace accidents, including legal and administrative costs, productivity costs (e.g., work shutdowns and production delays due to an accident), replacement costs (e.g., costs of replacing absent employees), and investigation costs. Gerbec and Kontić [44] suggested that reputation and client loss, in addition to impacts on the local/regional economy, can be considered as intangible indirect costs. While previous studies highlighted that estimating the cost of reputational damage following a major accident is a challenging task, recent publications have emphasized the criticality of considering the negative impacts of major accidents on a firm's share price and potential associated impacts to the firm's long-term economic performance [45, 46]. Reniers and Van Erp [41] suggested using a company's share price as a representation of investors' image of the company

(e.g., company reputation). Gerbec and Kontić [44] evaluated the impact of an explosion at a liquid cargo terminal, highlighting that consideration of indirect economic impacts (e.g., longer business interruption and the negative impacts on reputation), in addition to direct financial costs, is critical when assessing the business impacts of an accident.

Some of the indirect cost of accidents can be either considered as part of the direct arrow from Node 1 to Node 11 in Figure 1-1 (related to studies in Category II.1 of Table 2-1) or, more explicitly, be modeled as indirect causations (Category II.2 in Table 2-1). For example, an increase of labor costs due to accidents can either be considered as an indirect cost of an accident under Category II.1 or can be modeled more explicitly as an arrow from Node 1 to Node 8 (increase in management's commitment to safety due to accidents) and from Node 8 to Node 7 (the effects of management's commitment to safety on the increase in quantity or quality of safety practices). For these types of indirect costs of accidents, the analyst needs to be cautious to avoid double-counting them; if they are considered as parts of indirect costs under the direct causal path from Node 1 to Node 11, they should not be explicitly modeled using indirect causal paths or vice versa.

2.1.2.1.1 Existing Studies Related to the Direct Causal Path from Safety Performance to Financial Performance of NPPs

This section reviews studies focusing on the direct causal path from safety to financial performance (i.e., the direct arrow from Node 1 to Node 11 in Figure 1-1) for NPPs. The review covers a selection of highly relevant studies in the nuclear domain. The literature review in this section supports the development of a theory-based causal model (in Subsection 2.2.1) for evaluation of the financial consequences of accidents and incidents in NPPs. Previous studies by several authors of this report evaluated the costs of various design alternatives for a Diverse and Flexible Coping Strategies (FLEX) storage building subjected to an external hazard [4], where accident costs were considered as a summation of costs for compensating health and societal impacts following an accident. The literature review in this section more comprehensively identifies factors and their interactions that can affect the consequences of an accident or incident in NPPs to provide further context in estimating costs following an accident/incident. Identification of these factors and their paths of influence on NPP financial performance helps with the development of a theory-based causal model (in Subsection 2.2.1).

Previous studies [47-49] have suggested different categorization schemas for accidents and incidents in NPPs, considering their consequences. For example, NUREG/CR-3673 [47] identified three categories for LWR operational events resulting in societal costs: (i) forced outage events which do not result in core

damage or significant plant contamination, (ii) accidents leading to core damage and possible fuel melting but do not lead to breach of the reactor vessel or any significant release of radioactive materials into the environment, and (iii) accidents resulting in severe core damage and either reactor vessel breach or a significant release of radioactive material into the environment [50]. The reviewed articles in this section are categorized into three groups (A, B, and C):

A. *Cost of core damage accidents;*

B. *Cost of non-core damage accidents or incidents; and*

C. *Cost of occupational accidents*.

Category A in this report corresponds to the combination of the second and third categories in NUREG/CR-3673. Category B in this report is similar to the first category in NUREG/CR-3673. Category C is not in the scope of NUREG/CR-3673.

Cost of core damage accidents (Category A): Bizet and Lévêque [51] reviewed previous studies focusing on the evaluation of costs of major nuclear accidents. The authors noted that discrepancies in the assessment of accident costs in the literature may originate from (i) differences between the type and location of accidents, (ii) differences in boundaries of cost assessment, and (iii) the statistical representation of the costs. It is a widely held belief that the occurrence of a major accident at an NPP will result in the end of the plant service life and in the plant being decommissioned. As such, evaluation of the potential impact of changes in safety performance on financial performance should consider the potential occurrence of an accident (i.e., Core Damage Frequency [CDF]) during the remaining planned plant service life. This perspective indicates an uncertain annual cash flow throughout the period of interest in the financial analysis. An additional complicating factor is associated with risk-based costs and benefits associated with very rare events. When evaluating potential safety investments to reduce the likelihood or consequence of the very rare events, the benefits associated with such investments – while potentially substantial – are unlikely to be realized over the plant service life, while the costs of the investments will be realized immediately. This view represents another source of uncertainty in cash flow.

Previous studies identified several types of costs associated with major nuclear accidents. Selected studies are summarized as follows:

- Severe accident costs accrue both to society and the NPP, including administrative penalties, litigation costs, costs associated with changes in public perception and attitudes, regulatory compliance costs, and stock price changes, as seen following the TMI [52] and Fukushima accidents [53]. According to

Kanamori [54], the cost breakdown (as of December 2016) of the Fukushima-Daiichi nuclear disaster consists of costs associated with damage compensation (8 trillion yen), decontamination and interim storage (6 trillion yen), and decommissioning (8 trillion yen), where responsible parties included Tokyo Electric Power Company Holdings, Inc. (TEPCO), other nuclear plant operators, power producers and suppliers, and the national government.

- Silva et al. [55] developed a "cost per severe accident" model, where different cost components are considered, including costs associated with health effects (e.g., effects of radiation exposure and psychological effects), economic impacts (i.e., income losses, transportation costs, accommodation costs and capital utility losses of the sheltered, evacuated and relocated population), social impacts (e.g., harmful rumors), and environmental impacts (e.g., decommissioning and land decontamination). Their study identified factors that can affect decontamination costs, including decontamination techniques and associated unit costs, waste generated by each decontamination technique, and waste management [56]. In addition, dose reduction factors, the period of time the public remains in contaminated areas, and occupational exposure for workers involved in decontamination may impact radiation exposure costs, while decontamination speed may impact relocation costs. Their study also discussed the importance of a discount rate in accounting for the long-term impacts of severe accidents, utilizing the declining-balance method to aggregate all future impacts into a single economic value. A recent study by Silva and Vechgama [57] evaluated major accident costs, over time, associated with radiation effects, relocation, and decontamination. Their results showed that, while decontamination comprised a large portion of the total major nuclear accident cost during the first few years after an accident, their impact decreases over time. On the other hand, the radiation effects will be dominant contributors to accident costs from the second decade onward after occurrence of an accident.

- The MELCOR Accident Consequence Code System (MACCS) is a level 3 PRA code developed by the U.S. Nuclear Regulatory Commission [58]. MACCS can consider the economic costs of long-term protective actions (e.g., permanent relocation) and costs of emergency response actions (i.e., evacuation, sheltering, and relocation) [58]. MACCS is equipped with the Regional Disruption Economic Impact Model (RDEIM) that can account for the direct losses to a disrupted region affected by an accident as well as the indirect losses to the national economy due to supply chain disruptions and the induced losses from reduced spending by displaced workers [59]. Level 3 PRA outputs, including the averted population dose (using a conversion factor to assess the associated monetary value) and averted economic costs (e.g., offsite property damages), serve as inputs into the cost-benefit analysis [60]. For instance, MACCS is utilized in regulatory cost-benefit analyses for estimating the potential benefits of safety improvements, considering the averted accident consequences, and in

analyses of severe accident mitigation alternatives [61]. The changes in collective radiation exposure to the public due to plant safety enhancement multiplied by the monetary conversion factor (dollar per person-rem) are common attributes considered in cost-benefit analysis in NPPs. Zhang et al. [60] proposed a multi-criterion benefit evaluation methodology based on various evaluation criteria, including public risk, occupational risk, plant revenue and costs. While their mathematical formulation is similar to the U.S. NRC's cost-benefits analysis method, a major difference in Ref. [60] is the consideration of the cumulative prospect theory with some modifications to convert calculated costs and benefits to their perceived values.

- Nosek [62] developed the Fukushima-Informed Recovery and Cost Assessment approach to improve cost estimation by considering a more comprehensive set of impacts both inside and outside the interdicted area, including property damage, medical expenses, cleanup costs, waste management, compensation program, and burden of societal disruptions.

- Karanta [63] identified different seasonal and contextual factors (e.g., extreme snow) that can impact accident consequences in Level 3 PRA. These factors may ultimately affect population dose, evacuation processes, sheltering, and distribution of radionuclides in the environment [63].

- Bier et al. [64] highlighted that the number of people relocated can be considered as a proxy for the societal disruption following a severe nuclear accident. According to Denning and Mubayi [65], the societal impacts (e.g., costs of relocation; costs of housing of displaced personnel; costs of decontaminating large areas; and costs associated with loss of land use) and potential psychological impacts on relocated people following the Fukushima accident were substantial. They highlighted that long-term protective actions, emergency response delay time, and evacuation speed may affect the magnitude of accident consequences [65].

Cost of non-core damage accidents or incidents (Category B): Costs related to non-core damage plant states can affect NPP financial performance. Three main cost contributors following transients or non-core damage accidents are those associated with physical damage, generation loss, and regulatory impact [66]. For example, following an accident at an NPP, a licensee will be required to conduct corrective actions to address the root causes of the accident. Dube et al. [67] highlighted that these costs may be correlated; for example, regulatory impacts may extend a plant shutdown, increasing generation loss. Their paper also described the Exelon Economic Enterprise Risk model, which focuses on reactor transient and non-core damage accidents. A database was developed using historical data for events with significant regulatory and financial impacts such as loss of offsite power, fire, and external hazards. Information within this

database includes risk metrics (e.g., results of the significance determination process, accident sequence precursor results), outage duration, repair costs, and total costs. A set of casualty events and their associated non-core damage plant impact states was developed in a tabular format where cost data link each non-core damage event to the plant impact states, connecting the sequence cut-sets to the consequence bins in the plant PRA model [66].

In addition to regulatory penalties, civil lawsuits can result in significant costs to the NPP, either as a result of severe/rare accidents, or as a result of smaller incidents, both of which may have root causes in safety [68]. Costs associated with legal liability can include costs of legal counsel, administrative burdens during discovery, settlements, and damage awards, as well as the potential for legal injunctions. Although the extent of civil liability varies under different regimes around the world, and have sometimes been criticized as insufficient [69], it is clear that the costs of liability can be very high, as demonstrated by the Fukushima accident [70].

Cost of occupational accidents (Category C): NPP workers may be exposed to several hazards in their workspace, which may lead to the occurrence of occupational accidents causing injuries, illnesses, and deaths. Occupational hazards associated with nuclear power facilities can be categorized into four groups [71]: (i) radiation hazards, (ii) chemical hazards, (iii) condition of facilities, which can impact the safety of radioactive material, and (iv) condition of facilities which may cause occupational hazards not involving radioactive materials (e.g., exposure to non-radioactive toxic materials, hazards due to falls, electrical, confined space, and energization). Occupational injuries and illnesses generate direct costs via workers' compensation payments, medical expenses, and costs for legal services, as well as indirect costs associated with training replacement employees, accident investigations, lost productivity, and costs associated with lower employee morale and absenteeism [72].

2.1.2.2 Existing Studies Related to the Indirect Causal Paths between Safety Performance and Financial Performance (Category II.2)

Safety can indirectly affect NPP financial performance through multiple paths in the SoTeRiA framework (Figure 1-1). The indirect causal paths refer to the cases where safety outcome (e.g., increase in incident rate) can indirectly impact NPP financial outcomes (Node 11 in SoTeRiA) through its impacts on organizational safety culture (Node 8 in SoTeRiA) or through regulatory oversight and enforcement (Node 12 in SoTeRiA). For example, near-misses and incidents or safety-related interventions may increase organizational and individual safety consciousness, leading to organizational safety practice improvements (e.g., training quality) that affect PSFs (Node 4 in SoTeRiA) and the quality of activities within the unit process model (Node 3), ultimately impacting financial outcomes (Node 11 in SoTeRiA). Similarly, as

Figure 1-1 shows, changes in financial performance may affect organizational culture (Node 8 in SoTeRiA); for example, a reduction in management's commitment to safety can influence the quality of organizational safety practices (Node 7 in SoTeRiA), impacting the quality of activities within the unit process model (Node 3 in SoTeRiA) and leading to changes in safety performance (Node 1 in SoTeRiA) through changes in the quality of safety critical tasks (Node 2 in SoTeRiA).

Another indirect causal path from safety to financial performance is through regulatory environment (Node 12 in SoTeRiA). A significant increase in the number of incidents, for instance, may lead to changes in legislation [41, 73]. While changes in legislation are costly processes for government, they can result in an even larger financial, administrative, and operational burden for companies which have to evaluate and implement the altered regulations in order to ensure their compliance with the new regulations [41]. Because even well-meaning regulations can create countervailing risks—for example, by imposing costs that reduce overall safety—many regulatory theorists encourage careful analysis of regulatory programs to ensure that those programs are effective in promoting their goals [74]. Other scholars emphasize the perverse outcomes that can arise when regulatory programs intending to reduce risk ignore the systemic [75] or practical [76] implications of cost and other tradeoffs [77]. This literature suggests that the costs of compliance can perversely create challenges to compliance; in a study by Ruhl and Salzman [75], for example, three-quarters of environmental lawyers representing business clients reported that the cost of compliance was relevant to levels of compliance.

Since the unit process model (Node 3 in Figure 1-1) is the sharp end of causation in all indirect causal paths, the review in Subsection 2.1.2.2.1 focuses on modeling one unit of an NPP, i.e., a maintenance unit, and the connection of a maintenance unit process model to safety and financial performance. The review in Subsection 2.1.2.2.1 provides background for the theoretical development in Subsection 2.2.2 and for the methodological developments in Chapter 3. Future work will expand the review and modeling to explicitly include more in-depth organizational mechanisms (e.g., safety culture) that affect maintenance unit performance and to include other units of NPPs (e.g., main control room unit) and their common causations on both safety and financial performance.

2.1.2.2.1 Existing Studies Related to the Relationships of NPP Maintenance Performance with Financial Performance and Safety Performance

There are existing studies that only analyzed the impact of maintenance performance on safety but did not calculate any financial performance outputs (e.g., Refs. [78, 79]). There are also some studies that only analyzed the maintenance performance impact on financial performance but did not calculate any safety-

related outputs (e.g., Ref. [80]). The literature review in this section, however, focuses on the studies that explicitly incorporated the maintenance impact on both safety and financial performance. In this context, the "explicit" incorporation of maintenance impact means that maintenance-related parameters are treated as input parameters of the safety and financial performance models such that the sensitivity of the safety and financial performance metrics to the variation of the maintenance parameters can be analyzed.

In the reviewed literature, multiple types of models were utilized for computing the safety performance metrics with the explicit incorporation of maintenance impact. Examples of these models include reliability or unavailability functions [81-85], the combination of an event tree and fault trees under PRA[86-89], a simulation-based approach combined with an event tree [90], a simulation-based approach combined with a fault tree [91], and a Bayesian network [92]. An EPRI report [89] used PRA modeling techniques to model system safety, while also developing a comprehensive cost model for O&M costs including indirect costs (e.g., administrative costs) and direct costs (e.g., material costs, labor costs, production loss due to maintenance). The direct costs account for all costs associated with maintenance processes such as inspection, repair, and post-maintenance testing. Another type of model used in the existing studies is a renewal process model, such as a continuous-time Markov model [93] and a multi-phase Markov model [94-96]. The key benefit associated with renewal process modeling techniques, compared to the other model types, is the capability to include multiple states of an individual component or equipment (e.g., degradation and damage states), which can provide additional realism to the connection of maintenance performance to safety and financial performance, by improving the modeling of the progression of component/system degradation and its interactions with multiple types of maintenance strategies. The following reviews a set of relevant studies that used renewal process modeling and analyzes them with respect to the connection of maintenance performance to safety and financial performance.

Cluever et al. [93] developed a continuous-time Markov model, where each state represents a success or failure state at a certain time point. The effects of PM and CM are incorporated by generating a "modifying parameter" to the degradation rate, modifying the degradation rate depending on the effectiveness and frequency of occurrence of PM and CM. The modifying parameter value was quantified by expert opinion. This study develops a function for the expected cycle cost, including only direct maintenance costs without considering production loss resulting from maintenance. The total contribution of direct maintenance costs is computed by determining the frequency of occurrence for specific maintenance activities as well as the cost per occurrence of each maintenance activity.

Cowing et al. [95] developed a multi-phase Markov process model to simulate successive cycles of operation, consisting of a period of planned maintenance and a period of normal operation. The set of the

Markov states included several shutdown states where PM and/or repair may occur. The effects of the maintenance interval and duration on safety were explicitly modeled through the transition rates between operating and shutdown states, which were quantified using available data related to the failure rate of components as well as the maintenance cycle and outage length. Their study calculated the costs associated with a component being in a specific state, as well as the costs associated with transitioning to a specific state. The costs for planned maintenance states included costs associated with specific maintenance activities (e.g., inspection labor costs) and the costs associated with production loss resulting from maintenance activities. Their study also included additional costs related to regulatory penalties.

Wu et al. [94] used a multi-phase Markov model at the system level, where different system states may occur due to the failure or success of components within the system. Their study explicitly includes the interval, duration, and effectiveness of maintenance activities using expert judgment to quantify the maintenance parameters. Their approach lacks the explicit inclusion of PM strategies during operation and only considers in-service inspection during outages and CM. Direct maintenance cost is estimated as a function of the frequency of occurrence and cost per occurrence of each maintenance activity, as well as the system unavailability cost as a function of cost per unit time and duration of system downtime as a result of maintenance.

Du et al. [96] used a multi-phase Markov model for component reliability, where the component is subject to imperfect PM and inspection at fixed intervals. The effectiveness and interval for inspection and PM were explicitly incorporated into the multi-phase Markov model, but CM was not explicitly included. Maintenance effectiveness was modeled using a maintenance effectiveness curve for PM, derived using expert opinion. Inspection was assumed to be perfect, where the component state is perfectly known at the time of inspection. The maintenance costs were computed as a function of the cost per occurrence and frequency of PM and inspection/replacement. This study did not consider the costs associated with production loss due to maintenance.

The review highlighted that the studies using a continuous-time or multi-phase Markov model that only included functional success and failure states of components [93, 94] were limited in the comprehensiveness of the maintenance activities since the variations in maintenance strategy and effectiveness depending on physical damage states of the component cannot be explicitly modeled. The use of a multi-state, multi-phase Markov model [95, 96] allows for more comprehensive modeling of maintenance strategies by capturing the maintenance activities specific to the component damage states and maintenance events occurring at discrete time points such as scheduled inspection and repair. These existing studies, however, relied on data-driven approaches and/or expert judgment for quantification of the maintenance parameters

as inputs to the Markov model. The data-driven approaches are challenging especially when (i) the system being analyzed is new and has limited or no operational data; or (ii) the system has undergone significant modifications such as redesign and maintenance policy updates and, thus, its historical data are not relevant to the current system conditions. To overcome the limitations of existing studies, this research offers a new theory-based causal modeling approach, as explained in Subsection 2.2.2.

2.2 Theoretical Developments on Interconnections of Safety and the Financial Performance of NPPs

Based on insights from the literature reviewed in Section 2.1, this section shows new theoretical development for modeling the interconnections between safety and the financial performance of NPPs. The objective is to generate a model-based approach (developed in Chapter 3), rather than a correlation-based approach, to analyze the underlying causation affecting both safety and financial performance of NPPs. Compared to the existing approaches (reviewed in Section 2.1), the approach offered in this three-part article adds realism to the modeling of: (a) the influence of maintenance performance on the financial performance of NPPs, (b) the influence of maintenance performance on the safety of NPPs, and (c) the interconnections of safety and financial performance of NPPs. This section generates theoretical bases for accomplishing these advancements by:

- Theorizing the direct causal path from safety to financial performance (i.e., the direct arrow from Node 1 to Node 11 in SoTeRiA; Figure 1-1) by formalizing the financial consequences of system accidents and incidents as well as occupational accidents of NPPs in a unified causal model (Subsection 2.2.1); and

- Theorizing the indirect causal path between safety and financial performance mediated by the intra-organizational factors (e.g., organizational culture; Node 8 in SoTeRiA), external factors (e.g., regulatory environment; Node 12 in SoTeRiA), and organizational causal mechanisms (e.g., unit process model; Node 3 in SoTeRiA). The scope of this research focuses on theorizing the impact of maintenance unit processes, interacting with system and component degradation, on the safety and financial performance of NPPs. Subsection 2.2.2 develops a theoretical causal model for maintenance performance, which will be used in Chapter 3 for the methodological development for quantifying the maintenance causal model as well as its connections with financial performance considering the coupled effects of physics-of-failure and maintenance performance. This would allow the inclusion of interrelated impacts of underlying physical degradation causal factors and maintenance causal factors on the assessment of the relationships and dependencies between safety and the financial performance of NPPs.

2.2.1 Theoretical Causal Model to Formalize the Direct Causal Path from Safety to the Financial Performance of NPPs

This section offers a causal model to theorize the direct arrow from Node 1 to Node 11 in SoTeRiA (Figure 1-1), making two key contributions:

- Financial consequences of system accidents, system incidents, and occupational accidents of NPPs are included in a unified model. Several scholars previously examined the consequences of major nuclear accidents [55-59, 62]; however, there is no model to consider the combinatory financial consequences of system accidents, system incidents and occupational accidents of NPPs.

- A "theory-based" causal model is created, where the inclusion of accident/incident-induced cost factors and their interactions are justified by literature and, for some cases, by expert opinion. For example, cost elements identified by the recent studies discussed in Subsection 2.1.2.1.1 [55, 58, 62, 66] are utilized to justify the selection of the causal factors and their interrelationships. The proposed causal model provides the theoretical foundation for quantification of the financial consequences of accidents and incidents. In the scope of this causal model, factors affecting the magnitude of accident consequences, such as source terms [97], decontamination techniques [56, 98], and seasonal and contextual factors [63] are not included. These aspects require further research, which will expand the causal model by developing a quantification methodology and advance the Level 3 PRA of NPPs.

The proposed causal model (Figure 2-1) includes six layers of causality, starting from accidents/incidents (Node 1 in SoTeRiA; Figure 1-1) and ending in financial outcome (Node 11 in SoTeRiA; Figure 1-1). Each node in Figure 2-1 represents the total impacts over all periods of time. For example, the human health effects ("HHE" node) include both short- and long-term health effects, such as those resulting from radiation exposure. The formulation of the proposed causal model implicitly captures feedback mechanisms across causal layers, such as health effects during sheltering, decontamination, and decommissioning activities. Explicit consideration of feedback loops requires methodological developments in future research. The following provides theoretical justifications for the selection of factors in each layer of the causal model and for the relationships among the layers.

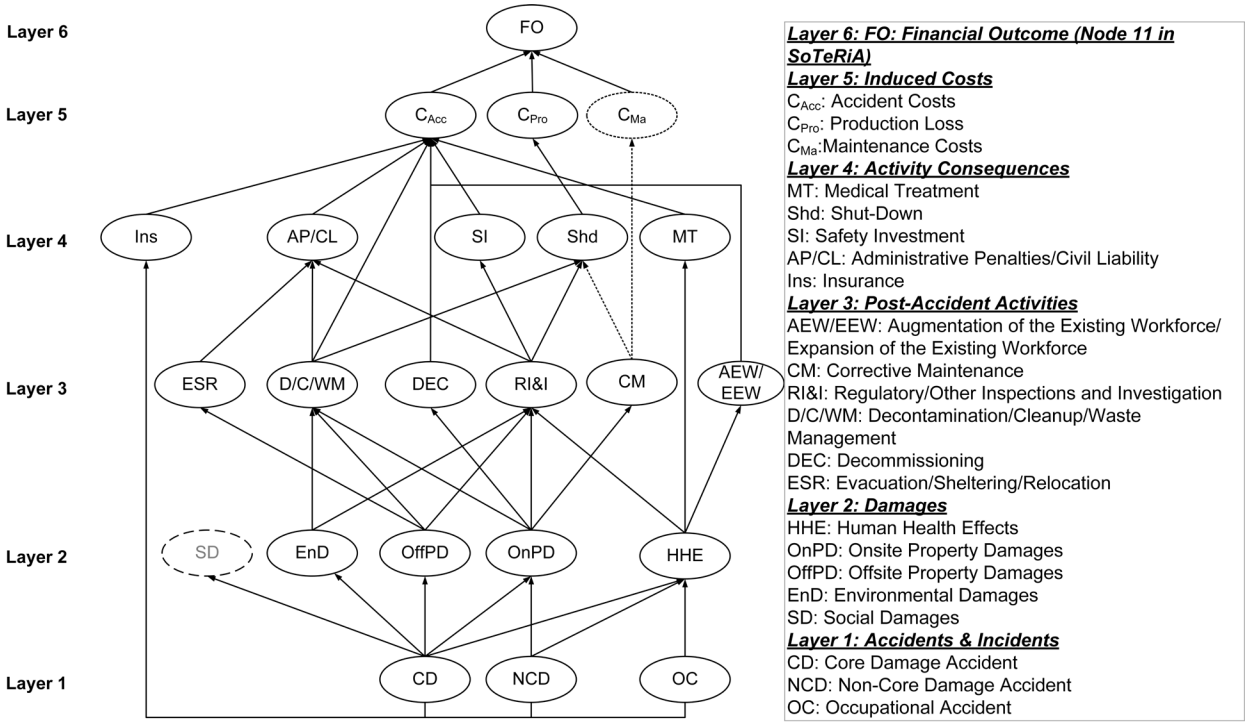


Figure 2-1: Theoretical Causal Model to Formalize the Direct Causal Path from Safety to the Financial Performance of NPPs (Detailed Model of the Direct Arrow from Node 1 to Node 11 in SoTeRiA).

Layer 1 of the causal model (Figure 2-1) focuses on the three accident types discussed in Section 2.1.2.1: (i) a major nuclear accident involving core damage (Node "CD"), with or without potential release of radioactive material, (ii) nuclear accidents/incidents not involving core damage (Node "NCD"), and (iii) occupational accidents (Node "OC").

Layer 2 of the causal model focuses on the potential damages associated with each accident type in Layer 1. Five types of damage are considered: (i) human health effects (Node "HHE"), including injuries and fatalities of involved workers, non-involved workers, and/or the public [60, 62, 99], (ii) onsite property damage (Node "OnPD") [62, 66, 99], (iii) offsite property damage (Node "OffPD") [62, 65, 99], (iv) environmental damage (Node "EnD") [55, 62], and (v) social damage (Node "SD"). While previous studies have highlighted the importance of social damage, including social [54, 55] and moral impacts [54], caused by a major nuclear accident (edge between Nodes "CD" and "SD" in Figure 2-1), the evaluation of how social damage influences the causal factors within different layers of the causal model is left for future work. Some studies considered economic and regional disruptions [59, 62] and suggested considering the impacts of a major accident on the nuclear industry. These impacts are related to other SoTeRiA connections (e.g., from Node 11 to Node 13 in Figure 1-1) and are not the focus of this research.

There are relationships between Layer 1 and Layer 2, as follows:

- Edge between "CD" and "EnD" in Figure 2-1: Released radioactive material following a core damage accident may cause significant environmental damage [55, 62] through radiation-induced effects (short- and long-term) as well as physical damage [62]. For example, the Chernobyl accident killed wildlife within a 10 square km area around the plant site [62].

- Edge between "CD" and "OffPD" in Figure 2-1: Offsite property damages following a major nuclear accident [99] are primarily associated with contamination of crops, livestock, and properties [55, 62], both inside and outside of the interdicted areas, leading to the loss of land use, indirect damages due to lack of property upkeep within the interdiction area, and decreased property values [62].

- Edge between "CD" and "OnPD" in Figure 2-1: A major nuclear accident may also cause significant onsite property damages [99], including physical damage (e.g., resulting from accident progression) and contamination within the NPP site [62].

- Edge between "CD" and "HHE" in Figure 2-1: A major accident can induce human health effects including population's short- and long-term health effects from radiation exposure [49, 55, 60, 62, 100]. The immediate and long-term health effects on plant personnel and external workers supporting plant response [60, 101] should also be included in the "HHE" node in Figure 2-1. Based on the lessons learned from the Fukushima accident, four major hazards for workers at the site should be considered, including radiation, heat, stress, and machine operation and manual handling [102].

- Edge between "NCD" and "OnPD" in Figure 2-1: A non-core damage accident/incident may cause onsite property damage. The severity and types of property damages can differ depending on the type of Initiating Events (IEs). For instance, based on the database developed by Dube et al. [66, 103], the physical damage to the plant following internal flooding and fire events can be significant (tens of millions of dollars), while the physical damage following non-flood events may be minimal.

- Edge between "NCD" and "HHE" in Figure 2-1: A Non-core damage accident/incident may also lead to occupational exposure, affecting worker health [49].

- Edge between “OC” and “HHE” in Figure 2-1: Plant workers may be injured during the conduction of O&M activities under normal conditions. Occupational hazards during maintenance activities may include physical hazards (e.g., heat exposure), physical workload (e.g., working in confined spaces or craning and hoisting operations), and chemical hazards [104-106].

Layer 3 of the causal model (Figure 2-1) identifies potential activities to resolve the damage included in Layer 2; thus, there are relationships between Layers 2 and 3, as follows:

- Edge between “OffPD” and Evacuation/Sheltering/Relocation (Node “ESR”) in Figure 2-1: Offsite damage may affect evacuation decisions by authorities. Other factors (e.g., location of homes relative to the plant, social status) may also affect the evacuation decision by individual and family units to voluntarily evacuate beyond the mandatory evacuation zone [107]. Staffing of local offsite response organizations supports these activities, while additional staffing from other facilities (e.g., emergency operation centers) supports emergency response decision-making [62].

- Edge between “OnPD” and Decommissioning (Node “DEC”) in Figure 2-1: Decommissioning may occur following onsite damages due to an accident or incident with significant damages to an NPP [49]. There were several reactors, in history, that were closed due to damages following accidents and serious incidents in several countries, such as Vandellos Unit 1 in Spain closed following a turbine fire and Bohunice A1 in Slovakia closed following core damage due to a fueling error [108]. The onsite property damages can increase costs of plant decommissioning [62].

- Edge between “OnPD” and Decontamination/Cleanup/Waste Management (Node “D/C/WM”) in Figure 2-1: Cleanup and decontamination activities, such as such as initial decontamination of building surfaces [109], may be required following onsite property damages due to an accident or incident [60] and may generate radioactive waste [62]. Decontamination of a damaged unit may require several years of extended planning and analysis [60]. For example, cleanup of the damaged nuclear reactor following the TMI-2 accident lasted from 1979 to 1993 as several tools for decontamination needed to be newly designed and manufactured [109]. For instance, in the case of the Fukushima accident, the treatment of the site’s contaminated water has become a controversial issue. The fundamental strategy to deal with contaminated water is to eliminate contamination sources, isolate water from contamination, and prevent leakage of contaminated water [110].

- Edge from “OffPD” and “EnD” to “D/C/WM” in Figure 2-1: Following a severe nuclear accident, decontamination, cleanup, and waste management are also required to remedy contaminated offsite property and environment in both restricted areas as well as habitable areas [62]. Disposal of

radioactive waste can be considered as part of decontamination [65]; hence, activities for disposal of radioactive waste are included in this node.

- Edges from the nodes in Layer 2 and Regulatory/Other Inspections and Investigation (Node "RI&I") [111-113] in Figure 2-1: As identified in U.S. NRC Management Directive 8.3, it is the policy of the U.S. NRC to identify the cause of each significant safety event at facilities licensed by the NRC through investigation (e.g., via an incident investigation team) or less formal inspection programs (e.g., via an augmented inspection team or a special inspection team) [114]. One goal of inspection and investigation is to inform corrective actions to prevent the recurrence of similar events [115].

- Edge from "OnPD" to corrective maintenance (Node "CM") in Figure 2-1: Repair and replacement of damaged equipment is one of the main remedial activities required to address onsite property damage [60, 99, 100]. CM node and its impacts on plant shutdown (edge between "CM" and Node "Shd" shown with dotted line in Figure 2-1) as well as maintenance costs (edge between "CM" and Node "C_{Ma}" shown with dotted line in Figure 2-1) are further discussed in Subsection 2.2.2.

- Edge from "HHE" to Augmentation of the Existing Workforce/Expansion of the Existing Workforce (Node "AEW/EEW") in Figure 2-1: Following an incident or occupational accident, injured workers may be temporarily unable or unavailable to carry out their jobs, requiring other workers to absorb the activities of their injured co-workers [43]. The costs of absenteeism depend on the severity of injuries, the number of injured workers, and the duration of workers' absenteeism (i.e., short-term vs. long-term). The short-term absenteeism of injured workers may necessitate the augmentation of the existing workforce or lengthening the working hours of other workers, affecting their productivity. For long-term absenteeism, expansion of the existing workforce can be necessary, requiring the hiring and training of new workers to replace the injured workers [42]. NUREG/BR-0058 highlights that worker productivity, turnover, and training should be considered in cost benefit analysis for NPPs [60].

Layer 4 of the causal model covers consequences resulting from post-accident activities (Layer 3). There are relationships between Layers 3 and 4, as follows:

- Edge between "RI&I" and Administrative Penalties/Civil Liability (Node "AP/CL") in Figure 2-1: Investigation following an accident/incident may lead to civil liability and bring costs for legal counsel, administrative burdens during discovery, settlements, and damage awards, and legal injunctions. As stated in Section 2.1.2.1.1, an organization may also receive regulatory penalties

[67]. In addition, administrative penalties may be levied by federal, state, or local regulatory authorities in the form of fines. Costs associated with lawsuits and trials may affect the liquidity of the company as civil lawsuits can, depending on the severity of an accident, last several years [41].

- Edge from "ESR" and "D/C/WM" to "AP/CL" in Figure 2-1: The NPP may be responsible for several compensation costs, such as the daily cost of compensation for evacuees and short-term relocation costs (edge between "ESR" and "AP/CL" in Figure 2-1) [58]. This can include compensation for voluntary evacuation [116]. The plant operator may also be responsible for costs associated with onsite and offsite decontamination, cleanup, and waste management (edge between "D/C/WM" and "AP/CL" in Figure 2-1) [117].

- Edge from "CM," "RI&I," and "D/C/WM" to Plant Shutdown (Node "Shd") in Figure 2-1: An NPP may remain in the shutdown state after an accident or incident due to investigation activities (imposed by regulators or the internal organization [66]) to identify the root cause of an accident/incident (edge between "RI&I" and "Shd" in Figure 2-1), plant cleanup activities (edge between "D/C/WM" and "Shd" in Figure 2-1), and corrective maintenance activities (edge between "CM" and "Shd" in Figure 2-1).

- Edge between "RI&I" and Safety Investments (Node "SI") in Figure 2-1: The outcomes of investigation by regulators or other organizations may lead to optional or mandated plant safety improvements. The results of the accident investigation may also result in mandatory safety investments across the nuclear industry; for example, a series of post-Fukushima safety enhancements required at U.S. NPPs associated with FLEX, spent fuel pool instrumentation, containment venting systems, seismic and flooding defense, and emergency preparedness [49, 118].

- Edge between "HHE" and Medical Treatment (Node "MT") in Figure 2-1: Accidents and incidents may lead to injuries requiring medical treatments [43, 60, 62] using on-site medical aid or treatment at off-site facilities.

- Edge between "CD/NCD/OC" and Insurance (Node "Ins") in Figure 2-1: Occurrence of an accident or incident may directly affect insurance premiums for an organization. Insurance may cover a portion of the potential impacts of different accident types, which should be considered in estimating costs incurred by the plant following different accident types [119, 120]. In the U.S. nuclear industry, the Price-Anderson Act covers liability claims due to damages and injuries following a commercial nuclear accident. Two tiers of insurance have been established for licensed

reactors: (i) available maximum liability insurance which is carried by each reactor site; and (ii) the nuclear industry self-insurance system (i.e., retrospective premiums). Aside from the mandated insurance coverage for the nuclear industry, nuclear power companies may elect to purchase additional insurance to augment the mandated coverage to cover costs such as property damage, physical loss, and premature decommissioning [120]. Expenses associated with post-accident action (e.g., relocation expenses, cleanup) as well as public liabilities can be covered by the Price-Anderson Act regime until these costs exceed the predefined cap [62].

Shutdowns would lead to production loss (in Layer 5), CM activities would lead to maintenance costs in Layer 5, and the rest of the nodes in Layer 4 and costs associated with "D/C/WM, DEC" and "AEW/EEW" in Layer 3 are mapped to accident costs in Layer 5. The cost elements in Layer 5, which generate NPP Financial Outcome in Layer 6, are utilized for developing the financial analysis module of the I-ERM framework in Chapter 3.

2.2.2 Theoretical Causal Model for the Performance of the NPP Maintenance Program

This subsection develops a theoretical causal model for the NPP maintenance program, i.e., a maintenance unit process model associated with Node 3 in SoTeRiA (Figure 1-1). For NPPs, the literature review in Subsection 2.1.2.2.1 has not identified any existing study that explicitly incorporates maintenance unit work processes into safety and financial performance; thus, the selection of factors and their relationships in the causal model are based on multiple other resources including: (i) a theoretical causal model for aviation maintenance performance [8], (ii) a theory-building process in the data-theoretical methodology [21], (iii) ASME standard for maintenance [121], and (iv) NPP expert opinion. Note that the ASME standard for maintenance refers to the ASME Boiler Pressure Vessel Code Section XI standards, which are only applicable for pressure retaining components. Further research may evaluate whether this standard can be generalized for other types of NPP components.

The target node in this causal model (Figure 2-2) is "Maintenance Program," describing the overall quality of the maintenance program in an NPP. Under the target node, seven causal layers are established and are consistent with phases of maintenance including inspection, diagnosis, repair, and post-repair action. The Structured Analysis and Design Technique (SADT) [8] is used to expand each phase to its direct causal factors including the direct resource/tool, procedure, and personnel in the sublayers. For example, in Figure 2-2, the quality of the factor in Layer 7 depends on the quality of factors in Sublayer 7-1. Using the SADT method, outputs from some nodes are considered as inputs to other nodes, creating a flow of information from the bottom of the causal model up (i.e., from Layer 7 to Layer 1).

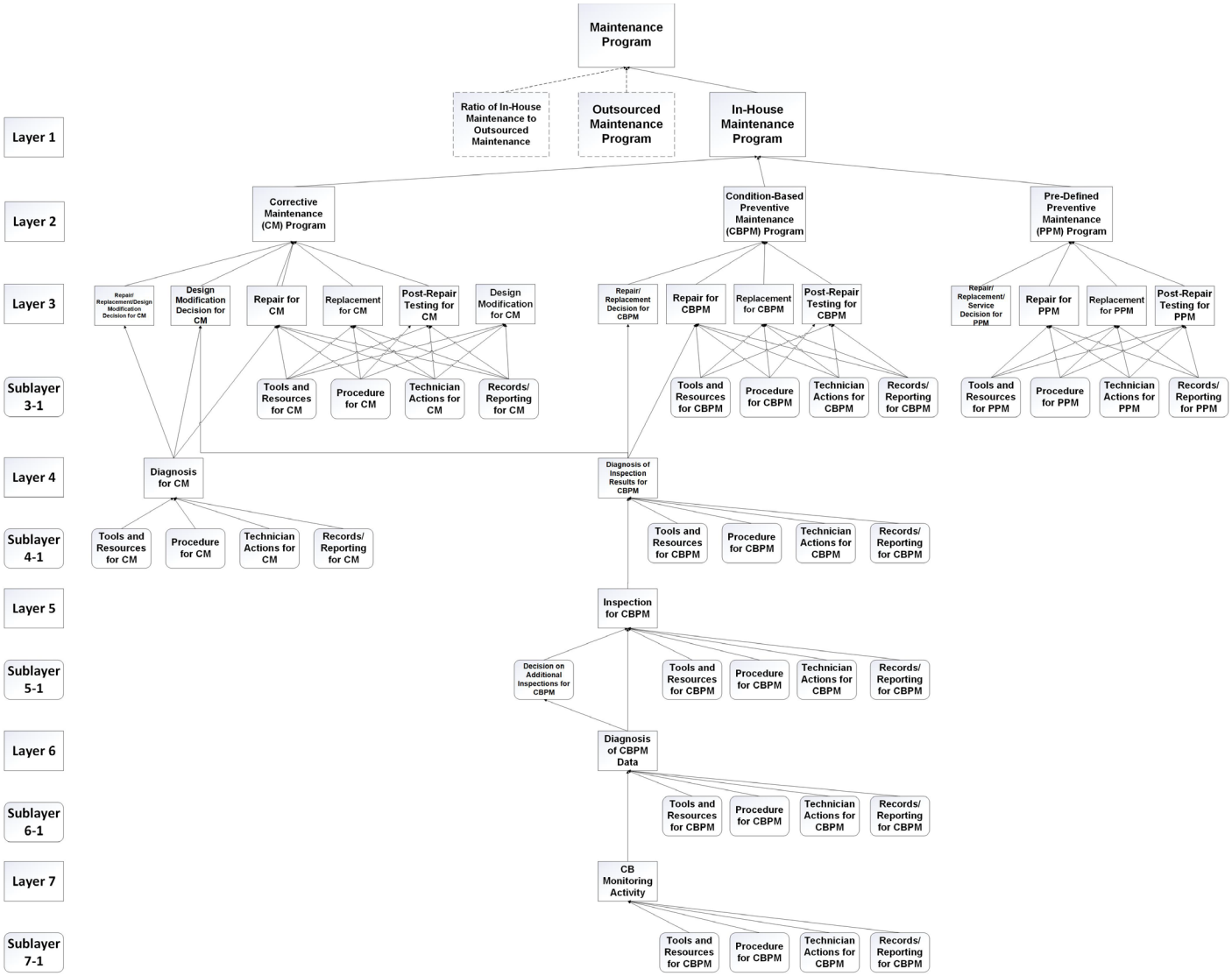


Figure 2-2: Proposed Causal Model for the Quality of the Maintenance Program in NPPs.

Layer 1 consists of three nodes, “Ratio of In-House Maintenance to Outsourced Maintenance”, “Outsourced Maintenance Program”, and “In-House Maintenance Program”. The current stage of development of this model focuses on the in-house maintenance programs; thus, “Ratio of In-House Maintenance to Outsourced Maintenance” and “Outsourced Maintenance Program” – dashed line in Figure 2-2 – are not further opened. Future research is needed to open these nodes to further investigation.

The quality of “In-House Maintenance Program” is influenced by the quality of maintenance program types shown in Layer 2, including: Corrective Maintenance (CM), Condition-Based Preventive Maintenance (CBPM), and the Pre-Defined Preventive Maintenance (PPM) [122]. The overall quality of these programs is influenced by the quality of maintenance activity and decisions shown by the nodes in Layer 3.

In the CBPM Program, three maintenance activities, “Repair for CBPM”, “Replacement for CBPM”, and “Post-Repair Testing for CBPM”, and one maintenance decision “Repair/Replacement Decision for CBPM” are included. The activity “Repair for CBPM” and the decision “Repair/Replacement Decision for CBPM” take inputs from the activity “Diagnosis for CBPM” (in Layer 4 of the causal model) to inform the strategies used for the repair, and the decision to repair or replace the component. In addition, using the SADT method, the three maintenance activities for CBPM in Layer 3 are influenced by four underlying factors including “Tools and Resources” (e.g., availability of a spare part for replacement), “Procedure” (e.g., complexity of written guidelines), and “Technician Actions,” and “Records/Reporting” in Sublayer 3.1. Although “Records/Reporting” can be part of procedures, it is considered as a separate causal factor (in the sublayers) since accurate reporting of the historical maintenance activities can have a significant impact on preventing future maintenance errors. “Technician Actions” describes the technicians’ performance quality. “Tool and Resource” refers to the quality and availability of tools and resources needed for each maintenance activity. The causal factor “Procedure” describes the quality and availability of the procedures for a specific maintenance activity, defined in the corresponding sections of the ASME Section XI standards [121].

In the CM program, four maintenance activities, “Repair for CM”, “Replacement for CM”, “Design Modification for CM”, “Post-Repair Testing for CM”, and two maintenance decisions, “Repair/Replacement/Design Modification Decision for CM” and “Design Modification Decision for CM”, are included. The two decision nodes, and the “Repair for CM” node are influenced by the “Diagnosis for CM” since the information from this activity will influence the repair strategy, or the plant may decide to modify the design of the component to prevent future damage or failure. The “Design Modification for CM” decision node also takes information from the “Diagnosis for CBPM” node since this failure analysis

may similarly influence the decision to modify the design of the component. The four maintenance activities in the CM program are also influenced by the four underlying sublayer causal factors. As an example, under the maintenance activity "Post-Repair Testing for CM", the sublayer factor "Procedure for CM" describes the quality of procedures for post-repair testing such as the clarity and comprehensiveness of the written procedure based on ASME.BPVC.XI.1.IWA-4540.

In the PPM Program, three maintenance activities, "Repair for PPM", "Replacement for PPM", and "Post-Repair Testing for PPM", are included along with one maintenance decision node "Repair/Replacement/Service Decision for PPM". The decision to repair, replace, or service the component is at the discretion of the operators. The three maintenance activities for PPM are similarly influenced by the four underlying sublayer causal factors previously discussed. As an example, under the activity "Replacement for PPM", the sublayer factor "Tools and Resources for PPM" includes the availability and quality of replacement components onsite.

Layer 4 of this causal model consists of "Diagnosis for CBPM" and "Diagnosis for CM". The node "Diagnosis for CBPM" describes the analysis of the information from inspection and thus takes inputs from the node "Inspection for CBPM". The node "Diagnosis for CM" describes the analysis of a failed component and may include a root cause investigation or an engineering review.

Layer 5 of the causal model remains within the CBPM Program and describes the maintenance activity "Inspection for CBPM", which takes inputs from the "Diagnosis of CBPM Data" since the information from the diagnosis activity can inform the inspection type or location. This activity is influenced by the four underlying sublayer factors similar to Layer 4, along with one additional sublayer factor, "Decision on Additional Inspections for CBPM". This decision takes inputs from the "Diagnosis of CBPM Data" to determine whether the component should undergo additional inspections beyond what is required by regulation, based on the trends detected in the performance data.

Layer 6 of the causal model remains within the CBPM Program and describes the maintenance activity "Diagnosis of CBPM Data", which takes inputs from the Layer 7 node "CB Monitoring Activity" to diagnose the logged information. In "Diagnosis of CBPM Data" activity, the performance parameters are tracked and trended to assess whether a component is functioning as intended or if it may be susceptible to failure or damage. This activity is influenced by the four underlying factors in Sublayer 6-1. As one example, the sublayer factor "Technician Actions for CBPM" describes the required actions needed to characterize and interpret the data collected by condition-based monitoring systems which can include the interpretation of various data types such as temperature, pressure, flow, etc. [122]

The Layer 7 node "CB Monitoring Activity" describes the condition-based (CB) monitoring conducted by plant operators. As an example, vibration sensors may be used to log and track information related to the performance of a component. This activity describes the collection and logging of the CB data. Like all other activities, there are four underlying causal factors in Sublayer 7-1. As an example, the sublayer factor "Tools and Resources for CBPM" may include the availability and/or quality of acoustic emission monitors used to monitor flaw or crack progression in NPP components [121].

2.3 Summary

This chapter begins with the review and analysis of literature on interconnections of safety and financial performance (Section 2.1). Previous studies that examined correlations between safety and financial performance are reviewed and analyzed, and the limitations of the correlation analysis are highlighted (Subsection 2.1.1.3) to establish the motivations for model-based approaches. The previous studies related to explicit modeling of underlying causations between safety and financial performance are then reviewed and analyzed (Subsection 2.1.2), focusing on two types of causal paths: (i) direct causal path, representing costs incurred by accidents and incidents; and (ii) indirect causal paths, where safety and financial performance interacts via intra-organizational factors (e.g., organizational culture) and/or external factors (e.g., regulatory environment). For the indirect paths, this research primarily focuses on the maintenance unit process, which is the sharp end of causation in all indirect causal paths associated with O&M activities of NPPs. The insights from the literature review are utilized for two purposes: (a) to justify the contributions of this research; and (b) to identify the factors and their connections in the theory-based causal models.

Compared to the existing studies reviewed and analyzed in Subsection 2.1.2, this research makes two key contributions. First, this research theorizes financial consequences of system accidents, system incidents, and occupational accidents of NPPs and, for the first time, develops a unified causal model including all the three types of financial consequences. The development of the financial causal model is presented in Subsection 2.2.1. The inclusion of accident/incident-induced cost factors and their interactions are justified mainly by literature reviewed in Subsection 2.1.2 and, for some cases, by NPP expert opinion.

Second, this research adds realism to the modeling of (i) the impact of maintenance performance on financial performance, (ii) the impact of maintenance performance on safety, and (iii) the interconnections of safety and financial performance. To achieve these, Chapter 3 develops an Integrated Enterprise Risk Management (I-ERM) methodological framework, capable of quantifying the causations underlying the impact of maintenance performance on both safety and financial performance of NPPs in a unified, multi-level platform. For the component level, a multi-state renewal process model is used to compute reliability

and availability, where maintenance strategies, such as preventive maintenance (PM) based on condition monitoring and in-service inspection and corrective maintenance (CM), are explicitly incorporated. In the previous studies, the maintenance parameters, as inputs to the renewal process model, were quantified by data-driven approaches. The data-driven approaches, however, are challenging especially if (a) no or limited operational data is available for the system being analyzed; or (b) significant modifications such as redesign and maintenance policy updates have been implemented; hence, the existing data are not fully relevant to the current system conditions. The proposed approach in this research addresses this gap by explicitly incorporating the models of maintenance performance and physics-of-failure into the renewal process model.

For the explicit modeling of maintenance performance, this project develops a theory-based maintenance organization causal model (Subsection 2.2.2). In Chapter 3, the maintenance causal model is quantified using a Human Reliability Analysis (HRA)-based method. This contribution helps avoid the reliance on data-driven approaches for the analysis of the safety and financial performance. The explicit modeling of maintenance performance can also add resolution to the modeling of the impact of maintenance performance on safety and financial performance; hence, it helps improve the efficiency of maintenance strategies by providing decision-makers with in-depth quantitative insights at the level of maintenance work processes and human performance. The explicit modeling of maintenance performance can add realism to the modeling of the impact of maintenance performance on safety and financial performance. Additionally, the coupled effects of physics-of-failure and maintenance performance are explicitly incorporated into the modeling of the interconnections of safety and financial performance. In Chapter 4, an advanced physics-of-failure model with higher spatial and temporal resolutions is developed and coupled with the maintenance performance model through the renewal process model. This contribution makes it possible to include the interrelated impacts of underlying physical degradation causal factors and maintenance causal factors on the interrelationships between safety and the financial performance of NPPs.

3. Methodological Developments and Case Study

This chapter develops a unified methodological framework - an Integrated Enterprise Risk Management (I-ERM) framework - to quantify the interrelationships between safety risk and the financial performance of NPPs based on the theoretical bases in Chapter 2. The I-ERM methodological framework can capture the coupled effects of physics-of-failure and maintenance performance (considering human and organizational factors) in a unified platform to quantify the interconnections of safety and financial performance with explicit modeling of the underlying causalities. An illustrative NPP case study (Section 3.2) is implemented to demonstrate the applicability of the I-ERM framework.

3.1 Methodological Developments to Quantify Relationships of Safety and the Financial Performance of Nuclear Power Plants

Subsection 3.1.1 provides an overview of the I-ERM framework, while Subsection 3.1.2 provides a detailed description of individual modules in I-ERM and the interfaces among them.

3.1.1 Integrated Enterprise Risk Management (I-ERM) Methodological Framework

The I-ERM methodological framework (Figure 3-1), developed based on the theoretical bases in Chapter 2, provides a unified computational platform to quantify interconnections between safety and financial performance, considering common causes rooted in maintenance work processes. Within the I-ERM methodological framework (Figure 3-1), safety risk consists of two dimensions: system risk estimated using Probabilistic Risk Assessment (PRA), and occupational safety risk estimated by the occupational health and safety risk assessment (OHSRA). These two dimensions of safety are quantified by the Organizational Safety Risk Assessment (OSRA) module in I-ERM (‘e’ in Figure 3-1). As the scope of safety in this research focuses on system safety, the PRA module is the primary focus from this point forward. Meanwhile, the financial performance of an NPP is quantified by the Financial Analysis module (‘g’ in Figure 3-1) considering both major and minor costs associated with plant operation and production such as O&M costs. At this stage of research, the financial performance model focuses on direct maintenance costs (e.g., material and labor costs) and production loss costs.

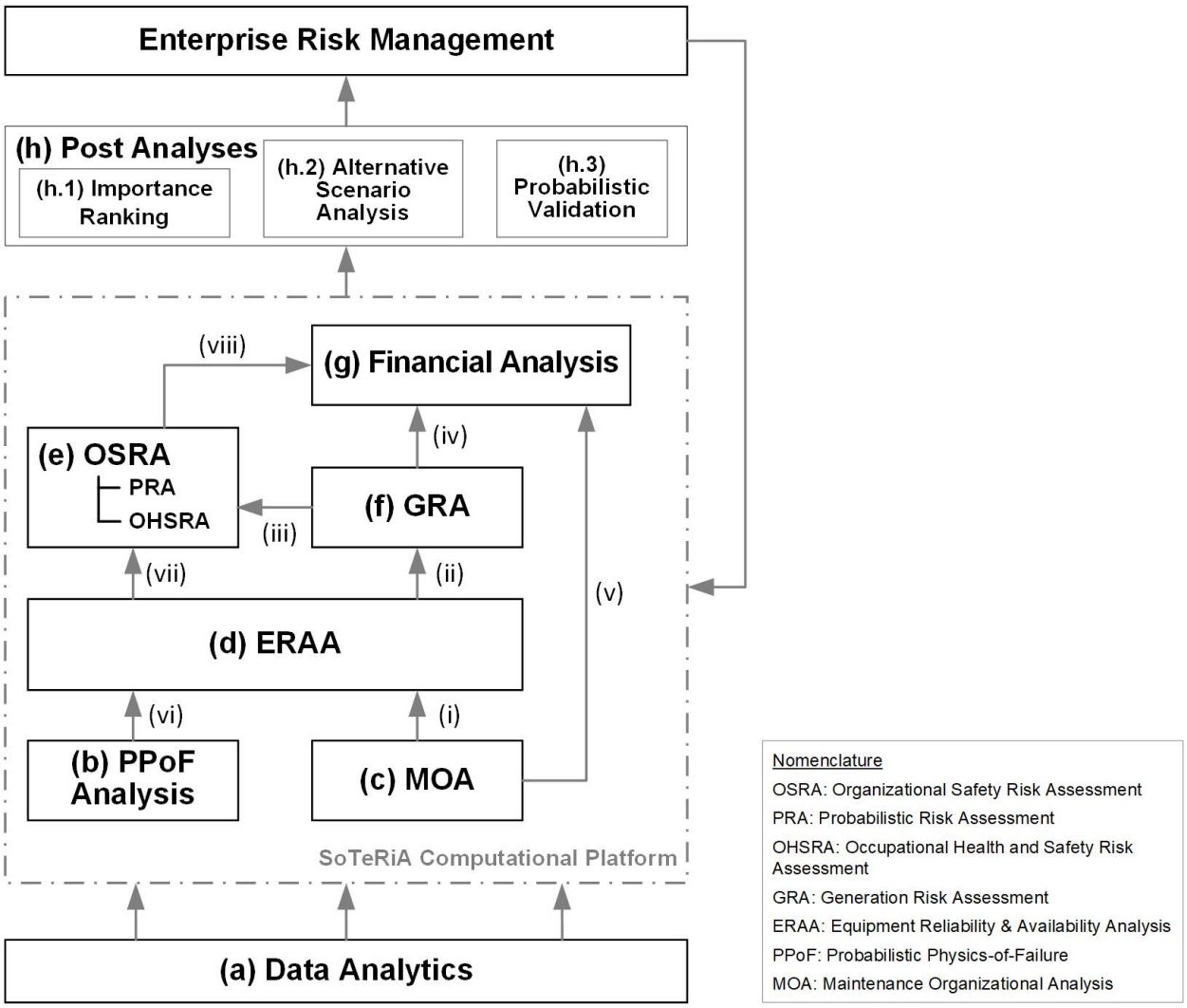


Figure 3-1. Integrated Enterprise Risk Management (I-ERM) Methodological Framework.

The PRA module uses Event Trees (ETs) and Fault Trees (FTs) to estimate plant risk metrics such as Core Damage Frequency (CDF). In addition to safety metrics related to severe accidents, I-ERM considers scenarios which do not lead to severe accidents but still lead to production loss and additional costs. The Generation Risk Assessment (GRA) module ('f' in Figure 3-1) uses systematic modeling techniques similar to those used in PRA to estimate the frequency and duration of production loss events.

The PRA and GRA modules both take inputs related to equipment reliability and availability, computed by the Equipment Reliability and Availability Analysis (ERAA) module ('d' in Figure 3-1) using a renewal process model. For ERAA, the physical degradation inputs are obtained from the Probabilistic Physics-of-Failure (PPoF) Analysis module ('b' in Figure 3-1). The advancements and implementation of the PPoF Analysis module are the focus of Chapter 4 of this report. The maintenance inputs are computed by the

Maintenance Organizational Analysis (MOA) module ('c' in Figure 3-1). MOA uses a Human Reliability Analysis (HRA)-based approach to model and quantify maintenance performance, considering the underlying human and organizational factors.

The Post Analysis module ('h' in Figure 3-1) includes three submodules. The Importance Ranking submodule ('h.1' in Figure 3-1) conducts importance measure analysis [123] to rank underlying physical and human/social contributing factors based on their impact on safety risk and financial performance. The Alternative Scenario Analysis submodule ('h.2' in Figure 3-1) generates alternative O&M strategies which satisfy safety margins and regulatory constraints. To validate the simulation models used in I-ERM, the probabilistic validation submodule ('h.3' in Figure 3-1) is included. The probabilistic validation characterizes and propagates the sources of epistemic uncertainty for each of the models used in I-ERM to generate uncertainty bounds representing the "degree of confidence (or validity)" for the simulation-based estimates of risk and profitability. The probabilistic validation methodology has been reported in previous publications by the PI's research team [13, 124].

The remainder of this section, which includes the PRA, Financial Analysis, GRA, ERAA, and MOA modules, details individual modules and their interfaces in I-ERM. The development of the PPoF module and its connection with other modules is reported in Chapter 4.

3.1.2 Developments and Integration of the I-ERM Modules

This section, including the PRA (Subsection 3.1.2.1), Financial Analysis (Subsection 3.1.2.2), GRA (Subsection 3.1.2.3), ERAA (Subsection 3.1.2.4), and MOA (Subsection 3.1.2.5) modules, describes individual modules of I-ERM. In Subsection 3.1.2.6, the integration among the modules (i.e., how to generate the input-output connection among these modules) is presented. A detailed description of the PPoF Analysis module is provided in Chapter 4 of this report.

In I-ERM, it is necessary to distinguish between the time when the reactor is operating (i.e., operational time) and the time when the reactor is in refueling outage. For this purpose, the following set of notations is used. The set of total time (t) for year i is defined as $\mathcal{T}^{(i)}$, consisting of the union of operational time and refueling outage time.

$$\mathcal{T}^{(i)} = (365(i-1), 365i], \qquad i = 1, \dots, y_{\text{plt}}, \tag{1}$$

where y_{plt} is the plant lifetime [years]. For simplicity, in equation (1), leap years are neglected. The first cycle of operational time ($\mathcal{T}_{\text{o},1}$) occurs from the beginning of the reactor life (t = 0) until the timing of the first refueling outage ($t_{\text{outage},1}$), as defined in equation (2):

$$\mathcal{T}_{\text{o},1} = (0, t_{\text{outage},1}], \tag{2}$$

At $t_{\text{outage},1}$, the first cycle of refueling outage time ($\mathcal{T}_{\text{ro},1}$) for the duration of a refueling outage (Δt_{outage}) occurs, as defined in equation (3):

$$\mathcal{T}_{\text{ro},1} = \left(t_{\text{outage},1}, t_{\text{outage},1} + \Delta t_{\text{outage}}\right] \tag{3}$$

It should be noted that equation (3) consists of planned outages, while unplanned plant shutdown and derate events are modeled in the GRA module (Subsection 3.1.2.3). Subsequent cycles of operation and non-operation time up to y_{plt} years of operation are defined below for the total number of cycles (N_{cycles}) before the end of the reactor life.

$$\mathcal{T}_{\text{o},j} = \left(t_{\text{outage},j-1} + \Delta t_{\text{outage}}, t_{\text{outage},j}\right], \qquad j = 2, \dots, N_{\text{cycles}} \tag{4}$$

$$\mathcal{T}_{\text{ro},j} \in \left(t_{\text{outage},j}, t_{\text{outage},j} + \Delta t_{\text{outage}}\right] \tag{5}$$

As the safety and financial performance are computed for each year in real time, an additional term is defined to represent the set of operational time for year *i,* as shown in equation (6):

$$\mathcal{T}_{\text{o}}^{(i)} = \bigcup_{j=1}^{N_{\text{cycles}}} \left[\mathcal{T}_{o,j} \bigcap \mathcal{T}^{(i)}\right] \tag{6}$$

For the simplicity of mathematical notations, the total set of operational time over all the operating cycles is defined as follows:

$$\mathcal{T}_{\text{o,all}} = \bigcup_{j=1}^{N_{\text{cycles}}} \mathcal{T}_{o,j} \tag{7}$$

3.1.2.1 Probabilistic Risk Assessment (PRA) Module

The PRA module ('e' in Figure 3-1) computes the estimation of the plant safety risk metrics (such as CDF and Large Early Release Frequency [LERF]) using the combination of two types of logical models: (i) ETs that map a set of possible accident scenarios based on the status of safety systems and the end states following an Initiating Event (IE) and (ii) FTs that model logical relationships between the safety systems included in the ET scenarios and smaller pieces of components and equipment comprising those safety systems. For quantification of ETs and FTs, a PRA mission time (t_{PRA}) is assigned, with the assumption that if the event progression has not yielded a catastrophic failure within t_{PRA}, a catastrophic failure will not occur. The combined solutions of the ET/FT structure are used to compute the plant risk metrics (e.g., CDF and LERF). In I-ERM, the frequencies of IEs induced by the production loss events are estimated by the GRA module (Subsection 3.1.2.3) and provided as inputs to the PRA module.

3.1.2.2 Financial Analysis Module

In I-ERM, the Financial Analysis module ('g' in Figure 3-1) computes the financial performance associated with O&M activities of an NPP. The quantitative financial performance model is developed based on the theoretical causal models developed in Section 2.2. The theoretical causal models focus on two paths of the interrelationships between safety and financial performance: (i) a direct causal path, where safety directly impacts the financial performance and (ii) an indirect causal path mediated by intra-organizational factors (e.g., organizational culture; Node 8 in SoTeRiA), external factors (e.g., regulatory environment), and organizational causal mechanisms. The primary focus in this research is to analyze the interrelationships between safety and financial performance induced by the component reliability and availability influenced by physical degradation and maintenance performance. For the direct path, the impact of the non-core-damage risk scenarios, initiated by the failure or unavailability of production systems on the financial performance through production loss, is assessed. For the indirect path, this project focuses on assessing how O&M decisions related to the selection of the maintenance programs and procedures, which should account for the financial performance of the organization as one of the key constraints, can impact plant safety and financial performance. It should be noted that other mechanisms of the direct and indirect paths between safety and financial performance, such as the direct paths due to onsite

and offsite damage from severe accidents and the indirect paths mediated by external factors such as regulatory environments, are not within the scope of this project and are left to future research.

In the Financial Analysis module, the financial performance is measured by a net value.

$$NV_m^{(i)} = B_{\mathrm{Rev},m}^{(i)} - C_{\mathrm{Ma},m}^{(i)} - C_{\mathrm{Acc},m}^{(i)}, \qquad i = 1, \dots, y_{\mathrm{plt}}, \qquad m = 1, \dots, M, \tag{8}$$

where

$NV_m^{(i)}$: Projected net value in year *i*, given the implementation of maintenance strategy *m*;

$B_{\mathrm{Rev},m}^{(i)}$: Projected revenue from electricity production in year *i*, given maintenance strategy *m*;

$C_{\mathrm{Ma},m}^{(i)}$: Projected costs of implementing the maintenance strategy *m* in year *i*;

$C_{\mathrm{Acc},m}^{(i)}$: Projected cost of accidents/incidents in year *i*, given maintenance strategy *m*.

Each term in Equation (8) represents "expected" profit or cost in the sense that it is computed as the expected value of the profit or cost over all possible outcomes, i.e., the sum of the products of profit or cost associated with each possible outcome and its frequency. Among the individual terms on the right-hand side of equation (8), this project focuses on generating a detailed model for $B_{\mathrm{Rev},m}^{(i)}$ and $C_{\mathrm{Ma},m}^{(i)}$, while $C_{\mathrm{Acc},m}^{(i)}$ is left for future research. In other words, the projected costs due to accidents/incidents are not explicitly included in the financial analysis; instead, the safety impact on the plant O&M decision-making, at this stage, is handled by considering the safety and financial risk metrics as two separate (but correlated) decision-making criteria.

Projected revenue: This term is related to the "direct path" from safety to financial performance induced by the production loss scenarios due to failure or unavailability of production systems. Plant trip and derate events due to GRA scenarios can cause production loss, followed by a transient initiating event in PRA, leading to either a non-core damage or core damage end state. The production loss induced by plant unavailability during maintenance activities to repair the production system is the focus of this project, while the production loss induced by post-accident/incident activities to deal with extensive damage to other systems and structures of the plant is left to future research. The projected revenue, with consideration of production loss due to GRA scenarios, is computed by equation (9):

$$B_{\mathrm{Rev},m}^{(i)} = c_{MWh}^{(i)} \left[\int_{t \in \mathcal{T}_{\mathrm{o,all}}^{(i)}} \dot{Q}_{\mathrm{Cap}} dt - \sum\nolimits_{l \in \mathcal{L}_{\mathrm{GRA}}} \left\{ fGRA_{l,m}^{(i)} \cdot Q_{\mathrm{Loss},l,m} \right\} \right], \qquad i = 1, \dots, y_{\mathrm{plt}}, \quad m = 1, \dots, M, \tag{9}$$

$$Q_{\mathrm{Loss},l,m} = \int_{t' \in (0, \Delta t'_{l,m}]} \left(\dot{Q}_{\mathrm{Cap}} - \dot{Q}_{\mathrm{DeCap},l,m}(t') \right) dt', \tag{10}$$

where

$c_{MWh}^{(i)}$: Unit revenue for electricity production [$/MWh] in year *i*;

$\dot{Q}_{\mathrm{Cap}}$: Electricity power capacity [MWe] of the plant; this variable is assumed to be constant over time (i.e., independent of year *i*);

$\mathcal{L}_{\mathrm{GRA}}$: Set of GRA scenarios, assumed invariant over time;

$fGRA_{l,m}^{(i)}$: Frequency of GRA scenario *l*, given the implementation of maintenance strategy *m*, in year *i* (obtained from the GRA module);

$Q_{\mathrm{Loss},l,m}$: Production loss [MWh] due to an occurrence of GRA scenario *l*, given the implementation of maintenance strategy *m*.

$\Delta t'_{l,m}$: Duration of the plant derate/outage event due to GRA scenario *l*, given the implementation of maintenance strategy *m*, including the time to repair, post-repair test, and the ramp-down and ramp-up time; this variable is assumed to be constant over time;

$Q_{\mathrm{DeCap},l,m}(t')$: Time profile of the derated power capacity at time t' after the beginning of the derate/outage event due to GRA scenario *l*, given the implementation of maintenance strategy *m*;

On the right-hand side of equation (9), in the squared brackets, the first term represents the production revenue, assuming that the plant is operating at its full capacity in year *i*, except for the scheduled/planned outage, while the second term represents the production loss induced by unplanned plant shutdown due to the GRA scenarios and the resultant maintenance activities. Among the input parameters in equations (9) and (10), $\mathcal{L}_{\mathrm{GRA}}$, $fGRA_{l,m}^{(i)}$, $Q_{\mathrm{DeCap},l,m}(t')$, and $\Delta t'_{l,m}$ are provided by the GRA module.

Projected maintenance cost: $C_{\mathrm{Ma},m}^{(i)}$ is quantified based on the theoretical maintenance causal model developed in Subsection 2.2.2. In the causal model, the in-house maintenance program is classified into three high-level types of maintenance programs ('Layer 2' in Figure 2-2): corrective maintenance (CM), condition-based preventive maintenance (CBPM), and pre-defined preventive maintenance. In 'Layer 3' of the causal model, each maintenance program is broken down into phases; for instance, the CM program consists of five phases, including repair/replacement and design modification decision, repair, replacement, post-repair testing, and design modification. If diagnosis is required to support the maintenance decision-making and implementation, it is included in 'Layer 4' of the causal model. In 'Sublayer 3-1' and 'Sublayer 4-1,' using the Structured Analysis and Design Technique [8], direct causal factors that can influence the performance of each maintenance phase, such as the resource/tool, procedure, and personnel, are identified.

In the MOA module (Subsection 3.1.2.5), maintenance scenarios are defined as the sequences of maintenance phases and their outcomes (e.g., success or failure). For each maintenance scenario $\mathrm{MS}_{m,\gamma,j}$ ($j = 1, \dots, , J_{m,\gamma}$, where $J_{m,\gamma}$ is the total number of maintenance scenarios for GRA equipment γ under maintenance strategy m) associated with GRA equipment γ under maintenance strategy m, an "expected" maintenance cost $C_{\mathrm{Ma},m,\gamma,j}^{(i)}$ in year i is computed by multiplying the costs associated with causal factors (maintenance phases, tasks, and resources) in the maintenance causal model ('Sublayers 3-1' and '4-1' in Figure 2-2) by the frequency of the corresponding maintenance scenario.

The total projected maintenance cost for $C_{\mathrm{Ma},m}^{(i)}$ is quantified as follows:

$$C_{\mathrm{Ma},m}^{(i)} = \sum_{\gamma \in \{1,\dots,\Gamma\}} \sum_{j \in \{1,\dots,J_\gamma\}} C_{\mathrm{Ma},m,\gamma,j}^{(i)}, \qquad i = 1, \dots, y_{\mathrm{plt}}, \qquad m = 1, \dots, M, \tag{11}$$

The computation of the expected maintenance cost $C_{\mathrm{Ma},m,\gamma,j}^{(i)}$ is related to how to interface the Financial Analysis module with the MOA module and is further described in Subsection 3.1.2.5.

3.1.2.3 Generation Risk Assessment (GRA) Module

The GRA module ('f' in Figure 3-1) provides (i) the plant unavailability scenarios and frequency estimates ($\mathcal{L}_{\mathrm{GRA}}$, $fGRA_{l,m}^{(i)}$, and $Q_{\mathrm{DeCap},l,m}(t')$) as input to the Financial Analysis module; and (ii) the IE frequency as an input to the PRA module ('e' in Figure 3-1). In this research, the FT-based GRA method, developed by the nuclear industry [125-129], is adopted with an advancement in the quantification of the component failure rates and unavailability estimates as inputs to GRA.

In the existing GRA, the GRA cut set frequency is computed as a function of the failure rate and unavailability of the GRA equipment estimated by data-driven approaches. For instance, supposing that a GRA cut set for the 0% event is (G, H). The existing GRA method computes the cut set frequency using equation (12):

$$fGRA^{(i)}_{\{\mathrm{G,H}\},m} = \lambda^{(i)}_{m,\mathrm{G}} \cdot UA^{(i)}_{m,\mathrm{H}} + \lambda^{(i)}_{m,\mathrm{H}} \cdot UA^{(i)}_{m,\mathrm{G}}, \tag{12}$$

where $\lambda^{(i)}_{m,\gamma}$ and $UA^{(i)}_{m,\gamma}$ represent the failure rate and unavailability, respectively, of GRA equipment γ (γ = 1, …, Γ, where Γ is the total number of GRA components) in year i, given the implementation of maintenance strategy m. In the existing GRA, the unavailability of a specific component is approximately computed by equation (13) as a function of failure rate and repair rate:

$$UA^{(i)}_{m,\gamma} = \lambda^{(i)}_{m,\gamma} / \left(\lambda^{(i)}_{m,,\gamma} + \mu^{(i)}_{m,\gamma}\right), \tag{13}$$

where $\mu^{(i)}_{m,\gamma}$ represents the repair rate for GRA equipment γ in year i, given the implementation of maintenance strategy m. In the existing GRA studies and applications, for each GRA component, the failure rate and the repair rate are estimated from historical data, such as test data and service records, using the reliability data analysis technique. Meanwhile, in I-ERM, the estimation of the GRA inputs is advanced using the model-based approach. The failure rate and unavailability of a subset of the GRA components that have significant impact on safety risk and financial performance are modeled by a renewal process model in the ERAA module. The renewal process model is developed for the subset of the GRA equipment considering various damage states of each piece of equipment, where the transitions among the damage states due to physical degradation and maintenance activities are modeled explicitly by the PPoF Analysis and MOA modules. The methodology for integrating ERAA with GRA is described in Subsection 3.1.2.6.

3.1.2.4 Equipment Reliability and Availability Analysis (ERAA) Module

The ERAA module computes the reliability and availability of individual equipment using a renewal process model. In this research, a multi-phase Markov process model [130] is selected due to its capability to capture the effects of maintenance events that occur at random (e.g., condition-based maintenance) as well as the ones that occur at predefined time points (e.g., in-service inspection).

A set of discrete states representing the possible degradation states of the equipment (e.g., 'No damage,' 'Minor damage,' and 'Failure') is defined based on (i) the dominant physical degradation processes and (ii) the practical information about the maintenance of the equipment such as detectability and repairability of each damage state. Let a set of discrete states for GRA equipment γ be $\mathcal{S}_\gamma = \left\{S_{\gamma,1}, S_{\gamma,2}, \cdots, S_{\gamma,N_\gamma}\right\}$, where N_γ is the number of the discrete damage states for component γ.

Two types of transitions between the damage states are considered. The first type represents an event that can occur at random timing and is modeled as a continuous-time Markov process. For this type of transition, the degradation transition rate $\nu_{m,\gamma,s,s'}$ from the state s to another state s' $(s, s' \in \mathcal{S}_\gamma, s \neq s')$ under maintenance strategy m is estimated from the PPoF Analysis module based on the explicit physics-based model (fully developed in Chapter 4), while the repair transition rate $\xi_{m,\gamma,s,s'}$ from state s to state s' $(s, s' \in \mathcal{S}_\gamma, s \neq s')$ under maintenance strategy m is estimated from the MOA module by developing a maintenance performance model (Subsection 3.1.2.5). The second type of transition represents maintenance events that can occur at a predefined discrete timing and is modeled by the transition rule $R_{m,\gamma,s,s'} = \left(\{s, s'\}, \mathcal{T}_{m,\gamma,s,s'}, \pi_{m,\gamma,s,s'}\right)$, where $\{s, s'\}$ is the transition path, $\mathcal{T}_{m,\gamma,s,s'}$ is a set of all predefined timepoints when the transitions occur, and $\pi_{m,\gamma,s,s'}$ is the corresponding transition probability.

The multi-phase Markov model is quantified by solving a set of differential equations and by using a set of initial conditions describing the initial state of the system. If the system is assumed to begin in the 'No Damage' state (represented by the first state S_1) at t = 0, the initial condition is [1, 0, 0, … 0]. To represent the effects of discrete transitions, the delta function δ is used. The multi-phase Markov model is solved using a set of N_γ differential equations with the following generic form, where all transition rates are set to zero during refueling outage time:

If $t \in \mathcal{T}_{\text{o,all}}$,

$$\frac{dP_{m,\gamma,s}}{dt} = \sum_{s' \in \mathcal{S}_{\gamma,-s}} \left[\left(\nu_{m,\gamma,s',s} + \xi_{m,\gamma,s',s}\right) P_{m,\gamma,s'} - \left(\nu_{m,\gamma,s,s'} + \xi_{m,\gamma,s,s'}\right) P_{m,\gamma,s} \right. \\ \left. - \sum_{t' \in \mathcal{T}_{m,\gamma,s,s'}} P_{m,\gamma,s} \delta(t - t') \pi_{m,\gamma,s,s'} + \sum_{t' \in \mathcal{T}_{m,\gamma,s',s}} P_{m,\gamma,s'} \delta(t - t') \pi_{m,\gamma,s',s} \right], \tag{14}$$

Otherwise,

$$\frac{dP_{m,\gamma,s}}{dt} = 0, \qquad s \in \mathcal{S}_{\gamma} \tag{15}$$

where $P_{m,\gamma,s}$ is the probability of state s of component γ under maintenance strategy m, while $\mathcal{S}_{\gamma,-s}$ is the set of the damage states of component γ, except for state s.

3.1.2.5 Maintenance Organizational Analysis (MOA) Module

This research develops the MOA module using an HRA-based method for maintenance analysis. This study, for the first time, interfaces the HRA-based maintenance model with a renewal process model (in ERAA) to explicitly analyze the time-dependent interaction between maintenance activities (including the selection of maintenance strategies and programs and maintenance crew performance) and physical degradation states of individual equipment. This section shows a methodology for developing the MOA module based on the maintenance causal model developed in Figure 2-2.

The MOA module is developed and quantified by the following three steps.

Step 1: Define maintenance programs and activities. This step includes the collection of information related to maintenance of the equipment of interest from various sources of information, such as historical records (e.g., event reports), and existing standards as well as procedures. After collecting the maintenance-related information, the maintenance causal model (Figure 2-2) is used to map the information to the relevant maintenance programs and activities for the selected equipment maintenance. Based on the scope of the analysis, the relevant decision nodes and underlying causal factors in the maintenance causal model are identified.

Step 2: Develop maintenance scenarios. For each type of maintenance program (denoted by γ), maintenance scenarios $\mathrm{MS}_{m,\gamma,j}$ $(j = 1, \dots, , J_{m,\gamma})$ are constructed using an ET technique to model the sequence of maintenance actions and their outcomes. The maintenance ET begins with an IE representing a failure event or other cues for maintenance execution. Following the IE, the maintenance activities, decision nodes, and underlying causal factors in the maintenance causal model (Figure 2-2) are used to construct sequential event-based models for the possible maintenance scenarios. The pivotal events in the maintenance ETs represent the performance (or outcome) of the maintenance activity included in the multiple layers of the maintenance causal model; for instance, inspection, condition monitoring, diagnosis,

and repair of the damaged or failed equipment. For each event sequence (or scenario), the end state consists of a set of (i) the resultant state transition in terms of the discrete damage states in ERAA $\{s_{\text{pre}}, s_{\text{post}}\}_{m,\gamma,j}$ ($s_{\text{pre}}, s_{\text{post}} \in \mathcal{S}_\gamma$), (ii) the conditional probability of the scenario, given the occurrence of the maintenance IE, $\pi_{m,\gamma,j}$, (iii) the duration of the corresponding maintenance scenario after the occurrence of the maintenance IE $\Delta t_{m,\gamma,j}$, and (iv) the expected maintenance cost $C^{(i)}_{\text{Ma},m,\gamma,j}$, i.e., the product of the scenario frequency and the annual maintenance cost associated with the phases, tasks, and resources of the corresponding maintenance scenario.

Step 3: Quantify maintenance scenarios. To quantify the end states in the maintenance ETs, the frequency of the maintenance IE and the conditional probabilities of each pivotal event in the ET are estimated. The quantification of these values is supported by the information collected from the review of the existing regulation and historical records in Step 1 above while focusing on the relevant activities, decisions, and underlying factors from the maintenance causal model (Figure 2-2) which correspond to the pivotal events in the ET. Three primary methods are used to quantify the maintenance IE and pivotal event probabilities: (i) quantification using engineering judgment based on the available historical records and input from a plant expert, (ii) quantification using existing literature, and (iii) quantification using HRA-based techniques such as the Integrated Decision-Tree Human Event Analysis System (IDHEAS) method [16].

3.1.2.6 Integration of Financial Analysis, PRA, GRA, ERAA, and MOA modules

This subsection describes how interfaces among the individual modules (Financial Analysis, PRA, GRA, ERAA, and MOA) are generated in the I-ERM framework. In Figure 3-1, the interfaces among these modules are numbered (i to viii). Among these interfaces, the methodological developments of this project focus on interfaces (i) through (v). Interface (vi) between the PPoF Analysis and ERAA modules is fully developed in Chapter 4 of this report. Interface (vii) between ERAA and PRA is not developed in this project; however, its methodology is essentially the same as that of Interface (ii) between ERAA and GRA. The development of interface (viii) from PRA to Financial Analysis is left to future research.

The key consideration in these interfaces is how to synchronize multiple modules that have different timescales. The timescale of PRA is defined by the PRA mission time, typically 24 hours after the occurrence of the PRA IEs. The timescale of the GRA and Financial Analysis modules is typically one year. The ERAA generates continuous-time prediction of equipment reliability and availability. The timescale of the MOA module is the duration of maintenance activities following the occurrence of the

maintenance IEs. The integration methodology in this subsection establishes a mathematical foundation to address the different timescales among individual modules.

3.1.2.6.1 Interface (i) between MOA and ERAA

Interface (i) between MOA and ERAA is generated by estimating the maintenance inputs to ERAA based on the outputs from MOA, i.e., $\left(\{s_{\text{pre}}, s_{\text{post}}\}_{m,\gamma,j}, \pi_{m,\gamma,j}, \Delta t_{m,\gamma,j}, C^{(i)}_{\text{Ma},m,\gamma,j} \right)$ as shown in Subsection 3.1.2.5.

As stated in Subsection 3.1.2.4, the ERAA module utilizes the multi-phase Markov process model, considering two types of transitions. For the first type of transition that can occur at random timing and is modeled as a continuous-time Markov process, for GRA equipment γ under maintenance strategy m, ERAA requires the maintenance transition rate $\xi_{m,\gamma,s,s'}$. Using the MOA outputs, $\xi_{m,\gamma,s,s'}$ is computed by equation (16):

$$\xi_{m,\gamma,s,s'} = \sum_{j \in \left\{ j \mid \{s_{\text{pre}}, s_{\text{post}}\}_{m,\gamma,j} = \{s,s'\} \right\}} \left(\pi_{m,\gamma,j} \cdot \frac{1}{\Delta t_{m,\gamma,j}} \right). \tag{16}$$

Equation (16) can be interpreted as a weighted average of the mean time to complete the maintenance activities under each maintenance scenario. For the second type of transition that can occur at predefined discrete timing, the transition rule for each path $\{s, s'\}$ $(s, s' \in \mathcal{S}_\gamma)$ requires the predefined time points when the transitions occur, $\mathcal{T}_{m,\gamma,s,s'}$, and the corresponding transition probability, $\pi_{m,\gamma,s,s'}$. $\mathcal{T}_{m,\gamma,s,s'}$ is obtained from the maintenance program specifications for equipment γ under maintenance strategy m. $\pi_{m,\gamma,s,s'}$ is obtained from the MOA outputs by equation (17):

$$\pi_{m,\gamma,s,s'} = \sum_{j \in \left\{ j \mid \{s_{\text{pre}}, s_{\text{post}}\}_{m,\gamma,j} = \{s,s'\} \right\}} \pi_{m,\gamma,j}. \tag{17}$$

In other words, in the case that maintenance activities under strategy m are performed at discrete time points, the transition probability is computed by the sum of the probabilities of the maintenance scenarios leading to the specific transition path.

3.1.2.6.2 Interface (ii) between ERAA and GRA

Interface (ii) between ERAA and GRA is created to estimate the GRA scenario frequencies using the equipment state probabilities $P_{m,\gamma,s}$ computed by ERAA, based on equations (14) and (15). For this purpose, a GRA-ERAA Interface ET is developed to represent the relationship between the GRA scenarios and the status (e.g., operating, under maintenance, and failure) of GRA equipment. The GRA-ERAA Interface ETs model the possible system production states by mapping the possible equipment states to the associated plant-level consequences in terms of production loss. The GRA-ERAA Interface ETs consist of Interface IEs (e.g., unavailability of GRA equipment due to planned/unplanned maintenance), followed by top events defined by the state of other GRA equipment in the system during the repair conducted in response to the Interface IEs. As a hypothetical example to illustrate the concept of the GRA-ERAA Interface ET, suppose that G and H are two critical pieces of GRA equipment and modeled by ERAA. G and H constitute a parallel production system, where each system train supports 50% production.

First, among the GRA scenarios, those that include any of the ERAA-modeled GRA equipment are identified (denoted by $\mathcal{L}'_{\mathrm{GRA}}$, which is a subset of $\mathcal{L}_{\mathrm{GRA}}$). Then, the GRA minimal cut sets, included in $\mathcal{L}'_{\mathrm{GRA}}$, are translated to GRA-ERAA Interface ETs. For the hypothetical example above, the GRA-ERAA Interface ET for the GRA scenarios initiated by unavailability of equipment 'G' is shown in Figure 3-2. The Interface IE involves the unavailability of 'G' due to maintenance, and the scenarios are generated based on the possible states of other GRA equipment in the minimal cut set, namely 'H,' during the repair time of 'G'. The end state of the GRA-ERAA Interface ETs consists of three elements: (i) the frequency of the corresponding GRA scenario, $fGRA^{(i)}_{l',m}$, (ii) the plant power output time profile during the GRA scenario, $\dot{Q}_{\mathrm{DeCap},l',m}(t')$, and (iii) duration of the GRA scenario, $\Delta t'_{l',m}$, where $l' \in \mathcal{L}'_{\mathrm{GRA}}$ and $i = 1, \ldots, y_{\mathrm{plt}}$.

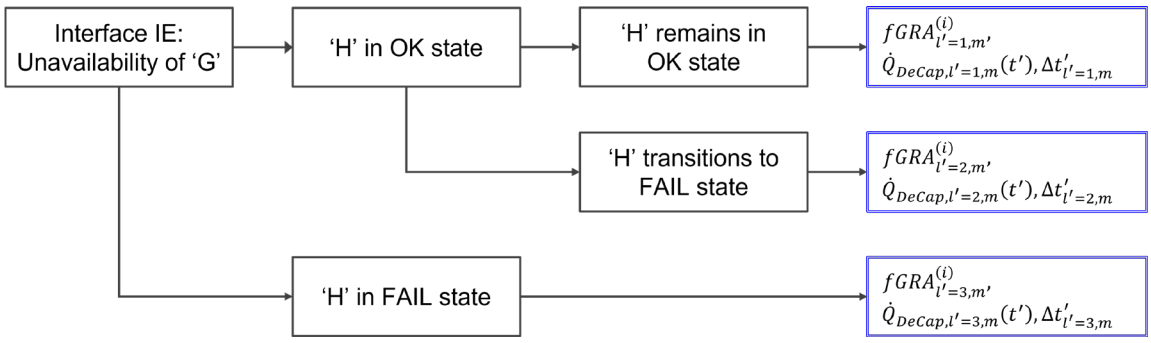


Figure 3-2: An Example of the GRA-ERAA Interface Event Tree.

Since the mission time of GRA is one year, the GRA scenario frequencies are computed for each year, i.e., the average frequencies over the period of one year. To quantify $fGRA_{l',m}^{(i)}$, the following three categories of input parameters are required from the other modules in I-ERM:

- Frequency of the Interface IE: This input is obtained from the ERAA module by calculating the annual expected frequency of the equipment unavailability event. It should be noted that this quantity is equivalent to the Rate of Occurrence of Failure (ROCOF) of the GRA equipment associated with the Interface IE. As an example, in Figure 3-2, the annual expected frequency of the unavailability event for equipment 'G' in year i is computed by

$$\bar{f}_{m,\mathrm{G}}^{(i)} = \int_{t\in\mathcal{T}_{\mathrm{o}}^{(i)}} \sum_{s\in\mathcal{S}_{\mathrm{G,FAIL}}} \sum_{s'\in\mathcal{S}_{\mathrm{G,OK}}} \left(\nu_{m,\mathrm{G},s',s} \cdot P_{m,\mathrm{G},s'}(t)\right) dt, \tag{18}$$

  where $\mathcal{S}_{\mathrm{G,FAIL}}$ and $\mathcal{S}_{\mathrm{G,OK}}$ are the sets of the ERAA damage states for which equipment 'G' is unavailable and available, respectively. $\mathcal{T}_{\mathrm{o}}^{(i)}$ is a set of the operational time during year i as defined in equation (6). $\nu_{m,\mathrm{G},s',s}$ is estimated by the PPoF analysis module developed for equipment 'G' (using the methodology in Chapter 4). $P_{m,\mathrm{G},s'}(t)$ is computed by ERAA developed for equipment 'G.'

- Probability that, upon the occurrence of the Interface IE, other GRA equipment included in the selected GRA MCS is also unavailable. This input is obtained from the ERAA module by calculating the annual expected unavailability of the GRA equipment. As an example, in Figure 3-2, the annual expected unavailability for GRA equipment 'H' is computed by

$$\bar{P}_{m,\mathrm{H=FAIL}}^{(i)} = \frac{\int_{\mathcal{T}_{o-all}^{(i)}} \left\{\sum_{s\in\mathcal{S}_{\mathrm{H,FAIL}}} P_{m,\mathrm{H},s}(t)\right\} dt}{\mathcal{T}_{o-all}^{(i)}}, \tag{19}$$

  where $P_{m,\mathrm{H},s}(t)$ is calculated by the ERAA module developed for equipment 'H.'

- Conditional probability that, during maintenance for the GRA equipment associated with the Interface IE, the other GRA equipment in the selected GRA MCS transitions to the unavailable states, given that it is in the available states upon the occurrence of the Interface IE. This quantity can be computed (approximately) by multiplying the transition rates from the available states to the

unavailable states with the duration of the maintenance activities for the GRA equipment causing the Interface IE. As an example, in Figure 3-2,

$$\bar{P}^{(i)}_{m,\mathrm{H,OK}\rightarrow\mathrm{FAIL}} = \sum_{s\in\mathcal{S}_{\mathrm{H,FAIL}}}\sum_{s'\in\mathcal{S}_{\mathrm{H,OK}}}\left(\nu_{m,\mathrm{H},s',s}\cdot\Delta t'_{l'=2,m}\right), \tag{20}$$

where $\mathcal{S}_{\mathrm{H,FAIL}}$ and $\mathcal{S}_{\mathrm{H,OK}}$ are the sets of the ERAA damage states for which equipment 'H' is unavailable and available, respectively. $\nu_{m,\mathrm{H},s',s}$ is obtained from the PPoF Analysis module for equipment 'H' (using the methodology in Chapter 4), while $\Delta t'_{l'=2,m}$ is obtained from the GRA module.

3.1.2.6.3 Interface (iii) between GRA and PRA

For interface (iii) between GRA and PRA, this research considers the scenarios where the production loss events in GRA trigger the PRA IEs. To model these scenarios, the PRA IE frequencies are computed by using the GRA outputs, leveraging the technique developed by Kee et al. [131]. The total frequency of the GRA scenarios leading to unplanned plant shutdown (i.e., 0% production state) is used as the transient IE frequency in the PRA module.

3.1.2.6.4 Interface between GRA and Financial Analysis

To generate interface (iv) between GRA and Financial Analysis, the outputs from the GRA-ERAA Interface ETs are directly utilized in the Financial Analysis module to compute the projected revenue using equations (9) and (10). $\dot{Q}_{\mathrm{DeCap},l',m}(t')$ and $\Delta t'_{l',m}$, computed by the ERAA-GRA Interface ETs for each GRA scenario $l'\in\mathcal{L}'_{\mathrm{GRA}}$ and in each year i ($i=1,\dots,y_{\mathrm{plt}}$), are used as inputs to equation (10). $fGRA^{(i)}_{l',m}$ from the ERAA-GRA Interface ETs are used as input to equation (9). It should be noted that the mapping between the GRA scenarios in the end states of the ERAA-GRA Interface ETs, $l'\in\mathcal{L}'_{\mathrm{GRA}}$, and those in the GRA module, $l\in\mathcal{L}_{\mathrm{GRA}}$, may be needed by matching the GRA cut sets and their associated production loss consequences.

3.1.2.6.5 Interface (v) between MOA and Financial Analysis

The interface (v) between MOA and Financial Analysis is generated by using the expected maintenance cost $C^{(i)}_{\mathrm{Ma},m,\gamma,j}$, computed as one of the outputs of the maintenance ET quantification in Subsection 3.1.2.5,

as an input to the projected maintenance cost calculation in the Financial Analysis module using equation (11).

3.2 Illustrative Case Study Implementation of the I-ERM Framework

In this section, an illustrative case study from an NPP is shown to demonstrate the implementation of the I-ERM framework with the primary focus on the PRA, Financial Analysis, GRA, ERAA, and MOA modules as well as on their interfaces (i through v).

3.2.1 Case Study Description

An illustrative case study assumes a plant consists of a production system that generates electricity outputs and a protection system required for preventing catastrophic failure (i.e., core damage) when a transient occurs. The production system (Figure 3-3) has three states in terms of the power outputs: full (100%), 50%, and 0%. The 0% production state leads to a transient leading to a PRA IE. To prevent the consequential event and catastrophic outcomes, the protective system needs to function properly. The production system (Figure 3-3) includes four blocks, consisting of two redundant pump trains (Blocks 2 and 3) and two valve trains including suction and discharge valves (Blocks 1 and 4). Each pump train contains four components, including a pump (P), pump prime mover motor (M), motor operated valve (V), and valve prime mover (O). The valve trains consist of two components, including valve (V), and valve prime mover (O). The pump failure mode of concern is "fails to run." For valve trains (Blocks 1 and 4), "fails closed" represents the functional failure mode of concern.

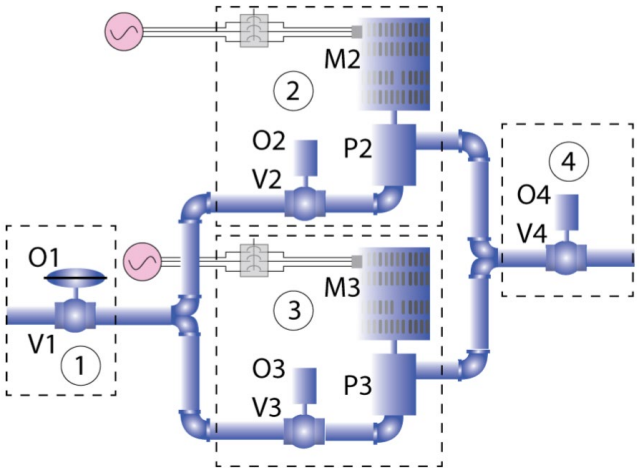


Figure 3-3: Illustration of Hypothetical Production System.

For this case study, the two pumps in the production system (P_2 and P_3) are modeled by ERAA, while the other pieces of GRA equipment are quantified using the failure rates and repair rates, shown in Table 3-1, obtained from historical data in NUREG/CR-6928 [132] and expert judgment. The two pumps (P_2 and P_3) are selected for the detailed modeling in the ERAA module since they are the most active components in the pump train and, therefore, are typically subjected to maintenance more regularly than are other types of equipment.

Table 3-1: Failure rate (λ) and repair rate (μ) of GRA equipment in the production system. Ci: components, FM: functional failure modes, FC: fails to close, and FTR: fails to run.

Train	C_i	FM	λ [hr^{-1}]	μ [hr^{-1}]
Pump i = 2,3	Pi	FTR	Modeled by ERAA (Subsection 3.2.2.4)	
	Oi	FC	2.50E-06	0.037
	Vi	FC	5.00E-07	0.056
	Mi	FTR	1.80E-06	0.024
Valve 1	O1	FC	2.00E-08	0.033
	V1	FC	2.00E-08	0.067
Valve 4	O4	FC	2.00E-08	0.033
	V4	FC	2.00E-08	0.067

If failures within the production system lead to the 0% production state, leading to a transient, the protection system (Figure 3-4) is necessary to operate in order to avoid core damage. If either of the protection system valve trains in the suction or discharge headers fails, the protection system will fail to operate. While the valve in the discharge header (V8 in Figure 3-4) normally remains closed to avoid inadvertently pumping into the downstream system or to prevent backflow into the supply tank, the valve in the suction header (V5 in Figure 3-4) is normally held open to ensure the readiness of the system and also functions as a second prevention against backflow into the tank. Table 3-2 shows the failure modes (FM), failure rate (λ), and repair rate (μ) for each component of the protection system. The failure probabilities in the 24-hour PRA mission time, assuming one demand for each component, are estimated based on NUREG/CR-6928 [132].

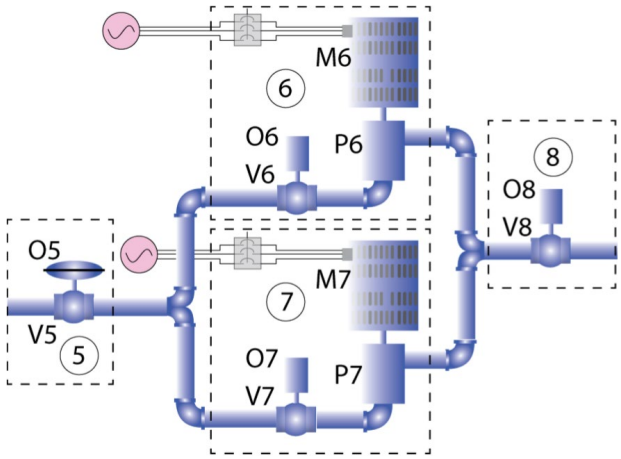


Figure 3-4: Illustration of Hypothetical Protection System.

Table 3-2: Failure probability in 24-hour mission time of components in the protection system. FM: functional failure mode, FC: fails to close, FTS: fails to start, and FTR: fails to run.

Train	Components	FM	Probability
Pump $i = 6,7$	O_i	FC	6.00E-05
	V_i	FC	1.20E-05
	M_i	FTS	1.16E-03
	M_i	FTR	4.32E-05
	P_i	FTS	3.33E-04
	P_i	FTR	1.01E-04
Valve 5	O_5	FC	2.40E-05
	V_5	FC	4.80E-05
Valve 8	O_8	FC	4.80E-05
	V_8	FC	2.40E-05

3.2.2 Case Study Implementation

Subsections 3.2.2.1 through 3.2.2.5 describe the developments of individual modules for the case study: PRA (3.2.2.1), Financial Analysis (3.2.2.2), GRA (3.2.2.3), ERAA (3.2.2.4), and MOA (3.2.2.5). Subsection 3.2.2.6 shows the interfaces among these individual modules for the case study focusing on the parts directly relevant to the methodological developments in this research.

In this subsection, the set of time notations introduced in Section 3.1.2 is utilized, while the other time sets are also defined: a set of normal in-service inspection times ($\mathcal{T}_{\text{NISI}} = \{t_{NISI,1}, \dots, t_{NISI,N_n}\}$) for a total

of N_{n} normal in-service inspections, and a set of overhaul in-service inspection times ($\mathcal{T}_{\mathrm{OISI}} = \{t_{OISI,1}, \dots, t_{OISI,N_o}\}$) for a total of N_{o} overhaul in-service inspections.

3.2.2.1 PRA Module for the Case Study

The PRA module uses the combination of ETs and FTs. As shown in Figure 3-4, the protection system consists of four blocks, including two parallel pump blocks (Blocks 6 and 7) and two valve blocks (Blocks 5 and 8). The ET logic (Figure 3-5) considers these blocks as the top events. The split fraction for each top event is calculated using the FTs in Figure 3-6. The mission time of the protection system is assumed to be 24 hours. The total frequency of the core damage scenarios is computed using the Riskman® software [133].

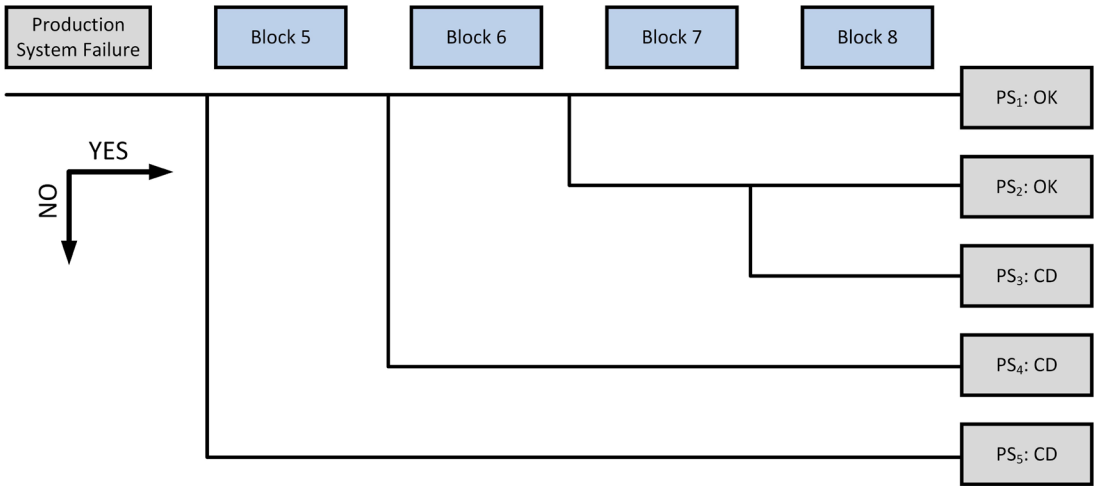


Figure 3-5: PRA event tree for the protection system, where OK: success and CD: core damage.

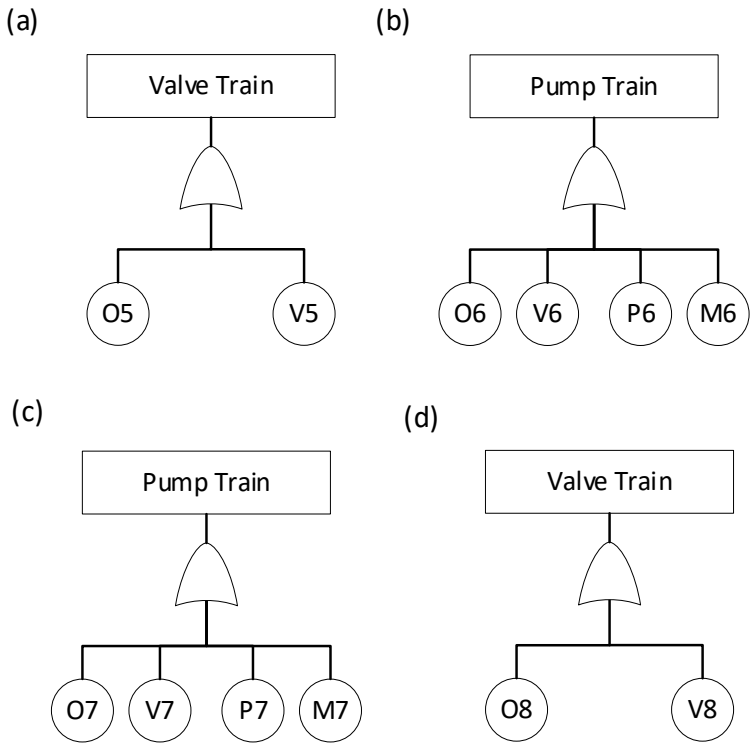


Figure 3-6: Protection system fault trees for (a) valve train in Block 5, (b) pump train in Block 6, (c) pump train in Block 7, and (d) valve train in Block 8.

3.2.2.2 Financial Analysis Module for the Case Study

The financial performance of the plant O&M is quantified using the financial analysis model in Subsection 3.1.2.2. The plant capacity ($\dot{Q}_{\text{Cap}}$) in this case study is assumed to be 1,000 MWe, and the unit revenue for electricity production ($c_{MWh}^{(i)}$) is assumed to be \$30 per MWh.

3.2.2.3 GRA Module for the Case Study

The GRA FT of the hypothetical production system (Figure 3-3) is shown in Figure 3-7. The basic events in the GRA FT represent the equipment in the production system. "Flag events" ("0%", "50%") are utilized so that system operational states are included explicitly in the GRA minimal cut sets. As shown in Figure 3-8, each block of the production system is further modeled by a fault tree. The GRA cut set frequencies are calculated using the failure rate and repair rate data for the components found in Table 3-1, while the two pumps in the production system (P2 and P3) are modeled using a renewal process model in the ERAA module.

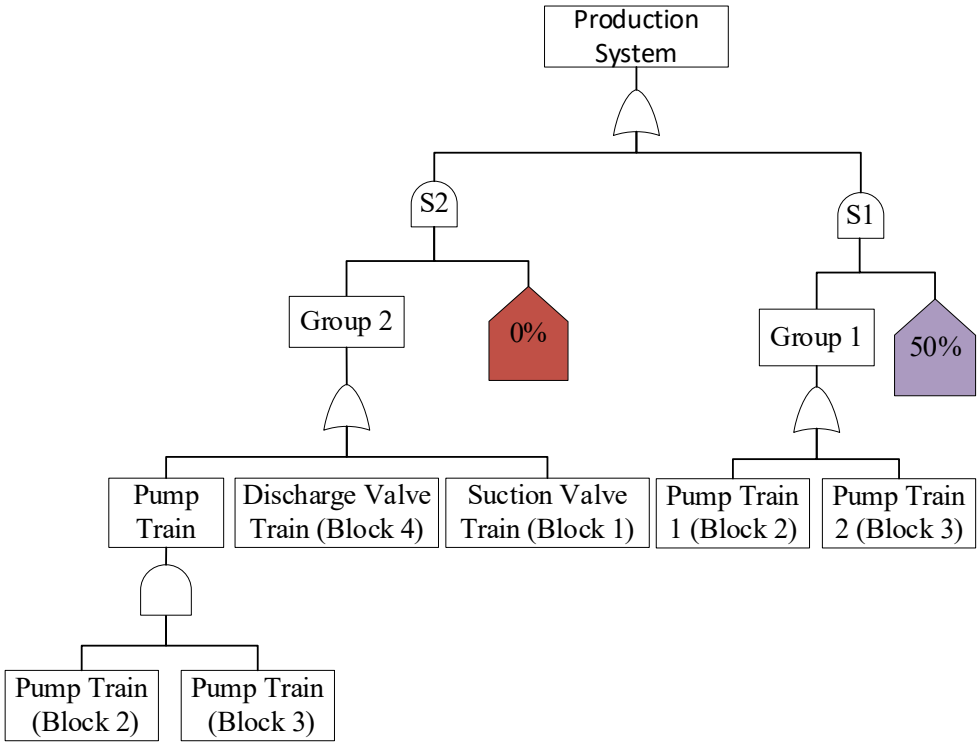


Figure 3-7: GRA fault tree for the production system.

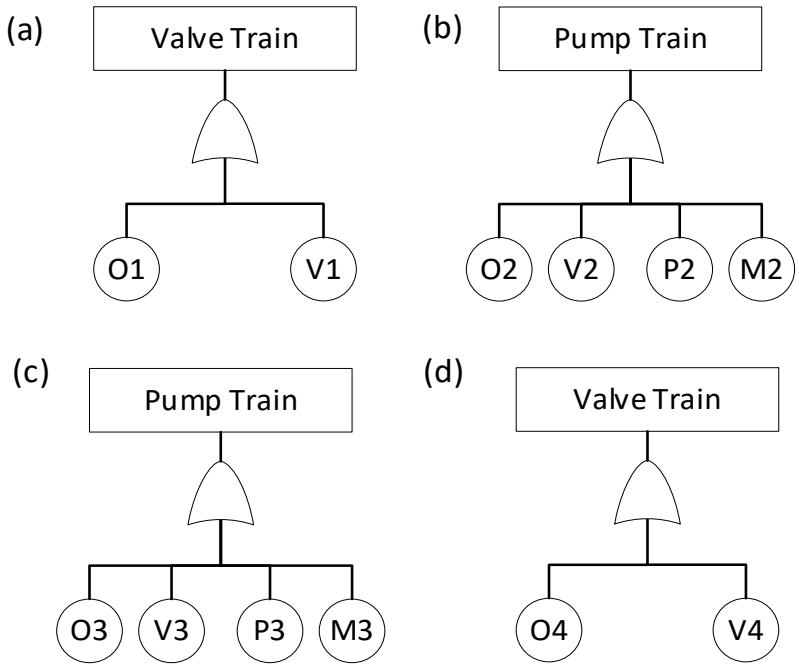


Figure 3-8: Fault trees for GRA systems: (a) Valve Train in Block 1, (b) Pump Train in Block 2, (c) Pump Train in Block 3, and (d) Valve Train in Block 4.

3.2.2.4 ERAA Module for the Case Study

For the pumps (P_2 and P_3) in Blocks 2 and 3 of the production system, a four-state multi-phase Markov process model (Figure 3-9) is developed, where each pump can be in a Success state (S), Damaged state (D), Condition-based Maintenance state (CBM), or Failure state (F). The multi-phase Markov model consists of two phases, the Operational Phase, and the In-Service Inspection Phase. In the Success state, the pump operates properly and without risk of entering the Failure state. The pump will, however, transition to the Damaged state with the transition rate (φ) due to physical degradation. While the pump is in the Damaged state, the pump still operates properly, but due to the physical degradation, if operation continues, the pump is at risk of entering the Failure state. The Damaged state is not self-evident, but the component can transition from the Damaged state to a Maintenance state as a result of online monitoring that may lead the component to enter the Condition-based Maintenance state, where the component is free of physical degradation but may transition to the Success state following a successful repair, or back to the Damaged state following an unsuccessful repair. From the Damaged state, the component may also transition to the Failure state with a transition rate (ρ) due to the physical degradation. From the Failure state, the component will undergo repair/replacement and will transition to the Success state or the Damaged state, dependent on the performance of the repair/replacement activities.

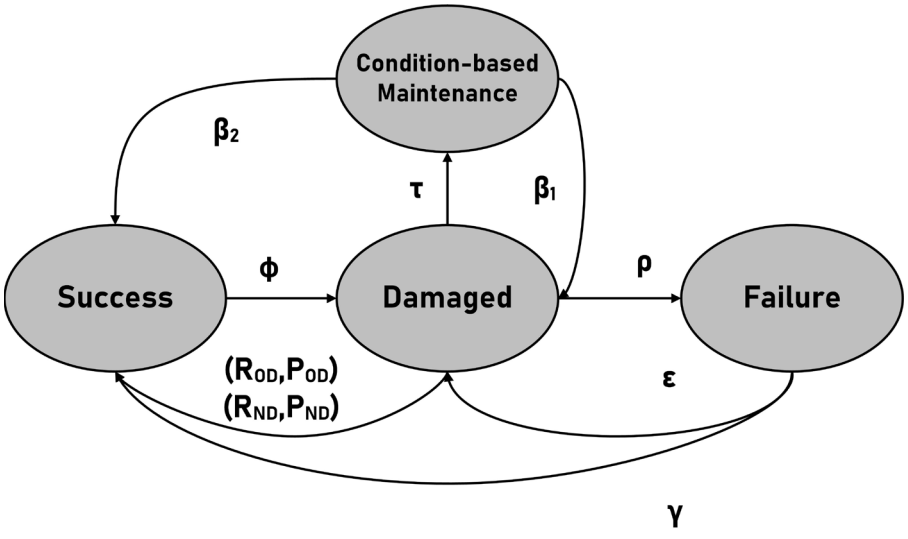


Figure 3-9: Multi-Phase Markov Process Model for Each Pump in the Production System.

The Operational Phase can be modeled as a continuous-time Markov model with transition rates related to maintenance and physical degradation. The maintenance activities during refueling outages cause discontinuities in the Operational Phase. These discontinuities are modeled in the In-Service Inspection Phase, which includes normal and overhaul inspections to detect pump damage during refueling outages.

The outcome of discontinuities from maintenance events is modeled as a reallocation of the state probabilities corresponding to the specific maintenance activity and a re-initialization of the Operational Phase. This re-initialization is modeled by a delta function, which models both the timing and impact of the maintenance events. To model the ISI Phase, each transition that may occur during the refueling outages is assigned a transition probability and transition rule. Two possible transition types are included in the ISI Phase for the case study: (i) normal inspection and repair for pump damage, and (ii) overhaul inspection and repair for pump damage. To define the rule associated with each transition, the timing when the transition may occur, the state the component must be in at the time when the transition may occur, and the end state following the transition are required. To define the transition related to normal inspection for pump damage during refueling outages (R_{ND}), the transition occurs at the timing of normal inspections, defined as $t = t_n$ for a total of N_n normal inspections where ($n = 1, \dots N_n$). The component must be in the Damaged state at $t = t_n$ for the transition to occur, where the component will transition to the Success state with the transition probability P_{ND}. For the second transition, the maintenance related to overhaul inspection and repair will occur at the timing of overhaul inspections, defined as $t = t_o$ for a total of N_o overhaul inspections where ($o = 1, \dots N_o$). The component must be in the Damaged state at $t = t_o$ for the transition to occur, when the component will transition to the Success state with the transition probability P_{OD}.

To solve the multi-phase Markov process model, a vector defining the time-dependent state probabilities of the multi-phase Markov process model is defined as [*S(t)*, *D(t)*, *CBM(t)*, *F(t)*] where the corresponding states are Success, Damaged, Condition-Based Monitoring, and Failure. The pump is assumed to be free of manufacturing defects at the beginning of its lifetime and thus begins in the Success state with certainty with initial conditions [1, 0, 0, 0]. The multi-phase Markov process model is solved from the beginning of the reactor lifetime ($t = 0$) to the expected end of reactor lifetime ($t = 60$ years) for both operational time and non-operational time, as shown in the equations below.

If $t \in \mathcal{T}_{o-all}$,

$$\frac{dS(t)}{dt} = -\varphi S(t) + \beta_2 CBM(t) + \gamma F(t) + \sum_{t' \in \mathcal{T}_{\mathrm{NISI}}} D(t)\delta(t - t')P_{ND} + \sum_{t' \in \mathcal{T}_{\mathrm{OISI}}} D(t)\delta(t - t')P_{OD} + \sum_{t' \in \mathcal{T}_{\mathrm{NISI}} \cup \mathcal{T}_{\mathrm{OISI}}} F(t)\delta(t - t')(1 - HEP_{FR}), \quad (21)$$

$$\frac{dD(t)}{dt} = \varphi S(t) - (\rho + \tau)D(t) + \varepsilon F(t) + \beta_1 CBM(t) - \sum_{t' \in \mathcal{T}_{\text{NISI}}} D(t)\delta(t - t')P_{ND} - \sum_{t' \in \mathcal{T}_{\text{OISI}}} D(t)\delta(t - t')P_{OD} + \sum_{t' \in \mathcal{T}_{\text{NISI}} \cup \mathcal{T}_{\text{OISI}}} F(t)\delta(t - t')HEP_{FR} \quad (22)$$

$$\frac{dCBM(t)}{dt} = \tau D(t) - (\beta_1 + \beta_2)CBM(t), \quad (23)$$

$$\frac{dF(t)}{dt} = \rho D(t) - (\gamma + \varepsilon)F(t) - \sum_{t' \in \mathcal{T}_{\text{NISI}} \cup \mathcal{T}_{\text{OISI}}} F(t)\delta(t - t'). \quad (24)$$

Otherwise,

$$\frac{dSu(t)}{dt} = \frac{dD(t)}{dt} = \frac{dCBM(t)}{dt} = \frac{dF(t)}{dt} = 0, \quad (25)$$

Table 3-3 lists the values of transition rates used in this case study application. At this stage of research, the physical degradation transition rates are estimated based on engineering judgment and generic pump failure data and using the assumption that damage to the pump and failure occur due to bearing failure. In the full implementation of the I-ERM framework, as developed and implemented in Chapter 4, the physical degradation transition rates are estimated by the PPoF Analysis module. The maintenance transition rates are estimated based on the MOA outputs (Subsection 3.2.2.5) using the interface methodology in Subsection 3.1.2.6.

Table 3-3: Transition Rates used for Quantification of the continuous-time Markov Model.

Transition Path/Parameter	Symbol	Value [yr^{-1}]
Success State to Damaged State	φ	8.67E-2
Damaged State to Condition-based Maintenance State	τ	1.04E+1
Damaged State to Failure State	ρ	2.63E+0
Condition-based Maintenance State to Damaged State	β_1	3.65E+0
Condition-based Maintenance State to Success State	β_2	6.94E+1
Failure State to Success State	γ	4.62E+1
Failure State to Damaged State	ε	2.43E+0

3.2.2.5 MOA Module for the Case Study

The structure of the maintenance models in the MOA module for this case study are derived from the paths of influence and structure of the maintenance causal model presented in Subsection 2.2.2, existing literature, and regulatory standards. The maintenance causal model describes the overall quality of the maintenance program and gives the underlying factors which influence the maintenance program quality. Maintenance models for two Level 2 Nodes in Figure 2-2, including "Corrective Maintenance Program" and "Condition-Based Preventive Maintenance Program," are developed. The nodes and paths of influence from the maintenance causal model inform the structure of the maintenance models for MOA.

Maintenance ETs, involving each maintenance strategy, are developed to map the possible maintenance scenarios which may occur. Quantification of the MOA maintenance models occurs by quantifying maintenance parameters from the models in one of three ways: (I) parameters quantified using a combination of engineering judgment and input from a plant expert, (II) parameters derived from the existing literature related to pump maintenance [134] and human error during the repair process [135], and (III) parameters quantified using the IDHEAS HRA method [136]. Square brackets are used to denote the corresponding Group for each parameter listed below.

For the condition-based maintenance (Figure 3-10), two primary pump inspection strategies to detect pump damage prior to failure are considered: (i) online condition-based maintenance occurring during operation, and (ii) preventive maintenance through ISI during refueling outages. For online condition-based maintenance, condition-based monitoring techniques, such as acoustic monitoring of pump vibration, are used to track the pump performance characteristics (e.g., pump flow, shaft vibration). Typically, the pump performance characteristics are tracked and logged on a monthly basis [134]. In this analysis, it is assumed that all damage to the production system pump will affect the pump performance to a level that could be detected by the condition-based monitoring systems. It is also assumed that the pump will not fail due to a sudden failure mechanism but may fail, over time, due to the propagation of a dominant physical degradation mechanism. In this analysis, the physical degradation rates for production system pumps are estimated based on existing failure rate data for bearing failure.

Maintenance-related scenarios 1 to 6, associated with condition-based maintenance of the production system pump, are shown in Figure 3-10. In this figure, the IE "Pump in Damaged state during operation" is used for all the maintenance scenarios. The maintenance ETs have three possible end states: (i) successful repair (scenarios 1 and 5), (ii) unsuccessful repair, where human error during the repair causes the pump to remain in the damaged state (scenarios 2 and 6), and (iii) no repair occurs and the pump remains in the damaged state (scenarios 3 and 4). The end state includes the resultant state transition path (in relation to

the ERAA module) and the associated expected cost. As an example, in the first scenario of Figure 3-10, the pump begins in the Damaged state, then transitions to the Condition-based Maintenance state, and finally to the Success state.

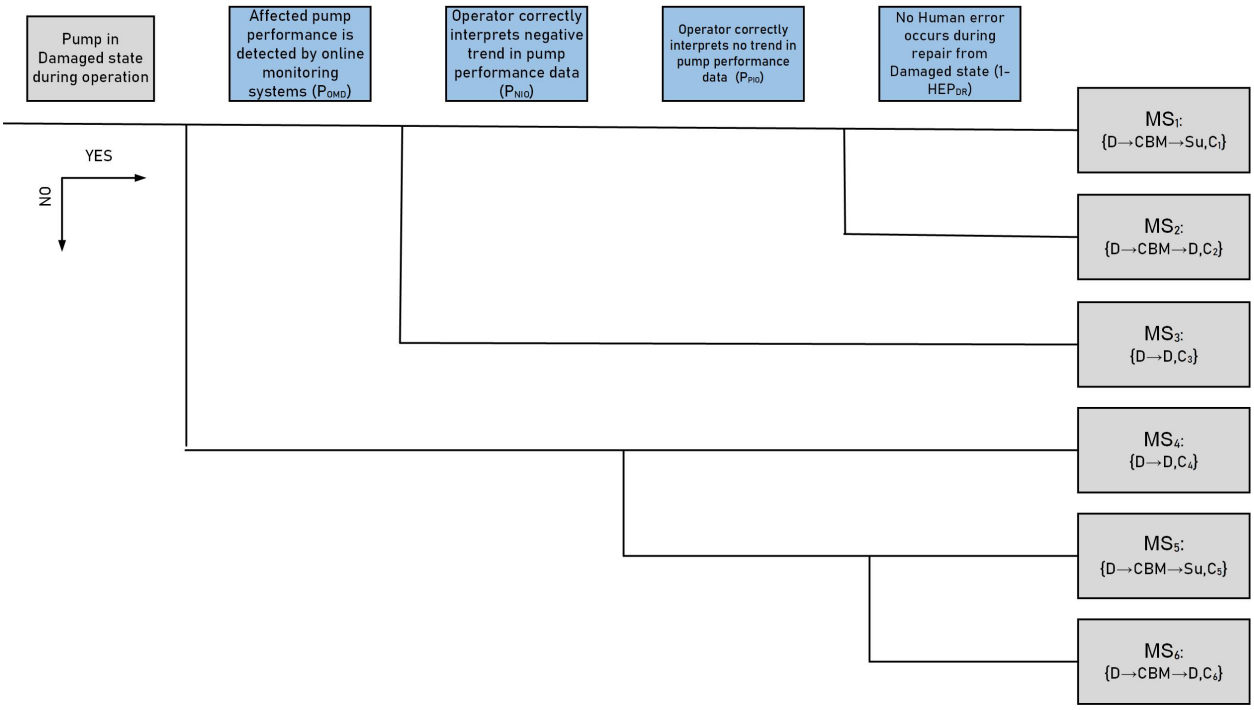


Figure 3-10: Maintenance Event Tree for Production System Pump during Operation as a Result of Condition-based Maintenance.

Maintenance scenarios 1 to 6 are quantified using the following maintenance input parameters:

- Probability that negative trends in pump performance data are detected by conditional monitoring systems (P_{OMD}) [I]. This case study assumes perfect reliability of condition-based monitoring systems.

- Probability that operators correctly interpret negative pump performance trends detected by condition-based monitoring systems (P_{NIO}) [III]. Failure of this event would cause a false negative diagnosis of the pump performance.

- Probability that operators correctly interpret no trend in pump performance data (P_{PIO}) [III]. Failure of this event would cause a false positive diagnosis of the pump performance.

- Probability that no human error will occur during repair process (1-HEP_{DR}) [I]. This parameter describes the probability that technicians will successfully repair the component. Failure of this event would cause the component to remain damaged following the repair. The value of this parameter is estimated from existing literature [135].

Preventative maintenance occurs during in-service inspections at refueling outages, which occur on average every 18 months for US NPPs [137]. Based on the EPRI maintenance procedures for the main feedwater pump, at the time of each ISI, only one pump in the two-pump system will undergo preventative maintenance [134]. Predictive maintenance tools are used to identify the pump to be selected for inspection at each refueling outage. In addition to either a typical inspection or a more robust overhaul inspection, a replacement of minor components (e.g., wear ring) may occur during ISI. The overhaul inspection is very comprehensive, and repair/replacement occurs at a very high rate for this maintenance strategy. EPRI recommends a realistic schedule of six years between major overhaul inspections [134]. Maintenance ETs representing the outcomes of normal and overhaul inspections are shown in Figure 3-11 and Figure 3-12 below, respectively.

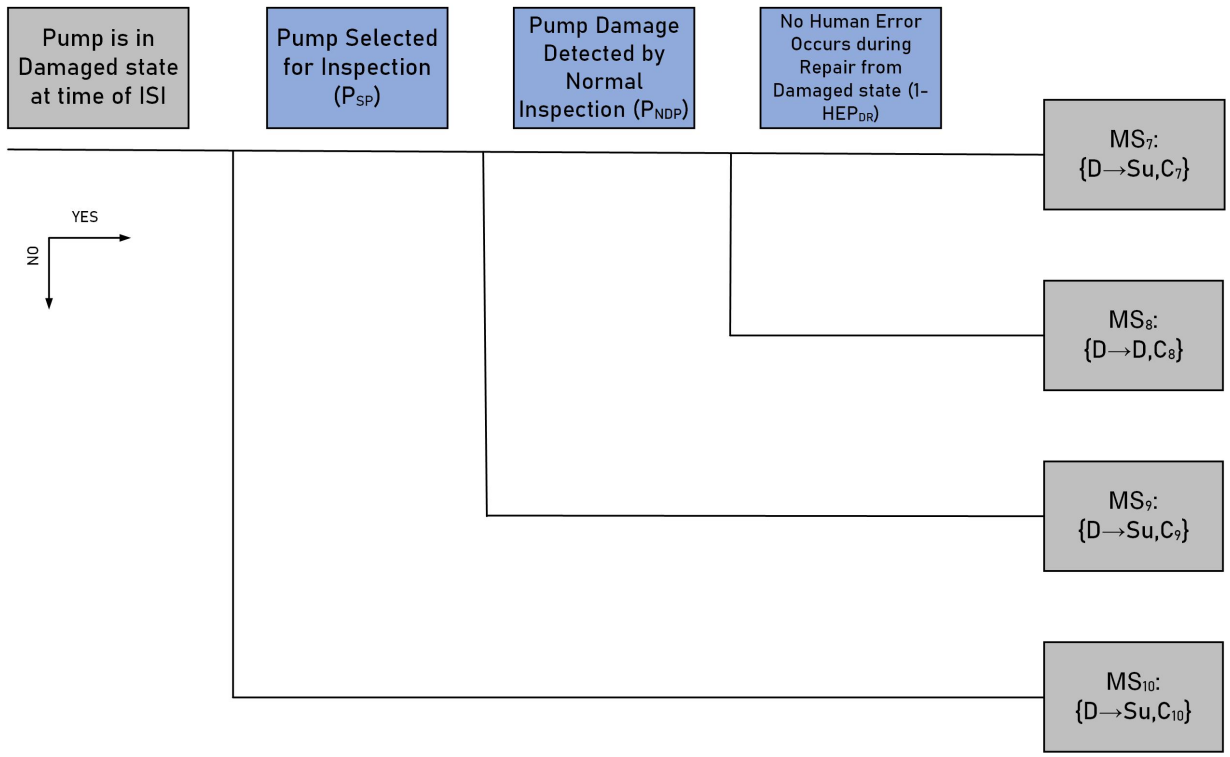


Figure 3-11: Maintenance Event Tree for Normal In-Service Inspections.

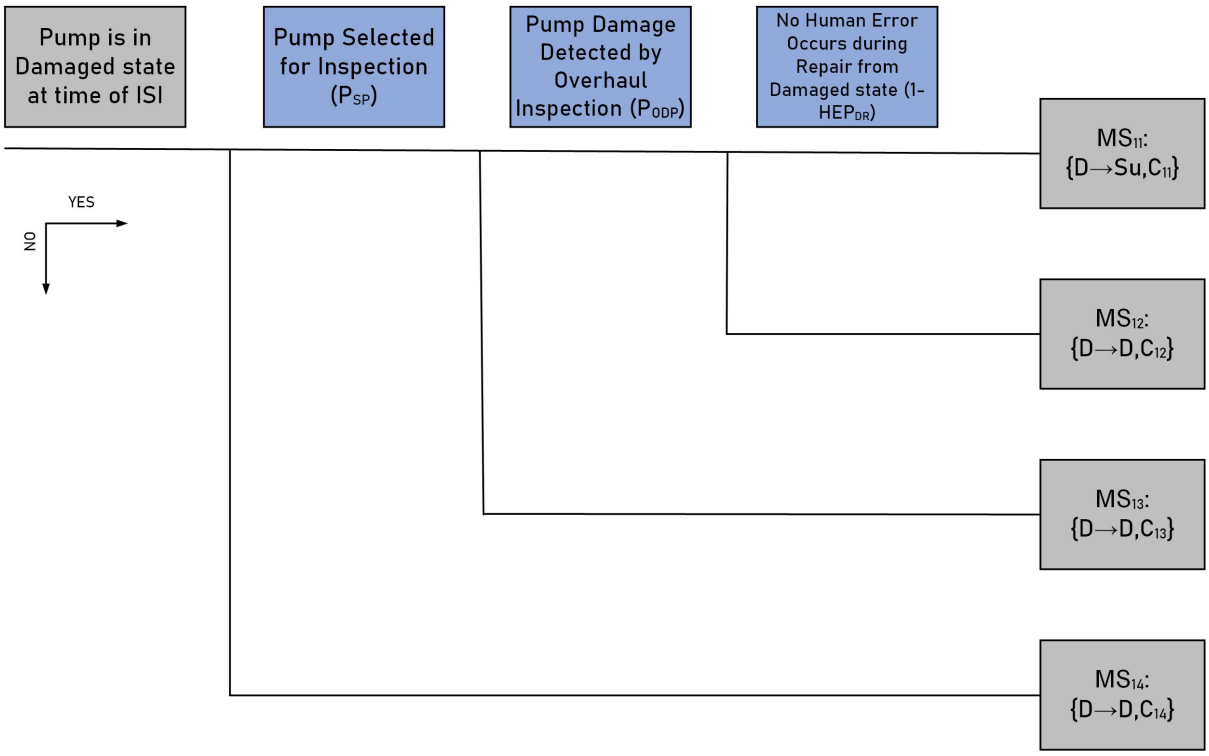


Figure 3-12: Maintenance Event Tree for Overhaul In-Service Inspections.

Seven possible maintenance scenarios 7 to 14 are quantified using the following maintenance parameters:

- Probability during refueling outage that the pump is selected for inspection at the time of ISI (P_{SP}) [II]. During each ISI event, only one pump is selected for inspection. In this analysis, it is assumed that each pump is equally likely to be inspected at the timing of each inspection.

- Probability that normal inspection detects pump damage during ISI (P_{NDP}) [I]. This parameter is estimated based on engineering judgment with consideration of the available inspection methods (e.g., ultrasonic inspection).

- Probability that overhaul inspection detects pump damage during ISI (P_{ODP}) [I]. During a major overhaul inspection, a very robust inspection process is used; thus, the value of this maintenance parameter will be very high. The estimation of this parameter is based on engineering judgment that the damage to the component will be detected with certainty.

- Probability that no human error will occur during the repair process from the Damaged state (1-HEP_{DR}) [I]. This parameter describes the probability that technicians will successfully repair the

component. Failure of this event would cause the component to remain damaged following the repair. The value of this parameter is estimated from literature [135].

Pump failure is assumed to be self-evident and the repair process following pump failure is assumed to begin immediately. Figure 3-13 shows the maintenance scenarios for the repair of a failed pump, where the relevant maintenance parameter is the probability of human error during repair from the Failure state (HEP_{FR}), estimated from existing literature [135].

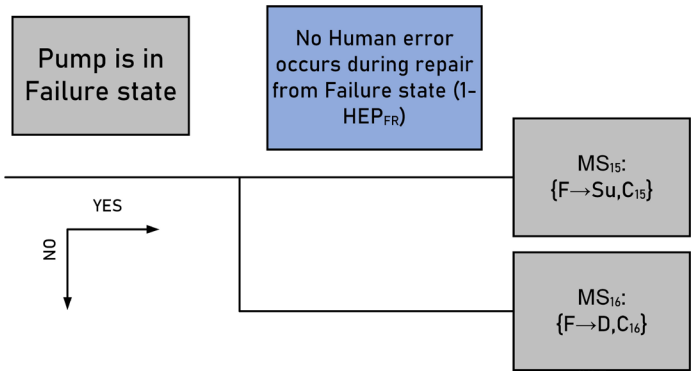


Figure 3-13: Maintenance Event Tree for Pump in Failure State.

Table 3-4 shows a list of the values used for the maintenance input parameters.

Table 3-4: Input parameters used to quantify the maintenance event trees.

Parameter	Symbol	Value Used
Probability that negative trends in pump performance data are detected by conditional monitoring systems	P_{OMD}	1
Probability that operators fail to correctly interpret negative pump performance trends detected by condition-based monitoring systems	$(1-P_{NIO})$	1.34E-1
Probability that operators fail to correctly interpret no trend in pump performance data	$(1-P_{PIO})$	9.80E-3
Probability that human error will occur during repair process from the Damaged state	HEP_{DR}	0.05
Probability that human error will occur during repair process from the Failure state	HEP_{FR}	0.05
Probability during refueling outage that the pump is selected for inspection at the time of ISI	P_{SP}	0.50
Probability that normal inspection detects pump damage during ISI	P_{NDP}	0.9
Probability that overhaul inspection detects pump damage during ISI	P_{ODP}	1

Additionally, the MOA module provides the estimated duration of each maintenance scenario, including:

- In-Service Inspection interval (T_{IS}) [I]. This case study assumes that ISI occurs at the timing of each refueling outage (i.e., every 18 months for U.S. NPPs); thus, T_{IS} = 18 months.

- Condition-based Monitoring Interval (T_{CBM}) [II]. Critical pump performance parameters for conditional monitoring are logged and trended on a monthly basis, per the EPRI maintenance guide for main feedwater pumps [134]; thus, T_{CBM} = 1 month.

- Mean Time to Repair Pump from Failure State ($MTTR_{FR}$) [I]. This parameter is estimated to be $MTTR_{FR}$ = 180 hours based on engineering judgment and input from an industry expert.

- Mean Time to Repair Pump from Damaged State ($MTTR_{DR}$) [I]. Based on engineering judgment and input from an industry expert, and with the consideration that the time to repair from the Damaged state is expected to be shorter than the time to repair from the Failure state, this parameter is assumed to be $MTTR_{FR}$ = 120 hours.

To estimate the total maintenance cost, two additional scenarios in Figure 3-14 (scenarios 17 and 18) are required to allow for the possibility of condition-based monitoring when the pump is in the Success state. In addition to the maintenance scenarios presented in the above ETs, one additional scenario, 19, is considered in which in-service inspection occurs with the pump in Success state where no false positive inspection result is possible, and the only cost incurred is the labor cost for the inspection.

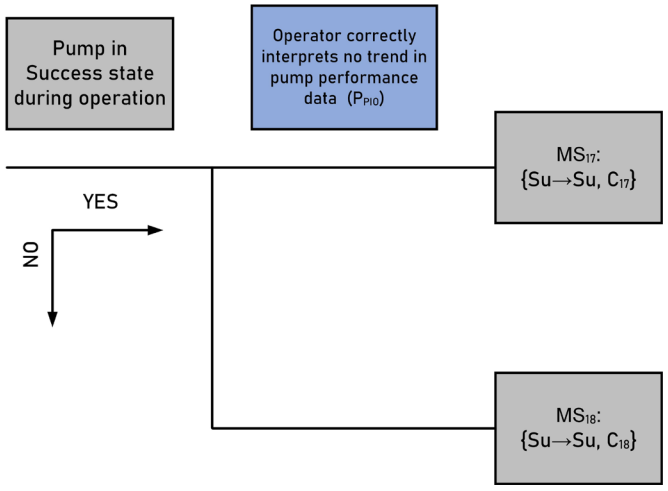


Figure 3-14: Maintenance ET during Operation with Component in Success State.

For each maintenance scenario (i.e., end states 1 to 19 in the maintenance ETs), a maintenance cost equation (Table 3-5) is developed to calculate the annual expected maintenance cost as one of the outputs from MOA. In 2020, the average refueling outage length was 33 days [138]. With this information, a rigid schedule of 18 months of operational time is assumed, followed by 33 days of refueling outage. The annual expected maintenance cost is computed by multiplying the frequency of occurrence and cost per occurrence of each maintenance scenario.

Table 3-5: Annual Maintenance Cost Equations for Maintenance Scenarios.

Maintenance Scenario	Cost Equation
MS_1	$\frac{P_{OMD}P_{NIO}}{T_{CBM}} \cdot L_{CM} \cdot \int_{t\in\mathcal{T}_{\text{o,all}}^{(i)}} D(t)\,dt + \frac{(1-HEP_{DR})}{MTTR_{DR}}(L_{RD}+M_{RD}) \int_{t\in\mathcal{T}_{\text{o,all}}^{(i)}} CBM(t)\,dt$
MS_2	$\frac{P_{OMD}P_{NIO}}{T_{CBM}} \cdot L_{CM}. \int_{t\in\mathcal{T}_{\text{o,all}}^{(i)}} D(t)\,dt + \frac{HEP_{DR}}{MTTR_{DR}}(L_{RD}+M_{RD}) \int_{t\in\mathcal{T}_{\text{o,all}}^{(i)}} CBM(t)\,dt$
MS_3	$\frac{P_{OMD}(1-P_{NIO})}{T_{CBM}} \cdot L_{CM} \cdot \int_{t\in\mathcal{T}_{\text{o,all}}^{(i)}} D(t)\,dt$
MS_4	$\frac{(1-P_{OMD}).P_{NIO}}{T_{CBM}} \cdot L_{CM} \cdot \int_{t\in\mathcal{T}_{\text{o,all}}^{(i)}} D(t)\,dt$
MS_5	$\frac{(1-P_{OMD})(1-P_{NIO})}{T_{CBM}} \cdot L_{CM} \cdot \int_{t\in\mathcal{T}_{\text{o,all}}^{(i)}} D(t)\,dt + \frac{(1-HEP_{DR})}{MTTR_{DR}} \cdot (L_{RD}+M_{RD}) \cdot \int_{t\in\mathcal{T}_{\text{o,all}}^{(i)}} CBM(t)\,dt$
MS_6	$\frac{(1-P_{OMD})(1-P_{NIO})}{T_{CBM}} \cdot L_{CM} \cdot \int_{t\in\mathcal{T}_{\text{o,all}}^{(i)}} D(t)\,dt + \frac{HEP_{DR}}{MTTR_{DR}}(L_{RD}+M_{RD}) \int_{t\in\mathcal{T}_{\text{o,all}}^{(i)}} CBM(t)\,dt$
MS_7	$P_{SP} \cdot P_{NDP} \cdot (1-HEP_{DR}) \cdot (L_{ISI}+M_{RD}+L_{RD}) \cdot \sum_{t'\in\mathcal{T}_{\text{NISI}}} \left[\int_{t\in\mathcal{T}^{(i)}} D(t)\delta(t-t')dt \right]$
MS_8	$(P_{SP}.P_{NDP}.HEP_{DR}) \cdot (L_{ISI}+M_{RD}+L_{RD}) \cdot \sum_{t'\in\mathcal{T}_{\text{NISI}}} \left[\int_{t\in\mathcal{T}^{(i)}} D(t)\delta(t-t')dt \right]$
MS_9	$P_{SP} \cdot (1-P_{NDP}) \cdot L_{ISI} \cdot \sum_{t'\in\mathcal{T}_{\text{NISI}}} \left[\int_{t\in\mathcal{T}^{(i)}} D(t)\delta(t-t')dt \right]$

MS_{10}	$(1-P_{SP})\cdot(0)\cdot\sum_{t'\in\mathcal{T}_{\text{NISI}}}\left[\int_{t\in\mathcal{T}^{(i)}}D(t)\delta(t-t')dt\right]$
MS_{11}	$P_{SP}\cdot P_{NDP}\cdot(1-HEP_{DR})\cdot(L_{ISI}+M_{RD}+L_{RD})\cdot\sum_{t'\in\mathcal{T}_{\text{OISI}}}\left[\int_{t\in\mathcal{T}^{(i)}}D(t)\delta(t-t')dt\right]$
MS_{12}	$P_{SP}\cdot P_{NDP}\cdot HEP_{DR}\cdot(L_{ISI}+M_{RD}+L_{RD})\cdot\sum_{t'\in\mathcal{T}_{\text{OISI}}}\left[\int_{t\in\mathcal{T}^{(i)}}D(t)\delta(t-t')dt\right]$
MS_{13}	$P_{SP}\cdot(1-P_{NDP})\cdot(L_{ISI})\cdot\sum_{t'\in\mathcal{T}_{\text{OISI}}}\left[\int_{t\in\mathcal{T}^{(i)}}D(t)\delta(t-t')dt\right]$
MS_{14}	$(1-P_{SP})\cdot(0)\cdot\sum_{t'\in\mathcal{T}_{\text{OISI}}}\left[\int_{t\in\mathcal{T}^{(i)}}D(t)\delta(t-t')dt\right]$
MS_{15}	$\frac{(1-HEP_{FR})}{MTTR_{FR}}\cdot(M_{RF}+L_{RF})\cdot\int_{t\in\mathcal{T}^{(i)}_{\text{o,all}}}F(t)\,dt$
MS_{16}	$\frac{HEP_{FR}}{MTTR_{FR}}\cdot(M_{RF}+L_{RF})\cdot\int_{t\in\mathcal{T}^{(i)}_{\text{o,all}}}F(t)\,dt$
MS_{17}	$\frac{P_{PIO}}{T_{CBM}}\cdot L_{CM}\cdot\int_{t\in\mathcal{T}^{(i)}_{\text{o,all}}}Su(t)\,dt$
MS_{18}	$\frac{(1-P_{PIO})}{T_{CBM}}\cdot L_{CM}\cdot\int_{t\in\mathcal{T}^{(i)}_{\text{o,all}}}Su(t)\,dt$
MS_{19}	$P_{PS}\cdot L_{ISI}\cdot\left[\sum_{t'\in\mathcal{T}_{\text{NISI}}}\left\{\int_{t\in\mathcal{T}^{(i)}}D(t)\delta(t-t')dt\right\}+\sum_{t'\in\mathcal{T}_{\text{OISI}}}\left\{\int_{t\in\mathcal{T}^{(i)}}D(t)\delta(t-t')dt\right\}\right]$

Table 3-6: Unit Cost Parameters used for Quantification of Maintenance Cost Scenarios.

Cost Elements	Unit Cost Parameters
Labor Cost for Condition-Based Monitoring (L_{CM})	$2,880
Material Cost for Repair from Damaged State (M_{RD})	$7,000
Labor Cost for Repair from Damaged State (L_{RD})	$11,520
Labor Cost for In-Service Inspection (L_{ISI})	$17,280
Material Cost for Repair from Failure State (M_{RF})	$7,000
Labor Cost for Repair from Failure State (L_{RF})	$11,520

3.2.2.6 Integration of Individual Modules for the Case Study

In the scope of the case study, the PRA, Financial Analysis, GRA, ERAA, and MOA modules are integrated using the interfacing methodologies shown in Subsection 3.1.2.6. This subsection shows the implementation of interfaces (i) between MOA and ERAA and (ii) between ERAA and GRA since these two interfaces are the key parts of the methodological developments in this research.

3.2.2.6.1 Interface (i) between MOA and ERAA for the Case Study

The interface from MOA to ERAA is created by estimating the maintenance transition rates in ERAA based on the MOA outputs using the methodology in Subsection 3.1.2.6.1. The maintenance transition rates are quantified as a function of the probabilities of maintenance scenarios (computed by multiplying the top event probabilities for each scenario) and the duration of each maintenance scenario. Table 3-7 shows the equations used and the resultant values of the maintenance transition rates in the multi-phase Markov process model (Figure 3-9).

Table 3-7: Quantification of Maintenance Transition Rates in the Multi-phase Markov Process Model.

Transition Path/Parameter	Symbol	Equation Used	Value [yr^{-1}]
Damaged State to Condition-based Maintenance State	τ	$\frac{P_{OMD} \cdot P_{NIO} + (1 - P_{OMD}) \cdot (1 - P_{PIO})}{T_{CBM}}$	1.04E+2
Condition-based Maintenance State to Damaged State	β_1	$\frac{HEP_{DR}}{MTTR_{DR}}$	3.65E+0
Condition-based Maintenance State to Success State	β_2	$\frac{1 - HEP_{DR}}{MTTR_{DR}}$	6.94E+1
Failure State to Success State	γ	$\frac{1 - HEP_{FR}}{MTTR_{FR}}$	4.62E+1
Failure State to Damaged State	ε	$\frac{HEP_{FR}}{MTTR_{FR}}$	2.43E+0

3.2.2.6.2 Interface (ii) between ERAA and GRA for the Case Study

As a result of solving the GRA FT (Figure 3-7) for the 0% production loss event, there are some minimal cut sets which involve only non-pump components and two types of minimal cut sets that involve pumps: Type A consisting of only pumps, Type B consisting of the mixture of a pump from one pump train, and a non-pump component from the remaining pump train. To compute the frequencies of the Type A and Type B GRA cut sets utilizing the ERAA outputs, GRA-ERAA Interface ETs are generated.

Figure 3-15 shows the GRA-ERAA Interface ET of the Type A scenarios that may occur due to the states of the two production system pumps (P_2 and P_3). The Interface IE in Figure 3-15 includes: (i) the planned repair of P_2 from the Damaged state following damage detection by in-service inspection or conditional maintenance inspection; and (ii) the unplanned repair of P_2 from the Failure state. Since there is no functional difference between P_2 and P_3 in terms of their impact on the production level, P_2 and P_3 are symmetric; therefore, the GRA scenarios induced by the repair of P_3 can be represented by the same ET structure, where P_2 and P_3 are flipped.

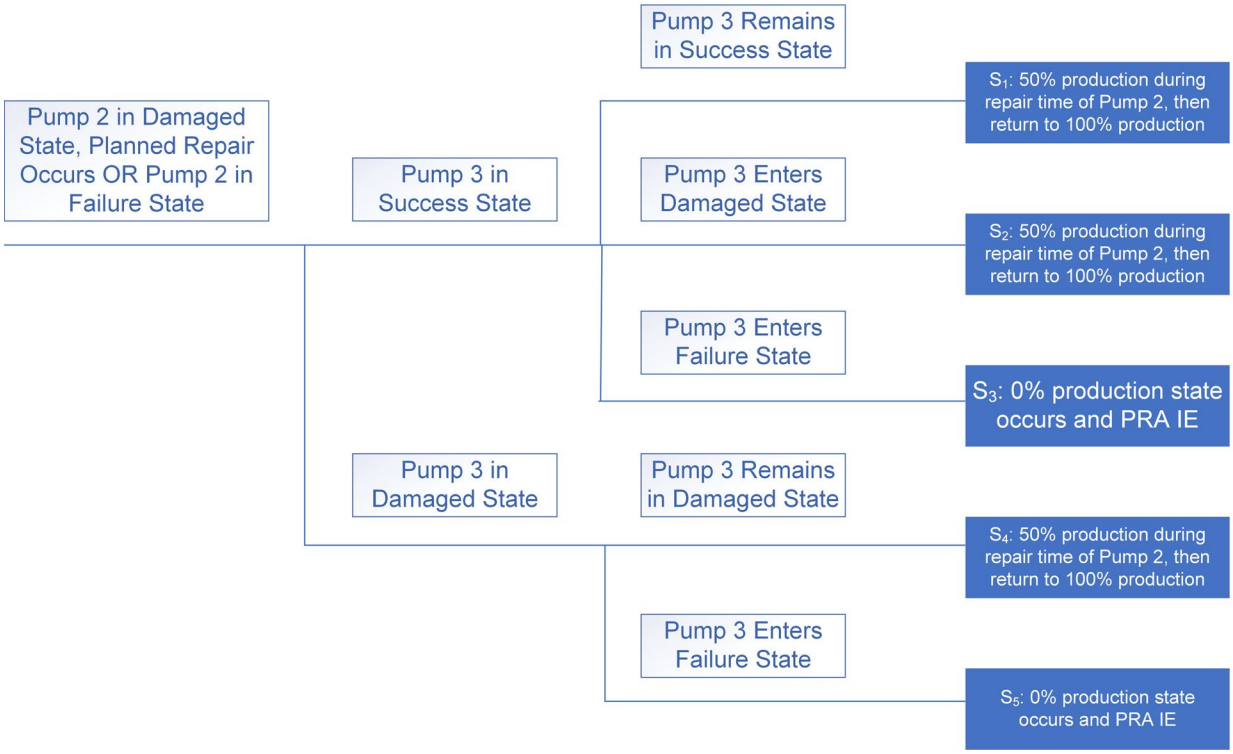


Figure 3-15: GRA-ERAA Interface Event Tree for Type A GRA cutsets.

During the repair of P_2 from either the Damaged state or Failure state, it is possible for P_3 to begin in the Success state or Damaged state when the repair is initiated. Scenarios 1-3 occur when P_3 is in the Success state when the repair of P_2 is initiated. In Scenarios 1 and 2, P_3 either remains in the Success state or enters the Damaged state during the repair time of P_2, which causes a 50% production state to occur during the repair time of P_2, but then a return to 100% production following the repair of P_2. In Scenario 3, P_3 enters the Failure state during the repair time of P_2, causing both pump trains to be unavailable and initiating the PRA IE caused by the 0% production state. In Scenario 4, P_3 begins and remains in the Damaged state, which causes the 50% production state during the repair time of P_2, and then a return to normal production. In Scenario 5, the PRA IE occurs as result of the failure of P_3 causing the 0% production state.

Type B GRA cut sets occur due to failure or repair to a pump along with failure or repair of a non-pump component in the parallel pump train. Figure 3-16 shows the Type B GRA cut sets, which begin with one of the pump trains being unavailable due to the failure or repair of a pump or non-pump component in the pump train. For the scenarios beginning with the unavailability of a pump, the GRA-ERAA Interface ET considers two Interface IEs: (i) the pump is in the Damaged state and a planned repair occurs, or (ii) the pump is in a Failure state. In Scenarios 6-7, the repair of one pump from the Damaged state or Failure state is initiated while the non-pump components in the remaining pump train are in the Success state. In Scenario 6, if the non-pump component remains in the Success state during the repair time of the pump, then a 50% production state will occur during the repair time and normal production will resume following repair. In Scenario 7, the non-pump component enters the Failure state during the repair of the pump, which causes both pump trains to be unavailable and the 0% production state and PRA IE will occur.

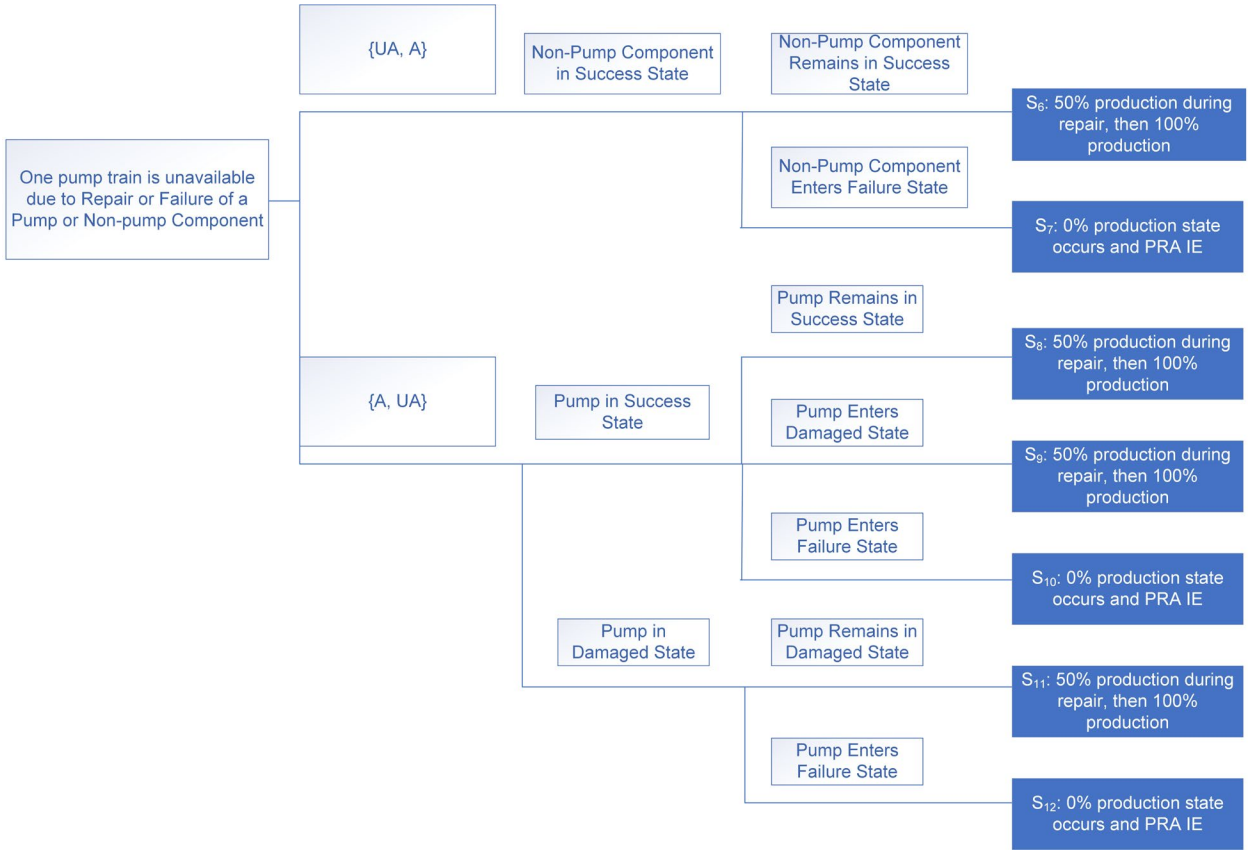


Figure 3-16: GRA-ERAA Interface Event Tree for Type B GRA cut sets. Two initiating events are included: (UA, A): A pump is not available, while a non-pump component is available; (A, UA): A pump is available, while a non-pump component is unavailable.

During the repair of a non-pump component from the Failure state, it is possible for the pump in the remaining pump train to begin in the Success state or Damaged state when the repair is initiated. Scenarios 8-10 occur when the pump is in the Success state when the repair of the non-pump component is initiated. In Scenarios 8-9, the pump either remains in the Success state or enters the Damaged state during the repair time of the non-pump component, which causes the 50% production state to occur during the repair time, but then a return to 100% production following the repair. In Scenario 10, the pump enters the Failure state during the repair time, causing both pump trains to be unavailable and initiating the PRA IE caused by the 0% production state. In Scenario 11, the pump begins and remains in the Damaged state, which causes the 50% production state during the repair time, and then a return to normal production. In Scenario 12, the PRA IE occurs as result of the failure of the pump causing the 0% production state.

The input parameters of the GRA-ERAA Interface ETs, including the Interface IE frequencies and the Top Event probabilities, are computed based on the ERAA outputs using the methodology introduced in Subsection 3.1.2.6.2. For each end state of the GRA-ERAA Interface ETs, the time profile of the electricity output during each GRA scenario is also calculated. Based on Ref. [139], a typical startup from cold shutdown, which includes a heat up and synchronizing to grid, takes approximately 34 hours. Once synchronized with the grid, the power output of the plant is gradually ramped up to full power, assuming a thermal power of around 25% of rated capacity at the time of grid synchronization and a ramp-up rate from this thermal power to full capacity of 1.65% of capacity per hour [139].

3.2.3 Case Study Results for Two Maintenance Alternatives

Two alternative maintenance strategies for preventive maintenance (PM) are considered. In the first PM strategy, only ISI is included, while in the second PM strategy both CBPM and ISI are included. In both cases, CM is assumed. The evaluation of multiple alternative O&M strategies demonstrates the value of the I-ERM framework to provide relevant outputs to NPP decision-makers. Safety and cost-related outputs for each maintenance alternative are provided in Figure 3-17. The annual expected CDF is computed as the key safety metric from the PRA module, while two financial performance metrics are computed for each maintenance alternative, the direct maintenance costs, and production loss costs.

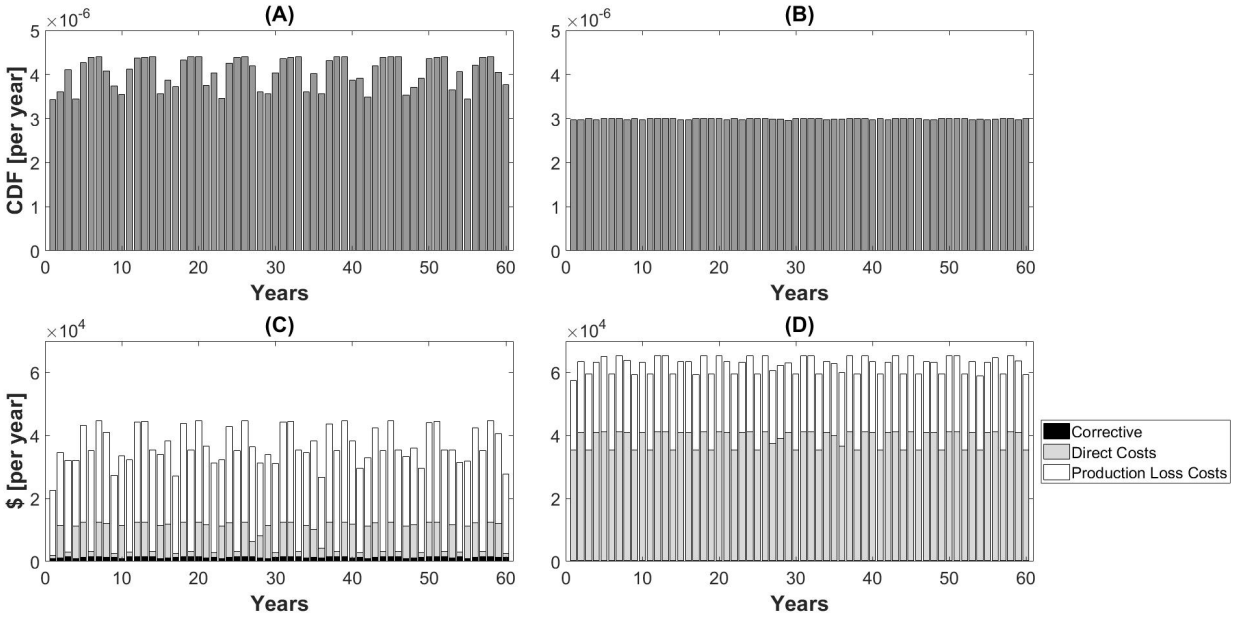


Figure 3-17: Safety and Financial Performance Metrics for two Maintenance Strategy Alternatives: CM + ISI (Subplots A and C), CM + CBPM (Subplots B and D).

From subplots A and B, the strong effect of CBPM in reducing safety risk is demonstrated. While in subplot A there is significant fluctuation in the annual expected CDF depending on whether ISI is planned for that specific year, the CDF in subplot B is both lower and more stable as the CBPM detects and repairs the component prior to failure. In subplot C, the expected annual production loss costs far outweigh the direct maintenance costs since direct maintenance costs are only accrued from ISI, which occurs sparingly, while in subplot D the direct maintenance costs account for a larger portion than production loss costs since CBPM is occurring on a monthly basis and generating larger direct maintenance costs but also reducing the amount of production loss costs by maintaining higher component reliability. Comparing subplots C and D, the total costs in subplot C are much lower than those in subplot D, indicating that the savings in production loss costs associated with using CBPM and ISI are not as significant as the savings in direct maintenance costs from using only ISI. Additionally, the costs of corrective maintenance are negligible in subplot D, due to the reduction in failure probability resulting from the use of CBPM. With the information contained in all of these plots, plant decision-makers can generate appropriate maintenance strategies to satisfy regulatory standards and ensure plant safety while maintaining a viable economic status.

3.3 Summary

A key output of the literature review in Chapter 2 has indicated that commonly used correlation-based approaches for modeling may not be sufficient and, thus, this chapter builds upon the theoretical foundation

established in Chapter 2 to develop a model-based approach to estimate safety and financial performance metrics for NPPs in a unified framework. The I-ERM framework is developed and implemented for an NPP case study in this chapter, demonstrating both the methodological contribution of the model-based approach and the practical value of the I-ERM framework.

I-ERM enables explicit incorporation of the underlying physical degradation mechanisms and maintenance performance (considering human and organizational factors) into the modeling of safety and financial performance of an NPP to capture the interconnections and dependencies between these two NPP performances. Explicit modeling of the underlying causations that can influence the interconnections of safety and financial performance empowers decision-makers to identify shared factors and causal mechanisms that impact both the safety and financial performance of an organization, providing an improved evaluation of the financial implications of safety strategies and of the cost-effectiveness of safety investments. Additionally, the explicit modeling of underlying causations can support simulation of the temporal interactions between safety performance and financial performance, contributing to an improved enterprise risk management that benefits management's critical decision-making in balancing these two organizational performances. This chapter focuses on the methodological developments of the I-ERM modules (Section 3.1) and the implementation of the I-ERM framework for an NPP case study (Section 3.2). The case study implementation demonstrates the viability of the I-ERM framework. By applying the I-ERM framework to an NPP case study, the results of the case study generate the types of valuable information encompassing both safety risk and financial performance, which can be provided to NPP decision-makers when faced with decisions related to O&M strategies. The case study generated time-dependent safety and financial performance metrics which can aid in determining appropriate maintenance strategies to satisfy safety requirements in a cost-effective manner.

4. Spatiotemporal Probabilistic Physics-of-Failure Analysis and Its Connection to Safety and Financial Performance

Chapter 3 of this report has introduced the I-ERM methodological framework (Figure 3-1) to quantify the interconnections of safety and financial performance with a focus on O&M of NPPs. Chapter 3 has also demonstrated the applicability and values of the I-ERM methodology through an NPP case study. In this chapter, detailed development and implementation of one of the I-ERM modules, i.e., probabilistic physics-of-failure (PPoF) analysis, and its connection with safety and financial performance is reported.

The I-ERM methodological framework (Figure 3-1) considers the coupled effects of physics-of-failure and maintenance performance (considering human and organizational factors) in a unified platform to quantify the interconnections of safety and financial performance with explicit modeling of the underlying causalities. To quantify the maintenance performance and its impact on safety and financial performance, Chapter 3 has developed the MOA module and interfaced it with the PRA and GRA modules through the ERAA module. The Financial Analysis module has also already been developed and connected to the PRA, GRA, ERAA, and MOA modules. In Chapter 3, physical failure behavior of individual equipment has been treated by a data-driven method, where the degradation- and failure-related inputs of the ERAA module have been estimated from failure event data. This chapter focuses on the development of the PPoF Analysis module, with explicit modeling of physical failure phenomena, and its interface with the ERAA module. The explicit incorporation of physics of failure model into the PPoF Analysis module of I-ERM in this chapter, combined with other modules of I-ERM developed in Chapter 3, makes incorporating physics-maintenance coupling into the safety and financial performance analysis of NPPs possible.

Previous research by the PI's research team [140] integrated a PPoF model with a renewal process model to estimate the probabilistic failure metrics (e.g., leak and rupture probabilities) of piping components. The PPoF analysis in this previous research was developed for stress-corrosion cracking induced by a static stress, where the applied stress was provided as an input to the PPoF model based on design information and operational data. This chapter advances the PPoF model, developed in the previous research [140], by incorporating finite element analysis (FEA) into the PPoF Analysis to simulate physical degradation mechanisms induced by dynamic and location-specific stress due to thermomechanical processes. For the piping reliability analysis of NPPs, there are several other studies that have connected a renewal process model to physics-based models [141-149]. Unlike the existing studies, this research, for the first time, uses the spatial (in addition to temporal) physical simulation data generated by FEA in the estimation of the physics-based transition rates. In this chapter, thermal fatigue is selected as the physical mechanism of interest since (i) thermal fatigue at NPPs is one of the dominant degradation mechanisms for

passive components, such as reactor pressure boundary components [150]; and (ii) the underlying physical processes are complex and involve spatial and temporal interactions between fluid and solid materials; thus, for a realistic depiction of the underlying physical phenomena, higher spatiotemporal resolutions are required in the PPoF analysis.

Section 4.1 explains the FEA-based PoF model for thermal fatigue developed in this research. Additionally, in Subsection 4.1.2, an interface between the PPoF Analysis module and the renewal process model in the ERAA module ('d' in Figure 3-1) is advanced with respect to how to utilize the spatiotemporal FEA data in the estimation of physical degradation and failure rates as inputs to the renewal process model in the ERAA module of the I-ERM framework. In Section 4.2, the FEA-based PPoF Analysis module and its interface with the ERAA module are applied to an NPP case study, where excess letdown elbow piping in the NPP is subjected to thermal fatigue due to thermal stratification.

4.1 Incorporation of Finite Element Analysis into the Probabilistic Physics-of-Failure Analysis module of the I-ERM Framework

This section describes the methodology for incorporating FEA into the PPoF Analysis module in I-ERM. While the methodological development is shown for an NPP pipe component subjected to thermal fatigue due to thermal stratification [151, 152], the FEA-based PPoF methodology can be applicable for pipe components subjected to thermal fatigue induced by other loading conditions [153, 154] and non-piping components subjected to thermal fatigue [155, 156]. To extend the PPoF methodology to different applications, the geometrical characteristics, material properties, loading conditions, underlying physical processes, and damage thresholds should be adjusted as needed. For instance, to extend the PPoF Analysis developed in this section to thermal fatigue of a steam turbine rotor caused by fluid temperature fluctuation [156], the geometrical characteristics, material properties, and loading conditions of the turbine rotor should be used as inputs to FEA. Additionally, the underlying physical processes should be modified based on the physical failure modes specific to the component and part being analyzed. For the example of the steam turbine rotor, a large fracture of the blade groove can lead to the failure of the turbine rotor; thus, the physical submodel for this specific failure mode should be added, while some of the piping-specific physical submodels, such as the leakage and rupture submodels, should be excluded.

There are three aspects for the PPoF Analysis module: (i) a PoF model for the physical degradation and failure mechanism, (ii) uncertainty quantification (UQ) to make the PoF model probabilistic, and (iii) estimation of the physics-based transition rates as inputs to the ERAA module. The PoF model simulates the physical degradation and failure processes, from their initiation up to equipment failure. The underlying physical processes of thermal fatigue are divided into six subprocesses: thermal fluid dynamics,

thermomechanical response, crack initiation, crack propagation, leakage, and crack instability. The PoF model is developed by coupling physics-based submodels developed for individual physical subprocesses.

Among the six physical subprocesses, due to thermal fatigue, the thermomechanical response induced by thermal fluid dynamics has a significant impact on the equipment failure [157], yet its treatment in the PPoF analyses has not been fully expanded in the literature. In Cheng et al. [158], the studies that estimated the probabilistic failure metrics (such as reliability and failure frequency) of reactor coolant pressure boundary components were reviewed. In previous studies, the thermo-mechanical response induced by thermal fluid dynamics was treated either by characterizing the applied stress using a data-driven approach [143, 145, 157, 159-169] or by using an analytical model derived for simplified geometries and stress conditions, such as the one derived for cylinder geometry [148]. These methods, however, may not generate an accurate depiction of the underlying physical processes, especially when (i) limited or no applied stress data directly relevant to the geometry and loading condition of interest is available, (ii) the geometry (e.g., a pipe with curvature) is too complex to be approximated by simplified geometries such as those for a straight pipe or a finite 1-D plate, and (iii) loading conditions involve a transient process. To address these limitations, this research equips the PPoF analysis with 3-D FEA for thermomechanical response, which provides spatiotemporal inputs to other PoF submodels, including crack initiation, crack propagation, leakage, and crack instability.

The development of the FEA-based PoF model is shown in Subsection 4.1.1. The 3-D FEA can consider the spatiotemporal temperature distribution of the fluids (e.g., movement of the thermal stratification layer) as its boundary conditions and initial conditions and compute time-dependent, location-specific stress and temperature distributions, thereby improving the spatiotemporal resolution of the PPoF analysis.

Section 4.1.2 describes UQ for the PoF model and estimation of the physics-based inputs to a renewal process model in the ERAA module. Compared to the previous study by the authors [140], this chapter advances (i) the UQ method to address the randomness associated with the crack locations based on the spatiotemporal FEA outputs; and (ii) the parameter estimation for the physics-based transition rates by using the right-censored data method and the Bayesian approach to enable the estimation of relatively small transition rates for a large portion of the PoF simulation output which consists of success data. For the piping reliability analysis of NPPs, there are several previous studies that have connected a renewal process model to physics-based models [140-149]. Unlike these studies, this research, for the first time, uses the spatial (in addition to temporal) physical simulation data generated by FEA in the estimation of the physics-based transition rates.

4.1.1 Development of a Finite Element Analysis (FEA)-based Physics-of-Failure (PoF) model

This section explains the development of a FEA-based PoF model, while demonstrating it for a pipe component subjected to thermal fatigue. For each physical subprocess, a physics-based submodel is developed, including (1) thermal fluid dynamics, (2) thermomechanical response, (3) crack initiation, (4) crack propagation, (5) leakage, and (6) crack instability. The causal connection among these submodels is created by considering multiple damage states. The crack initiation submodel (#3 in Figure 4-1) covers the physical process from the beginning of the component life to the time when an "engineering crack size" [170] is reached, represented by a "New" state. The crack propagation submodel (#4 in Figure 4-1) covers the crack growth until it causes a leak of the contained fluid, represented by a "Flaw" state. The leakage submodel (#5 in Figure 4-1) covers the physical process after a thorough-wall crack is formed and before the crack instability occurs, represented by a "Leak" state. The crack instability submodel (#6 in Figure 4-1) covers the physical process when the crack becomes instable and leads to rapid failure propagation, represented by a "Rupture" state. To allow for specifying multiple leak states, depending on the leak rates in relation to the operational and maintenance requirements, Figure 4-1 includes multiple leak states, Leakm, m = 1, 2, …, M, where M is the total number of leak states. Submodels #1 and #2 in Figure 4-1 cover the fluid and thermal-mechanical interactions using the 3-D FEA to compute the location-specific and time-dependent stress and temperature inputs to the other submodels. Each submodel is described below.

The thermal fluid dynamics submodel (#1 in Figure 4-1) provides the time-dependent and location-specific fluid temperature distribution $T_f(z, t, \boldsymbol{\zeta_1}, \boldsymbol{\eta_1})$, where z and t are the location of the fluid and time, respectively. $\boldsymbol{\zeta_1}$ is a vector of input parameters related to operating conditions, while $\boldsymbol{\eta_1}$ is a vector of model parameters of the fluid temperature distribution. Additionally, the heat transfer coefficients ($\boldsymbol{\zeta_2}$) are determined for the system surfaces (e.g., inner and outer surfaces of piping). $T_f(z, t, \boldsymbol{\zeta_1}, \boldsymbol{\eta_1})$ and $\boldsymbol{\zeta_2}$ are provided as boundary conditions and initial conditions for FEA in submodel #2.

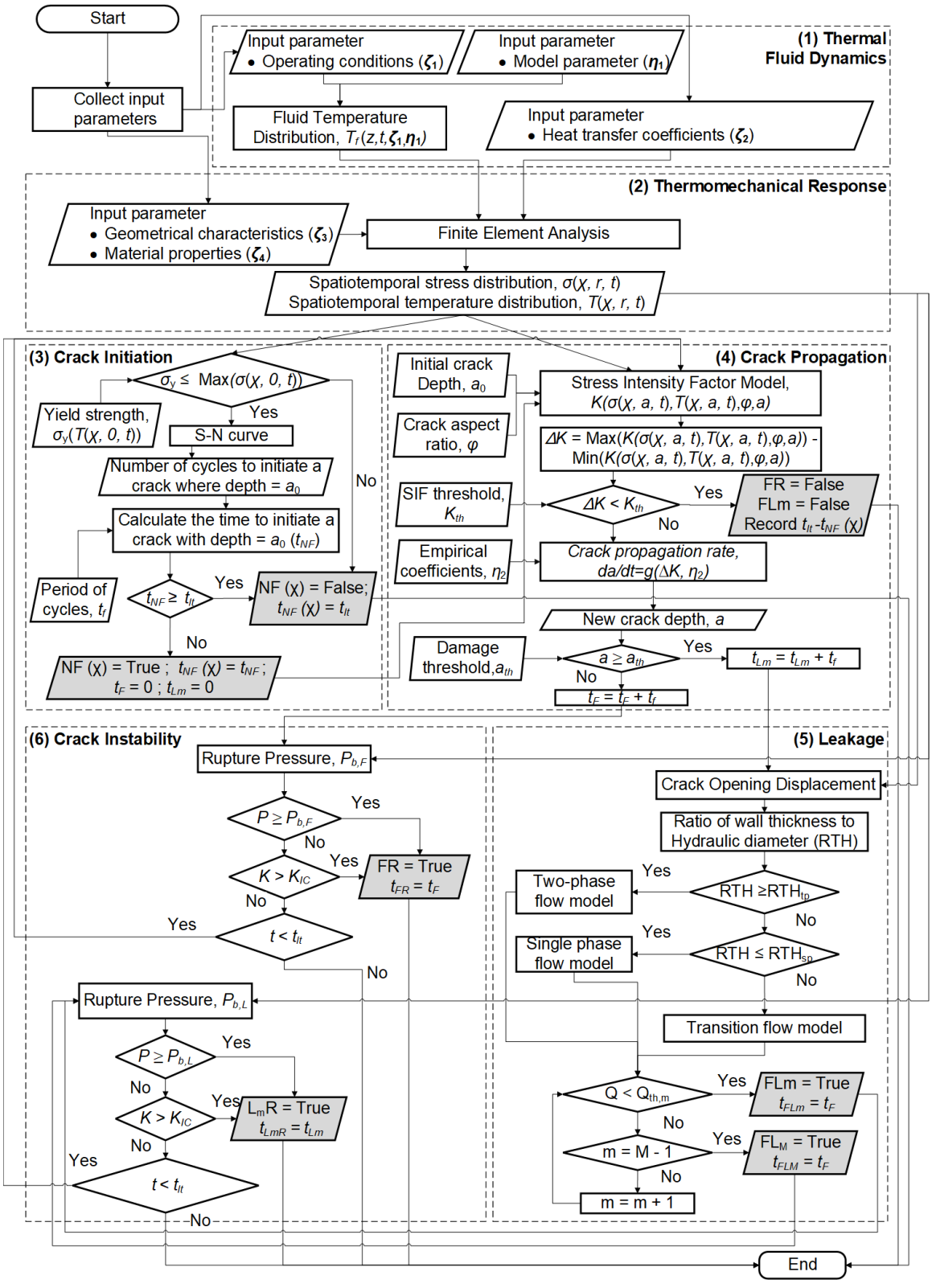


Figure 4-1. Finite element analysis (FEA)-based Physics-of-Failure (PoF) model for a pipe component subjected to thermal fatigue.

For the thermomechanical response submodel (#2 in Figure 4-1), a 3-D FEA is developed based on the geometrical characteristics ($\boldsymbol{\zeta_3}$) and material properties ($\boldsymbol{\zeta_4}$) of the component as well as $T_f(z, t, \boldsymbol{\zeta_1}, \boldsymbol{\eta_1})$ and $\boldsymbol{\zeta_2}$ obtained from submodel #1 above. As outputs from FEA, the spatiotemporal stress distribution $\sigma(\chi, r, t)$ and temperature distribution $T(\chi, r, t)$ are computed, where χ represents the FEA nodes (or locations) on the surfaces, while r represents the depth from the surface nodes. $\sigma(\chi, r, t)$ and $T(\chi, r, t)$ are used as inputs to other submodels (#3 through #6).

In the crack initiation submodel, for each node, a crack can be initiated if the maximum thermal stress is greater than the temperature-dependent yield strength $\sigma_y(T(\chi, 0, t))$. If this condition is satisfied, the time to crack initiation is predicted using an S-N curve, where the stress amplitude and temperature for the corresponding node χ are extracted from the FEA outputs in submodel #2. If the time to crack initiation (t_{NF}) is smaller than the component lifetime (t_{lt}), a crack is initiated on the node (represented by NF[χ]=True in Figure 4-1), and the time to crack initiation (t_{NF}) is recorded. Otherwise, a crack is not initiated on this node (NF[χ]=False) with the recorded component lifetime ($t_{NF}(\chi) = t_{lt}$), and the subsequent submodels (#4 through #6) are not evaluated for this location.

The crack propagation submodel (#4 in Figure 4-1) is then evaluated for an initiated crack. The stress intensity factor (SIF) at the crack initiation site χ as a function of time, denoted by $K(\sigma(\chi, a, t), T(\chi, a, t), \varphi, a)$, is computed by the SIF model, which requires multiple inputs including: $\sigma(\chi, r, t)$, $T(\chi, r, t)$, initial crack depth (a_o), and crack aspect ratio (φ). The SIF can be calculated by either conducting FEA [171] or adopting the SIF solutions benchmarked with FEA in the previous studies, for instance, Refs. [172-177]. In this study, the SIF solution approach is utilized, where the applied stress and temperature distribution computed by FEA are used as inputs. Based on the time profile of SIF at the crack initiation site χ, the SIF range ΔK is computed by the difference between the maximum and minimum SIFs. If ΔK is greater than a threshold (K_{th}), the initiated crack can further propagate with a rate calculated by Paris' law as a function of ΔK and empirical coefficients (denoted by η_2). An updated crack depth is obtained by multiplying the crack propagation rate with a time step. This study uses one period of the thermal cycle (t_f) as the time step. If ΔK is smaller than K_{th}, the crack does not propagate; thus, the transitions to the rupture and leak states do not occur, i.e., FR = False and $F2L_m$ = False, and the time duration of the flaw state (t_F) is recorded.

Once a predefined damage threshold between the flaw and leak states (a_{th}) is reached, the leakage submodel (#5 in Figure 4-1) calculates the crack opening displacement (COD) and the ratio of the wall thickness to the hydraulic diameter (RTH) in order to determine the appropriate leakage model (single-phase flow, two-phase flow, or transitional flow) to use. To calculate COD, the spatiotemporal temperature distribution $T(\chi, r, t)$ from FEA is used as input. In Figure 4-1, the threshold of RTH for the two-phase flow

is denoted as RTH_{tp} while the threshold of RTH for the single-phase flow is denoted as RTH_{sp}. If the calculated leakage rate (Q) is within the threshold of the leakage rate for m^{th} leak state ($Q_{th,m}$), the transition to the corresponding leak state (FL_m= True) and the time from an initiated crack to the m^{th} leak rate threshold (t_{FLm}) are recorded.

For each time increment and the updated crack depth, the crack instability submodel (#6 in Figure 4-1) checks whether the crack becomes unstable. A crack in the flaw state can become unstable if either the burst pressure for a flaw ($P_{b,F}$) is smaller than the internal pressure or the maximum SIF is greater than the fracture toughness (K_{IC}). $P_{b,F}$ is computed as a function of the spatiotemporal temperature distribution $T(\chi, r, t)$ from FEA. The time from an initiated crack to an unstable crack (t_{FR}) and the occurrence of the flaw-to-rupture transition (FR=True) are recorded. A stable crack continues to propagate until the simulation time reaches the component lifetime (t_{lt}) or the crack depth reaches the damage threshold (a_{th}). Meanwhile, the crack that has reached a_{th} and become a leak may continue to propagate until either the burst pressure for a leak ($P_{b,L}$) or K_{IC} is reached. If either condition is satisfied, the time to rupture (t_{LmR}) and the transition from the corresponding leak state to rupture (L_mR = True) are recorded.

4.1.2 Uncertainty Quantification for the FEA-based PoF Model and Estimation of Physical Transition Rates

UQ is conducted for the FEA-based PoF model to make it probabilistic and estimate the physical transition rates for the ERAA module based on the PoF outputs. In the UQ, aleatory uncertainty induced by natural variability and epistemic uncertainty induced by the lack of knowledge should be quantified separately [178]. In this research, the aleatory uncertainty associated with the PoF inputs (χ, φ, and S-N curve) is propagated by the Monte Carlo simulation (Figure 4-2).

Figure 4-2 has a loop structure over an index i, i = 1, 2, …, N_S, representing random samples in the Monte Carlo simulation, where N_S is the sample size. For each Monte Carlo sample, the PoF model, developed in Section 4.1.1, is executed. First, the spatiotemporal stress and temperature distributions for each node at the surface computed by FEA in the thermomechanical response submodel, $\sigma(\chi, r = 0, t)$ and $T(\chi, r = 0, t)$, are collected. Then, for each FEA node, where two sources of aleatory uncertainties are quantified, the crack initiation submodel (#3 in Figure 4-1) is executed. To quantify the aleatory uncertainty associated with the crack initiation time for each FEA node, the time to crack initiation is sampled from a family of the S-N curve with the associated probability density function (i.e., an S-N-P curve). As its outputs, the crack initiation submodel generates (i) a discrete variable indicating whether the crack initiation has occurred within the component lifetime, $NF(\chi)$ = True or False; and (ii) the time to crack initiation, $t_{NF}(\chi)$. Additionally, the aleatory uncertainty associated with the crack initiation location is considered by

generating random samples of the crack initiation time for all possible crack initiation sites, as shown by a loop over χ in Figure 4-2, $\chi = 1, 2, \ldots, \chi_{max}$, where χ_{max} is the number of the possible crack initiation sites. Among the possible crack locations considered in this algorithm ($\chi = 1, 2, \ldots, \chi_{max}$), the location with the minimum $t_{NF}(\chi)$ is selected as the location for crack propagation. It should be noted that this analysis focuses on a single crack, while the treatment of multiple cracks is left to future research.

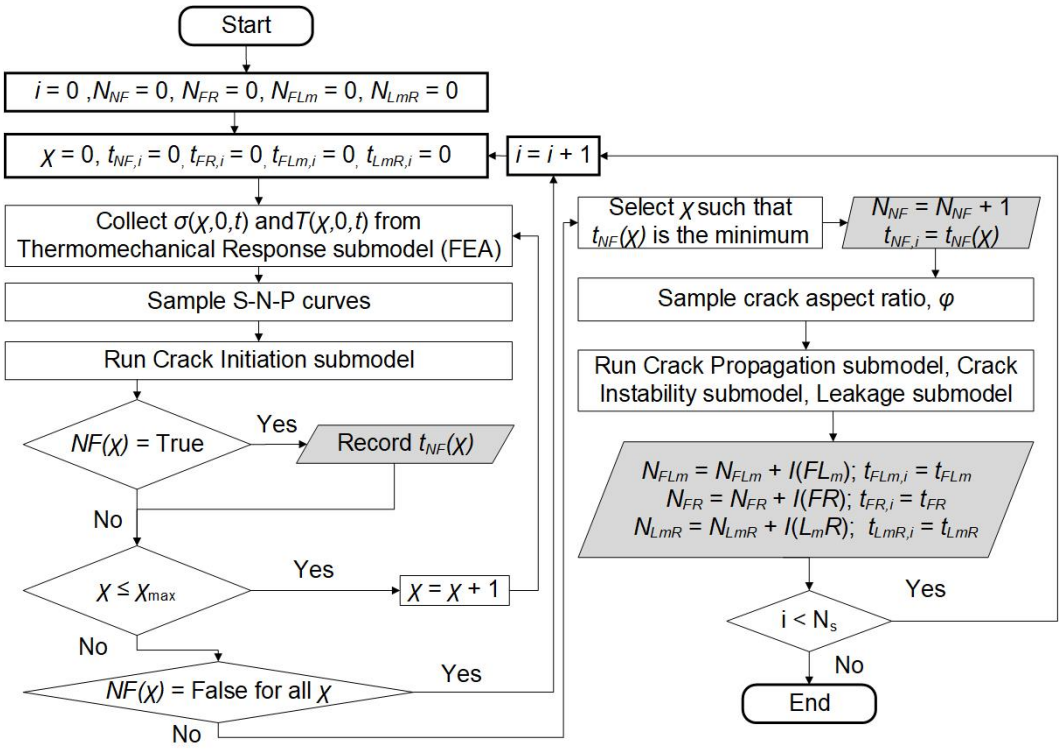


Figure 4-2. Uncertainty Quantification (UQ) Procedure in the PPoF Analysis Module of I-ERM.

For the selected crack location, the crack propagation, leakage, and crack instability submodels are executed, where the aleatory uncertainty for the crack aspect ratio φ is quantified by randomly sampling φ from its associated probability distribution. As a result, two types of data are recorded: (i) the number of each transition event, including N_{FLm} (from Flaw to the mth Leak state), N_{FR} (from Flaw to Rupture), and N_{LmR} (from the mth Leak state to Rupture); and (ii) the adjourn time of each damage state, including $t_{FLm,i}$ (the Flaw state duration for the samples that transitioned to the mth Leak state), $t_{FR,i}$ (the Flaw state duration for the samples that transitioned to the Rupture state), and $t_{LmR,i}$ (the mth Leak state duration for the samples that transitioned to the Rupture state). In Figure 4-2, an indicator function is used to represent the process for counting the number of transition events, $I(D_1D_2) = 1$ if the transition from one state (D_1) to another state (D_2) has occurred (D_1D_2 = True) and $I(D_1D_2) = 0$, otherwise.

The physical transition rates from state D_1 to state D_2 are estimated using the Bayesian approach. For each transition rate, a Jeffreys non-informative prior distribution, i.e., a gamma distribution with shape parameter $\alpha = 0.5$ and scale parameter $\beta = 0$, is used. The likelihood function is a Poisson distribution, where the evidence consists of (i) the number of the state transition events observed in the PoF runs, $N_{D_1D_2}$, and (ii) the state D_1 duration in the PoF runs for the samples that transitioned from D_1 to D_2, $t_{D_1D_2}$. Due to the conjugate property, the posterior distribution for each transition rate is a Gamma distribution with updated parameters, $\alpha' = \alpha + N_{D_1D_2}$, and $\beta' = \beta + t_{D_1D_2}$.

The state duration $t_{D_1D_2}$ for each type of transition path is computed using right-censored data. For New to Flaw, the New state duration t_{NF} is computed by Equation (26):

$$t_{NF} = (N_s - N_{NF})t_{lt} + \sum_{i=1}^{N_{NF}} t_{NF,i}, \tag{26}$$

where N_S is the number of random samples in the Monte Carlo simulation, and N_{NF} is the number of samples that have transitioned from New to Flaw during the component lifetime t_{lt}.

For Flaw to Rupture and Flaw to Leak$_m$, the Flaw state duration t_{FD_2} ($D_2 = R$ or L_m) is computed by Equation (27):

$$t_{FD_2} = \sum_{i=1}^{N_{NF}-\sum_{m=1}^{M} N_{FL_m}-N_{FR}} \left(t_{lt} - t_{NF,i}\right) + \sum_{m=1}^{M}\sum_{j_m=1}^{N_{FL_m}} t_{FL_m,j_m} + \sum_{k=1}^{N_{FR}} t_{FR,k}, \tag{27}$$

where N_{FL_m} is the number of samples that have transitioned from Flaw to Leak$_m$ before t_{lt}, while N_{FR} is the number of samples that have transitioned from Flaw to Rupture before t_{lt}. On the right-hand side of Equation (27), the first term includes the Monte Carlo samples that have remained in Flaw state until t_{lt}, the second term includes the Monte Carlo samples that have transitioned from Flaw to Leak$_m$ before t_{lt}, and the third term includes the Monte Carlo samples that have transitioned from Flaw to Rupture before t_{lt}.

For Leak$_m$ to rupture, the Leak$_m$ duration t_{L_mR} is calculated using Equation (28):

$$t_{L_mR} = \sum_{j_m=1}^{N_{FL_m}-N_{L_mR}} \left(t_{lt} - t_{NF,j_m} - t_{FL_m,j_m}\right) + \sum_{q_m=1}^{N_{L_mR}} t_{L_mR,q_m}, \quad (28)$$

where N_{L_mR} is the number of samples transitioned from Leak_m to Rupture before t_{lt}. On the right-hand side, the first term includes the Monte Carlo samples that entered Leak_m but have not transitioned to the Rupture state, while the second term includes the Monte Carlo samples that entered Leak_m and have transitioned to the Rupture state.

Within the scope of this research and in accordance with the current PRA practice [179], the epistemic uncertainties are analyzed by conducting sensitivity analysis. Advancements in the UQ for epistemic uncertainty are addressed in ongoing research by some of the authors [124, 180] by developing more comprehensive theoretical and methodological foundations for quantifying and interpreting the epistemic uncertainty associated with input data as well as for simulation models used in PRA.

4.2 Case Study Application

An excess letdown pipe of a chemical and volume control system (CVCS) connected to reactor coolant system (RCS) in a Pressurized Water Reactor (PWR) is selected as a case study (Figure 4-3). During times when the letdown pipe is isolated from the primary coolant loop, a thermal stratification layer can be formed. The flow in the main pipe can generate a turbulent penetration in the branched pipe [181], leading to the fluctuation of the interface layer and thermal cycling in the stratification zone.

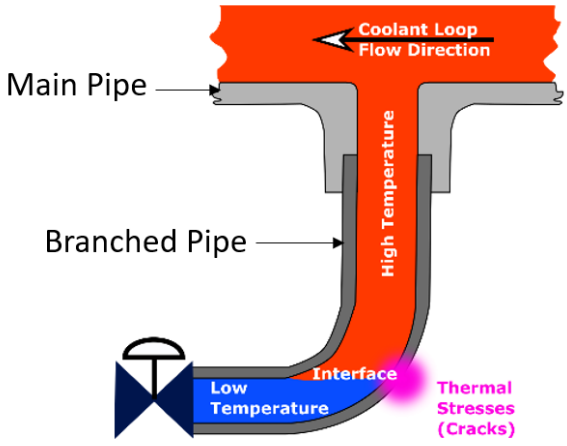


Figure 4-3. CVC system elbow pipe subjected to thermal stratification.

In relation to the I-ERM framework (Figure 3-1), the scope of the case study covers the PPoF Analysis, MOA, and ERAA modules. The outputs from this analysis (i.e., PPoF-MOA-ERAA) can be connected to other modules in I-ERM, such as PRA, GRA, and Financial Analysis, using the methodologies developed in Chapter 3. Below, Subsection 4.2.1 describes the development of the ERAA module for the case study. In Subsection 4.2.2, an FEA-based PoF model for thermal fatigue, induced by the fluctuating thermal stratification layer, is developed, and UQ is conducted to make the PoF model probabilistic, generating the PPoF analysis. The PPoF Analysis module is then used to estimate the physical transition rates as inputs to the renewal process model in ERAA. Subsection 4.2.3 shows the estimation of the maintenance input parameters of the ERAA module. The results of the probabilistic failure metrics, including leak and rupture probabilities, are reported in Subsection 4.2.4. Subsection 4.2.5 shows sensitivity studies and discussion of the results.

4.2.1 Developing a Renewal Process Model for the ERAA Module of the I-ERM Framework

For the ERAA module, a Multi-Phase Markov Process (MPMP) model [182] is used since it can model maintenance activities that occur on a discrete pre-defined schedule, such as in-service inspection (ISI), more realistically than the continuous-time or discrete Markov chain, where the impact of such maintenance activities is averaged over time. For the case study in this chapter, the MPMP model is developed considering eight damage states:

- New: No axial defect with crack depth greater than 3 mm on the inner surface.
- Flaw: An axial partial through-wall crack (PTWC) with crack depth exceeding 3 mm but smaller than 80% wall thickness.
- $Leak_0$: A PTWC reaching 80% wall thickness, with a leak rate lower than the minimum leak detection limit of the Leakage Monitoring System (LMS). Based on the Standard Technical Specification for a Westinghouse PWR plant [183], the minimum detectable leak rate of 0.05 gpm is selected.
- $Leak_1$: A TWC with a leak rate more than 0.05 gpm but less than 1 gpm. Per the Standard Technical Specification for the Westinghouse PWR plant [183], if an unidentified leakage from RCS exceeds 1 gpm, the plant needs to be shut down.
- $Leak_2$: A TWC with a leak rate greater than 1 gpm.

- Rupture: A PTWC or TWC becomes unstable and satisfies the rupture criteria.

- Two repair states, Leak Repair$_1$ and Leak Repair$_2$, representing the repair from the Leak$_1$ and Leak$_2$ states initiated by the leak detection during operation, respectively.

In the MPMP model, two phases are considered: (i) Operational Phase, which represents the time during which the plant is operating normally; and (ii) ISI Phase, which corresponds to the timing of flaw and leak inspections based on the ISI program occurring during refueling outages. During the Operational Phase, the component is subjected to both physical degradation and maintenance resulting from leak detection by LMS. In the ISI Phase, as well as during the Operational Phase, if the component is in the LeakRepair$_1$ and LeakRepair$_2$ states, it is assumed that the component is not subjected to the active physical degradation mechanism but is subjected to maintenance in the form of flaw or leak inspections and subsequent repair. It should be noted that in this chapter, the variable t refers only to the operational time of the component. Thus, while the MPMP model does capture the effects of in-service inspection and maintenance activities during refueling outages, these effects are assumed to occur instantaneously.

Figure 4-4 shows the MPMP model structure, including the transition rates associated with physical degradation and maintenance processes as well as the transition probabilities associated with ISI and subsequent repair actions during refueling outages. The Operational Phase is modeled as a continuous-time Markov process model. Meanwhile, maintenance actions during refueling outages (i.e., at the preplanned, discrete timing) cause discontinuities in the Markov model. These discontinuities are modeled by the ISI Phase, which includes flaw and leak inspections and repair. The outcome of a discontinuity occurring at a specific timepoint is modeled as a re-initialization of the continuous-time Markov process model by re-allocating the state probability distributions at the timepoint of the discontinuity. This re-allocation is modeled using a delta function which models both the timing and effect of the ISI maintenance event. To model the ISI Phase, a transition probability and transition rule are assigned to each transition that may occur during the refueling outages. Four transitions are included in the ISI Phase: (i) Flaw detection and repair (R_{FD}, P_{FD}), (ii) Leak$_0$ detection and repair (R_{LD0}, P_{LD0}), (iii) Leak$_1$ detection and repair (R_{LD1}, P_{LD1}), and (iv) Leak$_2$ detection and repair (R_{LD2}, P_{LD2}). As an example, to define the transition rule associated with Flaw detection and repair (R_{FD}), the transition will only occur at timepoints when flaw inspections occur, defined as $t = t_h$ for a total of N_f flaw inspections where ($h = 1 \ldots N_f$). The component must be in the Flaw state at $t = t_h$ for the transition to occur, where the component will transition to the New state with the transition probability P_{FD}. For the remaining three transitions, the timing is the same, and the transition may occur at timepoints when leak inspections occur, defined as $t = t_i$ for a total of N_m flaw inspections where ($i = 1 \ldots N_m$). The rules for transitions R_{LD0}, R_{LD1}, and R_{LD2}, specify that the component must be in the Leak$_0$,

Leak$_1$, or Leak$_2$ state respectively at $t = t_i$, and in each case will transition to the New state with probability P_{LD0}, P_{LD1}, or P_{LD2}, respectively.

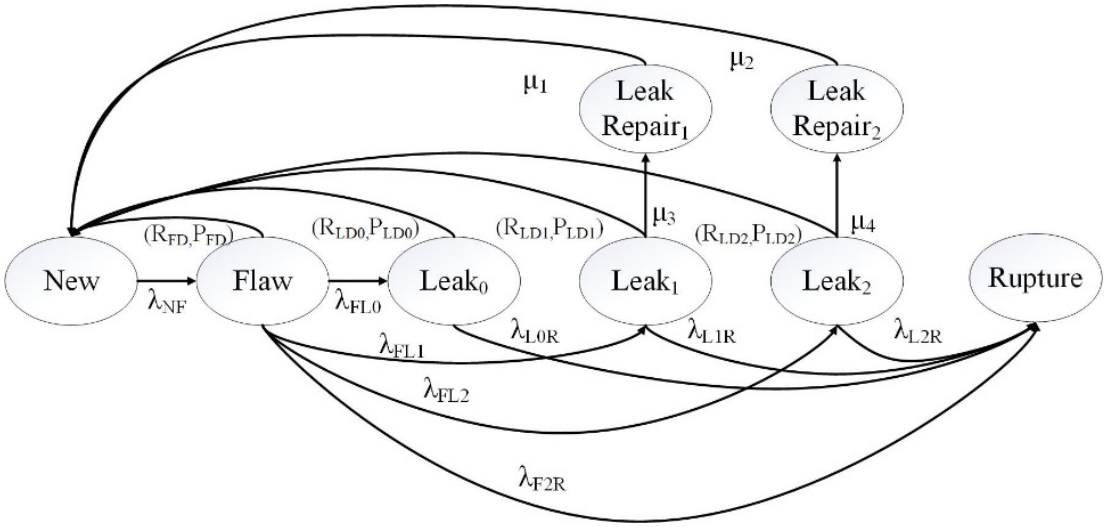


Figure 4-4. A Multi-Phase Markov Process (MPMP) model structure.

To solve the MPMP model, a vector defining the time-dependent state probabilities of the MPMP model is defined as [$N(t)$, $F(t)$, $L_0(t)$, $L_1(t)$, $L_2(t)$, $R(t)$, $LR_1(t)$, $LR_2(t)$] where the corresponding states are New, Flaw, Leak$_0$, Leak$_1$, Leak$_2$, Rupture, LeakRepair$_1$, and LeakRepair$_2$. At $t = 0$, the component is assumed to begin its lifetime in the New state (i.e., no axial surface defect with crack depth greater than 3 mm). This initial condition is used to solve the set of differential equations:

$$\frac{dN(t)}{dt} = -\lambda_{NF}N(t) + \sum_{k=1}^{2}[LR_k(t)\mu_k] + \sum_{i=1}^{N_m}\sum_{j=0}^{2}\left[L_j(t)P_{LDj}\delta(t-t_i)\right] + \sum_{h=1}^{N_f}[F(t)P_{FD}\delta(t-t_h)], \tag{29}$$

$$\frac{dF(t)}{dt} = \lambda_{NF}N(t) - \sum_{h=1}^{N_f}[F(t)\,P_{FD}\delta(t-t_h)] - (\lambda_{FR} + \lambda_{FL0} + \lambda_{FL1} + \lambda_{FL2})F(t), \tag{30}$$

$$\frac{dL_0(t)}{dt} = \lambda_{FL0}F(t) - \sum_{i=1}^{N_m}[L_0(t)\,P_{LD0}\delta(t-t_i)] - (\lambda_{L0R})L_0(t), \quad (31)$$

$$\frac{dL_1(t)}{dt} = \lambda_{FL1}F(t) - \sum_{i=1}^{N_m}[L_1(t)\,P_{LD1}\delta(t-t_i)] - (\lambda_{L1R} + \mu_3)L_1(t), \quad (32)$$

$$\frac{dL_2(t)}{dt} = \lambda_{FL2}F(t) - \sum_{i=1}^{N_m}[L_2(t)\,P_{LD2}\delta(t-t_i)] - (\lambda_{L2R} + \mu_3)L_2(t), \quad (33)$$

$$\frac{dLR_1(t)}{dt} = \mu_3 L_1(t) - \mu_1 LR_1(t), \quad (34)$$

$$\frac{dLR_2(t)}{dt} = \mu_4 L_2(t) - \mu_2 LR_2(t), \quad (35)$$

$$\frac{dR(t)}{dt} = \lambda_{L0R}L_0(t) + \lambda_{L1R}L_1(t) + \lambda_{L2R}L_2(t) + \lambda_{FR}F(t). \quad (36)$$

where δ is the delta function. The degradation transition rates (λ_{NF}, λ_{FR}, λ_{FL0}, λ_{FL1}, λ_{FL2}, λ_{L0R}, λ_{L1R}, and λ_{L2R}) are estimated from the PPoF Analysis module (Subsection 4.2.2), while the maintenance transition rates and probabilities ($\mu_1, \mu_2, \mu_3, \mu_4$, P_{FD}, P_{LD0}, P_{LD1}, and P_{LD2}) are estimated from the MOA module (Subsection 4.2.3).

4.2.2 Development of the FEA-based PPoF Analysis Module of the I-ERM Framework

Subsection 4.2.2.1 shows the development of the FEA-based PoF model for thermal fatigue caused by the fluctuating thermal stratification layer. Subsection 4.2.2.2 describes the UQ for the FEA-based PoF model to generate the PPoF Analysis module of the I-ERM framework. Subsection 4.2.2.2 also describes the estimation of the physical transition rates as inputs to ERAA.

4.2.2.1 Development of the FEA-based PoF model

The FEA-based PoF model for thermal fatigue (Figure 4-1) consists of six submodels, including (1) thermal fluid dynamics, (2) thermomechanical response, (3) crack initiation, (4) crack propagation, (5) leakage, and (6) crack instability. The development of each submodel is described below.

Thermal Fluid Dynamics:

The spatiotemporal fluid temperature distribution at the interface level ($T_f(z,t)$) is assumed to follow a hyper-tangent function as follows [184-186]:

$$T_f(z,t) = \frac{T_{f,h} - T_{f,c}}{2}\tanh[f_s \cdot g_1(z,t)] + \frac{T_{f,h} + T_{f,c}}{2},$$

where:

$$g_1(z,t) = z - (z_0 + D(t)), \tag{37}$$

$$D(t) = \frac{2d_{SL}}{t_f t},$$

z: Vertical coordinates of the nodes on the pipe (mm)

t: Time (sec)

$T_{f,h}$: Hot fluid temperature (Table 4-1)

$T_{f,c}$: Cold coolant temperature (Table 4-1)

t_f: Period of the cyclic thermal stratification layer (Table 4-1)

f_s: A factor related to the thickness of the stratification layers representing the region that has a temperature gradient when transitioning from the cold layer to the hot layer (Table 4-1)

d_{SL}: Half displacement of the stratification layer in one cycle (Table 4-1)

z_0: The initial centroid position of the stratification layer (Table 4-1)

Table 4-1. Parameters of the Thermal Fluid Dynamics Submodel.

ζ_1: Operating conditions		
Hot fluid temperature, $T_{f,h}$	560.93 (K)	[187]
Cold fluid temperature, $T_{f,c}$	444.26 (K)	[187]
Period of the cyclic stratification layer, t_f	100 (sec)	[187]
η_1: Model parameters for fluid temperature distribution		
Factor related to the thickness of the stratification layers, f_s	10	[186]
Half displacement of the stratification layer in one cycle, d_{SL}	8 (mm)	[186]
The initial centroid position of the stratification layer, z_0	-108 (mm)	[186]
ζ_2: Heat transfer coefficients		
Heat transfer coefficient on the inner surface of the pipe, h_i	1.784 (mW/mm^2·K)	Calculated based on $T_{f,h}$-$T_{f,c}$ [181]
Heat transfer coefficient on the outer surface of the pipe, h_o	0.01 (mW/ mm^2·K)	Engineering Judgment

Additionally, the heat transfer coefficients ($\boldsymbol{\zeta}_2$), including those at the inner (h_i) and outer (h_o) surfaces, are obtained. h_i is estimated by an engineering correlation developed in Ref. [181]. h_o is estimated based on engineering judgment by the authors with consideration of the range of natural convection flow heat transfer coefficients.

Thermal Stress Analysis:

The 3-D FEA is performed using a commercial software ABAQUS [188]. The fluid temperature distribution in Equation (37) and the heat transfer coefficients h_i and h_o are treated as the boundary conditions. The initial condition is calculated given the initial centroid position of the stratification layer (z_0). The FEA inputs for geometrical characteristics and material properties are listed in Table 4-2. A coupled thermal-stress analysis is conducted in ABAQUS to obtain the spatiotemporal stress and temperature distribution, which are provided as the inputs to other PoF submodels.

Table 4-2. Inputs to Finite Element Analysis of Thermomechanical Response Submodel

	Values (SI-mm)	Reference
ζ_3: Geometrical characteristics		
Inner diameter, d_i	66.65 (mm)	Design Information
Wall thickness, d_w	11.125 (mm)	Design Information
Radius of the elbow part, θ	125 (mm)	[186]
Vertical extension	400 (mm)	Design Information
Horizontal extension	100 (mm)	Design Information
ζ_4: Material properties (stainless steel type 316)		
Density	8.0E-9 (T/mm^3)	[189]
Specific heat	Temp. dependent	[189]
Thermal conductivity	Temp. dependent	[189]
Young's modulus	Temp. dependent	[189]
Poisson ratio	0.3	[189]
Thermal expansion coefficient	Temp. dependent	[189]
True stress-strain curve	Temp. dependent	[190]

Crack initiation:

The spatiotemporal stress distribution $\sigma(\chi, 0, t)$ and temperature distribution $T(\chi, 0, t)$ of the selected surface nodes (χ) are extracted from the FEA and used as inputs to the S-N-P curves for stainless steel types 306 and 316 in the water environment adopted from NUREG-6674 [191]. If the time to initiation is less than the component lifetime (t_{lt} = 60 years), it is assumed that a semi-elliptical axial crack at the inner surface of an elbow pipe is initiated.

Crack propagation:

An initiated crack can propagate from the inner surface to the outer surface if the calculated SIF is greater than a threshold value by assuming Mode I behavior (i.e., the direction of the crack growth is always perpendicular to the applied stress). The crack propagation rate is calculated using an engineering correlation for the water environment adopted from ASME BPVC.CC.NC.XI [176].

$$\frac{da}{dN} = C S_T S_R S_{ENV} (K_{\max} - K_{\min})^{2.25},$$

$$C = \begin{cases} 9.10E-6 & for\ K_{max} - K_{min} \geq K_{th} \\ 0 & for\ K_{max} - K_{min} < K_{th} \end{cases}, \qquad K_{th} = 1.1\ \text{MPa}\sqrt{\text{m}},$$

$$S_T = \begin{cases} e^{-\frac{2516}{T_K}} & \text{for } 423.15 \leq T_K \leq 616.15 \\ (3.39\text{E-}5) e^{\left[-\frac{2516}{T_K} - 0.0301 T_K\right]} & \text{for } 293.15 \leq T_K < 423.15 \end{cases}, \tag{38}$$

$$S_R = \begin{cases} 1.0 & \text{for} \frac{K_{min}}{K_{max}} < 0 \\ 1 + e^{8.02\left[\frac{K_{min}}{K_{max}} - 0.748\right]} & \text{for } 0 \leq \frac{K_{min}}{K_{max}} < 1.0 \end{cases},$$

$$S_{ENV} = \left(\frac{t_f}{2}\right)^{0.3}$$

where, $K_{\max}$ is the maxium SIF and K_{min} is the minimum SIF at the crack tip. T_K is obtained from the average of the maximum and minimum values of the spatiotemporal temperature distribution $T(\chi, r, t)$ extracted from FEA. The SIF is computed using the an analytical model adopted from article A-3411 (c) of ASME BPVC.XI.1 2019 [192].

$$K_I = \left[(B_0 + P)G_0 + B_1\left(\frac{a}{d_w}\right)G_1 + B_2\left(\frac{a}{d_w}\right)^2 G_2 + B_3\left(\frac{a}{d_w}\right)^3 G_3 + B_4\left(\frac{a}{d_w}\right)^4 G_4\right]\sqrt{\frac{\pi a}{Q}},$$

$$Q = \psi - q_y,$$

$$\psi = 1 + 1.4593\left(\frac{a}{2c}\right)^{1.65}, \tag{39}$$

$$q_y = \frac{1}{6}\left\{\frac{\left[(B_0+P)G_0 + B_1\left(\frac{a}{d_w}\right)G_1 + B_2\left(\frac{a}{d_w}\right)^2 G_2 + B_3\left(\frac{a}{d_w}\right)^3 G_3 + B_4\left(\frac{a}{d_w}\right)^4 G_4\right]}{\sigma_y\left(T(\chi,a,t)\right)}\right\}^2,$$

where a is the crack depth, c is the half crack length, and P is the internal pressure. The temperature-dependent yield strength, $\sigma_y(T(\chi, a, t))$, is obtained by interpolating the data for stainless steel type 316 in ASME BPVC.II.D [189], where the corresponding wall temperature $T(\chi, a, t)$ is extracted from the FEA results. The coefficients G_0, G_1, G_2, G_3, and G_4 are obtained from article A-3552 of ASME BPVC.XI.1

2019 [192] for a semi-elliptical axial PTWC. The coefficients B_0, B_1, B_2, B_3, and B_4 are obtained by fitting the hoop stress through the thickness obtained from the FEA results to the polynomial in Equation (40), where d_w is the wall thickness:

$$\sigma_h(a) = B_0 + B_1\left(\frac{a}{d_w}\right) + B_2\left(\frac{a}{d_w}\right)^2 + B_3\left(\frac{a}{d_w}\right)^3 + B_4\left(\frac{a}{d_w}\right)^4. \quad (40)$$

The calculated SIF is used to update the crack propagation rate and obtain an updated crack depth until the threshold of the damage (i.e., 80% of wall thickness) is reached.

Leakage:

If the crack reaches 80% wall thickness, but the rupture criteria are not satisfied, COD and RTH for the semi-elliptical crack are computed for selecting an adequate leak rate model [193]. The COD solutions are adopted from Kim et al. [194] for a constant depth TWC. As an input, the temperature-dependent yield strength extracted from the FEA outputs is considered. The threshold for the two-phase flow ($RTH_{tp} = 30$) and the single-phase flow ($RTH_{sp} = 4.6$) are adopted from the PRO-LOCA code specification [193]. The Henry and Fauske models [195-197] are used to obtain the leakage rates for a two-phase flow (RTH >30). A single-phase flow model from PRAISE [165, 198-200] is applied for a single-phase flow (RTH <4.6). For RTH between 4.6 and 30, the transition-flow model from PRO-LOCA [193] is applied. If the calculated leak rate is greater than or equal to 1 gpm, the crack transitions to $Leak_2$. If the calculated leak rate is smaller than 1 gpm but greater than or equal to 0.05 gpm, the crack transitions to $Leak_1$. If the calculated leak rate is smaller than 0.05 gpm, the crack transitions to $Leak_0$.

Crack instability:

Once the crack becomes unstable, the crack is assumed to transition to the Rupture state. A rupture is determined when the burst pressure is less than or equal to the internal pressure or the maximum SIF is greater than or equal to the fracture toughness of stainless steel type 316. This study adopts a burst pressure model proposed by Wang and Zhou [201] for a corroded elbow with an axial semi-elliptical defect:

$$P_b = \frac{2f_c}{\sqrt{4 - 2f_c + {f_c}^2}} \frac{d_w \sigma_y\left(T_{\text{avg}}(\chi, a)\right)}{R_m} \frac{\left(1 - \frac{a}{d_w}\right)}{\left(1 - \frac{a}{d_w Q'}\right)}, \quad (41)$$

where $f_c = \frac{R+R_m \sin\theta}{R+\frac{1}{2}R_m \sin\theta}$ and $Q' = \sqrt{1+\frac{0.31(2c)^2}{(d_i+2*d_w)d_w}}$. R is the neutral line bend radius (125 mm for this case study as shown in Table 4-2). R_m is the mean radius of the pipe. θ is angle of the elbow part ($\pi/2$). $\sigma_y\left(T_{\text{avg}}(\chi,a)\right)$ is the temperature-dependent yield strength, where the time-averaged temperature $T_{\text{avg}}(\chi,a)$ is obtained by averaging the time profile of the temperature at location χ and depth a during the cycle extracted from the FEA.

4.2.2.2 Uncertainty Quantification and Estimation of Physical Transition Rates as Inputs to ERAA

To quantify the aleatory uncertainty associated with the crack locations, based on the FEA results, the FEA nodes in the elbow region with non-negative hoop stress are collected as potential crack initiation sites. These potential crack locations are screened using two criteria. First, the nodes with the maximum hoop stress greater than the yield strength are identified as the vulnerable places for crack initiation. For instance, Figure 4-5 (a) and (b) show the hoop stress and the temperature distribution for the FEA nodes on the inner surface along the center line of the elbow pipe. The hoop stress for each node shown in Figure 4-5 (a) is plotted for four periods in Figure 4-6.

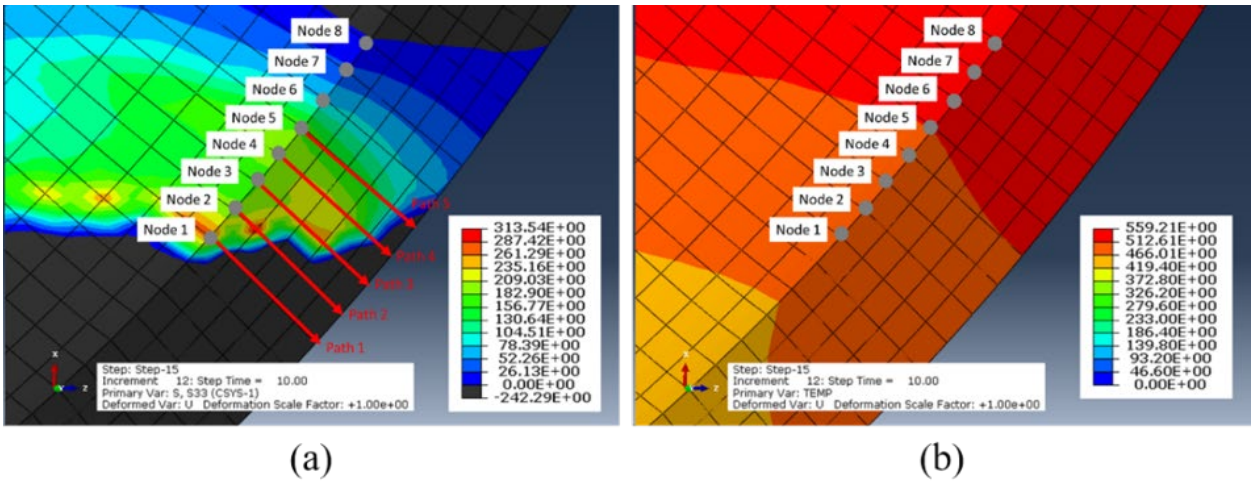


Figure 4-5: (a) Hoop stress and (b) Temperature distribution along the inner surface of the elbow at the halfway point in the second period (t_f = 100 sec).

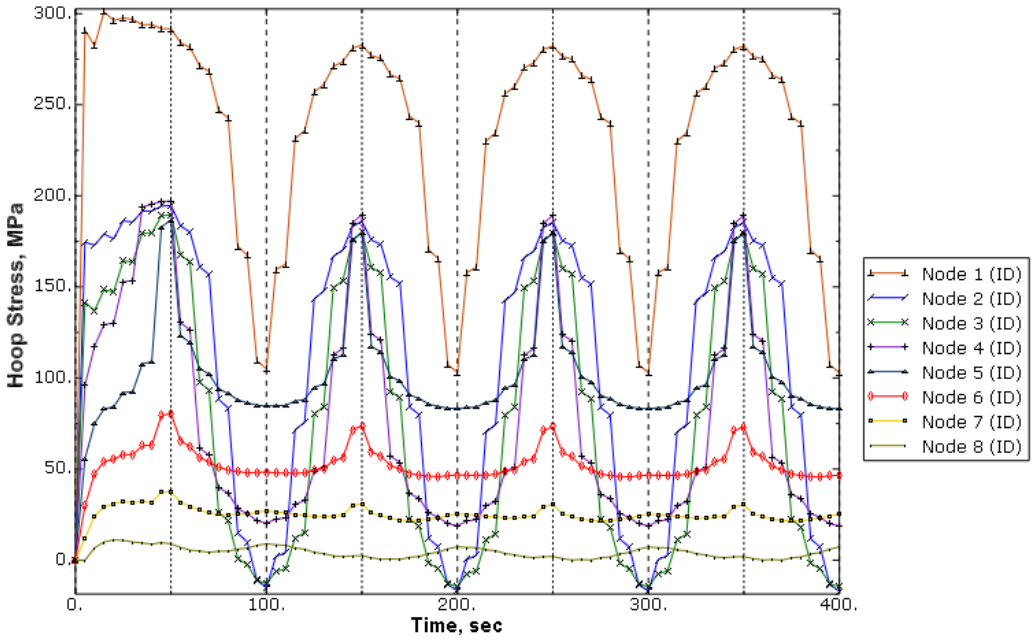


Figure 4-6: Time profile of hoop stress at Node 1 to Node 8 in Figure *4-5 (a).*

As shown in Figure 4-6, the hoop stresses in the first period of the cycle are sensitive to the initial conditions, while a limited variation is observed among the second, third, and fourth periods; thus, the results of the second period of the cycle are applied for all selected nodes. During the second period, the maximum hoop stress occurs at the halfway point of the cycle (at 150 sec), while the minimum hoop stress occurs at the end of the cycle (at 200 sec). In Figure 4-7, the yield strength calculated, based on the temperature obtained at 150 sec, is compared with the maximum hoop stress at the halfway point of the second cycle.

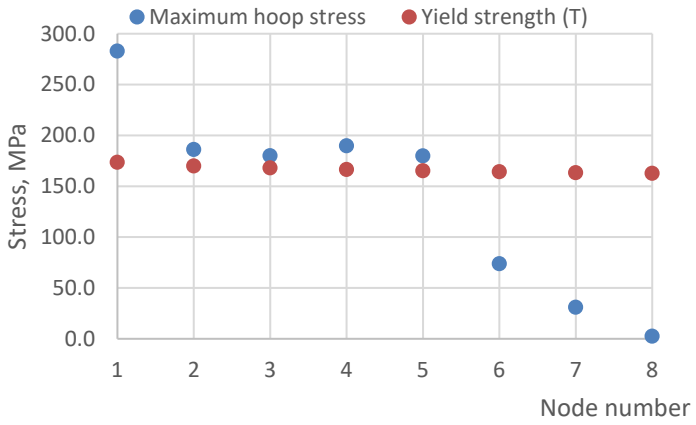


Figure 4-7: Comparison of maximum hoop stress vs. yield strength for each node in Figure 4-5.

Figure 4-7 indicates, among the eight nodes in Figure 4-5, the five locations where it is possible to initiate a crack based on the first criterion. Repeating this process for all nodes around the thermal stratification layer, a total of 42 locations are identified as potential crack initiation sites. The second criterion is then considered by evaluating the impact of the hoop stress range, defined as the difference between the maximum and minimum hoop stresses, on the transition rate from New to Flaw (λ_{NF}). It is found that the hoop stress range below 120 MPa has a negligible impact on the point estimate of λ_{NF}; therefore, the FEA nodes with the hoop stress range greater than 120 MPa are retained for further analysis. As a result, 18 locations are retained as crack initiation sites.

The aleatory uncertainty associated with the S-N-P curves is characterized by a standard cumulative normal distribution [191]. For each location, an S-N curve is randomly sampled from the S-N-P curves for estimating the time to crack initiation. The location with the minimum time to crack initiation is assumed to be the crack initiation site, where the crack can propagate along the radial direction as highlighted by red arrows shown in Figure 4-5 (a) if the threshold of SIF is satisfied, assuming Mode I behavior for a semi-elliptical axial crack.

For crack propagation, the aleatory uncertainty associated with the crack aspect ratio ($\varphi = a/2c$) is considered. Gosselin et al. [202] reviewed the thermal fatigue cracking events in the nuclear industry and identified nine events caused by thermal fatigue due to thermal stratification and turbulence penetration cycling. The crack aspect ratios for the nine events are calculated based on the crack length and depth reported in Ref. [202] and fitted to a shifted exponential distribution [203]. The K-S test result (p-value = 0.508) indicates that the shifted exponential distribution is not rejected with a 5% significance level. This study assumes that the initial crack depth is 3 mm [203], and the crack aspect ratio does not change during crack propagation.

The sample size of the Monte Carlo simulation is determined by the convergence study such that the relative half-width of the 90% credible interval, normalized by the expected value, is less than a predefined threshold 100γ% [204]:

$$\arg\min_{n>0}\left\{n \middle| \frac{\left(\lambda_{\mathrm{D1D2};\,0.95}-\lambda_{\mathrm{D1D2};\,0.05}\right)/2}{\bar{\lambda}_{\mathrm{D1D2}}} < \frac{\gamma}{1+\gamma}\right\}. \tag{42}$$

where $\lambda_{\mathrm{D1D2};\,0.95}$ and $\lambda_{\mathrm{D1D2};\,0.05}$ represent the 95th and 5th percentiles of the posterior distribution for the physical transition rate λ_{D1D2}, respectively, obtained from Bayesian updating (Subsection 4.1.2). In this

study, γ = 20% is used. The sample size is gradually increased and, when the criterion in Equation (42) is satisfied for all the transition paths that have at least one transition observed in the Monte Carlo simulation, the corresponding sample size is selected. The median, 5th and 95th percentile of the posterior distributions of the physical transition rates using the selected sample size are shown in Table 4-3.

Table 4-3. PPoF-based Estimation of the Physical Transition Rates.

Physical Transition Rates	Median [per year]	5th percentile [per year]	95th percentile [per year]
λ_{NF}	1.281E-04	1.268E-04	1.295E-04
λ_{FR}	1.486E-04	1.195E-04	1.821E-04
λ_{FL0}	2.725E-04	2.324E-04	3.171E-04
λ_{L0R}	2.910E+00	2.481E+00	3.385E+00
λ_{FL1}	5.059E-03	4.879E-03	5.244E-03
λ_{L1R}	5.018E+00	4.839E+00	5.201E+00
λ_{FL2}	4.804E-03	4.628E-03	4.984E-03
λ_{L2R}	9.036E+00	8.706E+00	9.374E+00

4.2.3 Estimating Maintenance Transition Rates as Inputs to the ERAA Module of I-ERM Framework

The maintenance transition rates, as inputs to the ERAA module, are estimated by the MOA module. In this case study, a data-driven approach, based on historical data as well as on standards and technical specifications, is utilized for estimating the maintenance transition rates since the focus of this case study is to demonstrate the application of the FEA-based PPoF analysis. The I-ERM methodological framework, however, includes a model-based MOA module, as shown in Chapter 3.

As stated in Subsection 4.2.1, two types of maintenance events are considered: (i) those initiated by scheduled ISI at discrete time points; and (ii) those initiated by leak detection by LMS.

For the first type of maintenance events initiated by ISI, three inspection strategies are considered (Table 4-4): (i) Periodic ISI using Ultrasonic Testing (UT); (ii) Visual inspection (VT-2); and (iii) Condition-based UT inspection based on the Usage Factor (UF) of the component. The first of these

strategies, UT testing for flaws, per ASME B&PV Code Section XI, Article IWB-2411 (Inspection Program), takes place during a refueling outage after 10 years have passed between inspections. The second of these strategies, VT-2, is aimed at detecting leaks and includes a visual inspection for leak evidence (e.g., boric acid crystals) during the refueling outage and a visual inspection for leaks during plant heat up and pressurization. The VT-2 inspections take place during every outage per ASME B&PV Code Section XI, Article IWA-2212 and Article IWB-5222(a). The third strategy, the condition-based UT inspection based on UF, is performed using NDE when the computed UF exceeds 1. The calculation of UF is done based on ASME BPVC.III.A-2017, Mandatory Appendix XIII, XIII-3520. The probability of detection (POD) of the inspection and the timing of each ISI event used in this case study are summarized in the third column of Table 4-4.

Table 4-4. Inspection Strategies and the Corresponding Transition Probabilities.

Inspection Strategies	Timing	Transition Probabilities
ASME Section XI: UT	The first planned outage after a ten-year period	$P_{FD} = 0.894$
ASME Section XI: VT-2	Every planned outage (every 18 months)	$P_{LD} = 0.990$
Condition-based Inspection (Usage Factor): UT	Determined based on the fatigue design curve and the period of cyclic stress	$P_{FD} = 0.894$

For the second type of maintenance event due to leak detection by LMS, the maintenance-related transition rates from $Leak_1$ to $LeakRepair_1$ and $Leak_2$ to $LeakRepair_2$ (μ_3 and μ_4) are estimated using the Mean Time to Shutdown (MTTS) the reactor following the LMS alarm as specified in the Standard Technical Specification for a Westinghouse PWR plant [183]. The maintenance transition rates from $LeakRepair_1$ and $LeakRepair_2$ to the New state (μ_1 and μ_2) are estimated based on the Mean Time to Repair (MTTR), the component estimated from the U.S. Nuclear Regulatory Commission (NRC) Licensee Event Report (LER) database.

4.2.4 Case Study Results

The annual and cumulative probabilities of the Leak and Rupture states, calculated by solving the MP Markov process model, are plotted in Figure 4-8.

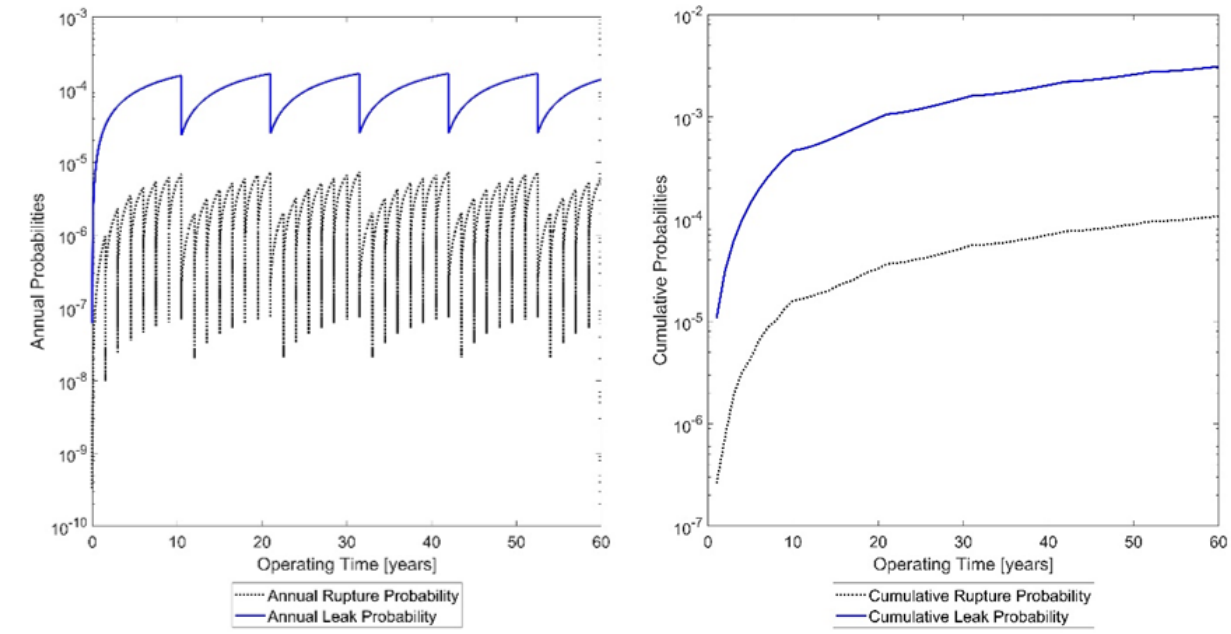


Figure 4-8. Annual and Cumulative Probabilities for Leak and Rupture States.

For the annual rupture probability (dotted line on the left plot), there are discontinuous drops at the timing of every refueling outage, representing the recovery of the leak state due to the VT-2 inspection (Table 4-4). Meanwhile, the annual leak probability (solid line on the left plot) shows the frequency of the occurrence of any leak state ($Leak_0$, $Leak_1$, or $Leak_2$) and has discontinuous drops at the timing of the UT inspections (the first planned outage after a ten-year period as shown in Table 4-4). The UT inspections can detect and repair the component in the Flaw state, reducing the frequency of the leak occurrence.

4.2.5 Sensitivity Analysis

The impact of epistemic uncertainties associated with the thermal stratification layer modeling in FEA on the estimates of the probabilistic failure metrics (i.e., leak and rupture probabilities) is investigated by conducting sensitivity analysis. Four FEA input variables are considered, including (i) the heat transfer coefficient on the inside surface h_i, (ii) fluid temperature difference across the stratification layer $T_{f,h}-T_{f,c}$, (iii) the period of the cycles t_f, and (iv) displacement of the thermal stratification layer d_{SL}. Aside from the baseline case, four sensitivity cases are analyzed as listed in Table 4-5.

Spain et al. [205] reported that $T_{f,h}-T_{f,c}$ can range from 116.67 to 244.44 K. While the baseline case used the lower bound of this range (116.67 K), the four sensitivity cases analyzed the impact of assuming the upper bound of this range (244.44K). h_i for both the baseline case and the sensitivity cases are computed using an engineering correlation developed in Ref. [181]. Among Cases 1 to 3, t_f is varied based on the

range reported by Spain et al. [205]. In Case 4, the d_{SL} of Case 2 is changed based on the range reported by Spain et al. [205] The annual leak and rupture probabilities at 60 years, computed for the baseline case as well as the sensitivity cases, are compared in Figure 4-9.

Table 4-5. Sensitivity Cases and Input Parameters

Parameters	h_i [mW/mm^2·K]	$T_{f,h}-T_{f,c}$ [K]	t_f [sec]	d_{SL} [mm]	Description
Baseline	1.784	116.67	100	8	Based on Table 4-1
Case 1	1.920	244.44	120	8	$T_{f,h}-T_{f,c}$ is the upper bound in Ref. [205]; t_f is within the range reported in Ref. [205]
Case 2	1.920	244.44	300	8	$T_{f,h}-T_{f,c}$ is the upper bound in Ref. [205]; t_f is within the range reported in Ref. [205]
Case 3	1.920	244.44	360	8	$T_{f,h}-T_{f,c}$ is the upper bound in Ref. [205]; t_f is within the range reported in Ref. [205]
Case 4	1.920	244.44	300	66.65	$T_{f,h}-T_{f,c}$ is the upper bound in Ref. [205]; t_f is within the range reported in Ref. [205]; d_{SL} is the upper bound in Ref. [205]

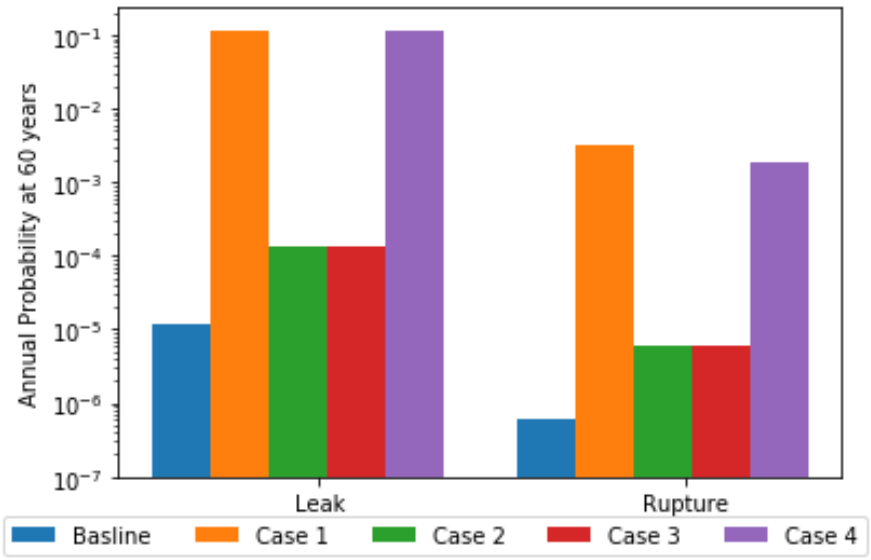


Figure 4-9. Annual Leak and Rupture Probabilities at 60 Years for Sensitivity Cases.

Based on Figure 4-9, the baseline case leads to the lowest leak and rupture probabilities, while the annual probabilities for Cases 1 and 4 are significantly higher (by several orders of magnitude) than the baseline case. The results indicate that the epistemic uncertainties associated with the thermal stratification layer modeling in FEA, especially the ones for $T_{f,h}-T_{f,c}$ and d_{SL}, can have a significant impact on the estimates of the leak and rupture probabilities; thus, more structured quantification of epistemic uncertainties would be required. To address this gap, ongoing research by some of the authors [124, 180] advances UQ for simulation models used in PRA by developing a Probabilistic Validation (PV) methodology. PV consists of theoretical and methodological foundations to identify, characterize, and propagate sources of epistemic uncertainties in the simulation models, rank them based on their uncertainty contribution, and utilize the uncertainty information in risk-informed decision-making. Beal et al. [14] presented a preliminary algorithm to implement PV for the MOA module in I-ERM, which is being extended in ongoing research by some of the authors.

4.3 Summary

To analyze the relationships between safety and financial performance and inform Enterprise Risk Management (ERM) of nuclear power plants (NPPs), Chapter 2 covers a categorical review of relevant literature as well the theoretical bases that support the methodological developments. Chapter 3 introduces an Integrated Enterprise Risk Management (I-ERM) methodological framework to quantify the interconnections of safety and financial performance with a focus on operation and maintenance (O&M) of

NPPs. In Chapter 3, the applicability and values of the I-ERM methodology have been also highlighted by applying I-ERM to an NPP case study.

Compared to existing studies, the I-ERM methodology, explicitly incorporates maintenance performance, coupled with physical failure mechanisms, into safety and the financial performance. The "explicit incorporation" means that the physical and maintenance causal factors are treated explicitly as inputs so that the sensitivity of the safety and financial performance to these inputs can be quantified. In Chapters 2 and 3, the explicit causal connection of the maintenance performance model to safety and the financial performance has been developed, while the physical failure behavior of components has been treated by a data-driven approach. This chapter advances the physical failure modeling for components by developing an advanced probabilistic physics-of-failure (PPoF) analysis, coupling it with the maintenance performance, and connecting the physics-maintenance coupling to safety and financial performance.

The PPoF development in this chapter focuses on thermal fatigue since the operating experience shows that thermal fatigue is one of the dominant failure mechanisms that has led to safety- and cost-significant events at NPPs. Additionally, in the authors' perspective, thermal fatigue is the failure mechanism that can benefit the most from the enhanced resolution by the advanced PPoF analysis as it involves highly spatial and temporal physical phenomena. The explicit incorporation of a physics of failure model into the PPoF Analysis module of I-ERM in this chapter, combined with other modules of I-ERM developed in Chapters 2 and 3 of this report, allows for the possibility of incorporating physics-maintenance coupling into the safety and financial performance analysis of NPPs.

This chapter makes two methodological contributions. One is that this research is the first to incorporate finite element analysis (FEA) into the PPoF model of thermal fatigue for NPP components. FEA can calculate location-specific and time-dependent stress and temperature distributions, which are then used as inputs to the PoF models for the subsequent physical subprocesses such as crack initiation, crack propagation, leakage, and crack instability. The incorporation of the spatiotemporal FEA can enhance the resolution of the PPoF analysis by excluding the need for simplified assumptions to reduce the spatial and temporal dimensions (e.g., using the maximum, minimum, or average stress and temperature over time and space) or analytical stress and temperature solutions derived with reduced spatial and temporal dimensions. The other contribution is that this research advances the probabilistic interface between the PPoF analysis and a renewal process model, used for computing component reliability and availability in the I-ERM framework. The interface developed in previous research [140] is advanced by (i) adding a computational procedure to deal with aleatory uncertainty associated with crack locations using the spatial stress and temperature distributions from FEA; and (ii) equipping it with a Bayesian updating method using the right-

censored data as evidence so that the physical transition rates of the renewal process model can be estimated efficiently, even when a majority of the PPoF outputs consists of success data. The advanced PPoF analysis and its coupling with the renewal process model are applied to an excess letdown elbow piping subjected to thermal fatigue due to thermal stratification in the chemical and volume control system of a Pressurized Water Reactor. The leak and rupture probabilities are computed with explicit incorporation of underlying physics-of-failure and maintenance characteristics.

The sensitivity study (Subsection 4.2.5) shows that the estimations of the leak and rupture probabilities are sensitive to the FEA inputs related to the thermal stratification layer modeling. To address this challenge, two directions of future research are suggested. The first research direction is an advancement in the uncertainty analysis, especially the characterization and propagation of epistemic uncertainties for the thermal stratification layer modeling. The PI's research team, in their ongoing work [14, 124, 180], is developing a Probabilistic Validation (PV) methodology for comprehensive uncertainty analysis for simulation models used in probabilistic risk assessment (PRA). PV will be implemented for the I-ERM framework in future work. The second research direction is to further improve the resolution of the PoF model with a focus on thermal stratification layer modeling. Ongoing research by the PI's research team is evaluating coupled Computational Fluid Dynamics (CFD) and FEA, which can solve the temperature distribution in fluid and piping material simultaneously, instead of adopting a separate analytical model for the fluid temperature distribution; namely, a hyper-tangent function in Equation (37).

5. Conclusions

The objective of this project is to theorize and quantify the relationships between safety and the financial performance of nuclear power plants (NPPs). In this research, safety refers to both occupational safety and system safety (estimated from Probabilistic Risk Assessment, PRA), and financial performance refers to the monetary values associated with NPP operation and maintenance (O&M) strategies. A comprehensive description of the work conducted, including theoretical bases, methodologies, results, and products are provided in this report.

The Socio-Technical Risk Analysis (SoTeRiA) theoretical framework (Figure 1-1), which connects the social aspects (e.g., safety culture) and structural features (e.g., safety practices) of an organization with organizational safety and financial risks, is used to theorize the direct and indirect relationships between safety and the financial performance of NPPs. In Chapter 2, the justifications and theoretical bases for the new model-based approach are established. Theoretical causal models are developed for (i) direct causal paths from safety to financial performance; and (ii) indirect causal paths between safety and financial performance through a maintenance unit process.

In Chapter 3, based on the theoretical bases developed in Chapter 2, an Integrated Enterprise Risk Management (I-ERM) methodological framework is developed to operationalize SoTeRiA to quantify NPP safety and financial performance in a unified platform, where the underlying physical degradation mechanisms, coupled with maintenance performance (considering human and organizational factors), are explicitly incorporated to depict the interconnections and dependencies between safety and financial performance. The development of explicit maintenance models and the coupling with physics-of-failure models enable the explicit consideration of the interconnections and dependencies between safety and financial performance. The I-ERM methodological framework aids NPP decision-making by providing a higher resolution model to identify cost-saving O&M strategies that satisfy safety requirements.

In Chapter 4, detailed development and implementation of one of the I-ERM module, i.e., probabilistic physics-of-failure (PPoF) analysis and the connection of the PPoF analysis with safety and the financial performance are provided. The physical failure modeling for hardware components is advanced by incorporating finite element analysis (FEA) into PPoF analysis and coupling the FEA-based PPoF with the maintenance performance through a renewal process model. Through the incorporation of FEA, the resolution of the PPoF analysis is enhanced as spatiotemporal conditions such as stress and temperature can be considered explicitly instead of relying on simplified assumptions or analytical models with reduced spatiotemporal dimensions. An application of the FEA-based PPoF analysis and its coupling with

maintenance through the renewal process model are demonstrated using a case study of a reactor coolant pressure boundary pipe.

Compared to previous relevant studies, the approach offered in this research makes the following key contributions:

1. Theorizes financial consequences of system accidents, system incidents, and occupational accidents of NPPs in a unified causal model as, previously, there was no such combinatory model.

2. Adds realism to (i) modeling the influence of maintenance performance on financial performance, (ii) modeling the influence of maintenance performance on safety, and (iii) modeling the interconnections of safety and financial performance by creating an integrated methodological environment (I-ERM) that can quantify the causal effects of maintenance performance on both safety and financial performances in a unified, multi-level platform. For the component-level analysis of I-ERM, this research explicitly incorporates models of maintenance performance and physics-of-failure into a multi-phase Markov process model. The previous studies relied on data-driven approaches and/or expert judgment for quantification of the maintenance parameters as inputs to the Markov model. The data-driven approaches are challenging especially if (a) the system being analyzed is new and has limited or no operational data; or (b) the system has undergone significant modifications such as redesign and maintenance policy updates and, thus, its historical data are not relevant to the current system conditions. To address this gap, the proposed approach in this research explicitly incorporates causal models of maintenance performance and FEA-based PPoF analysis into a multi-phase Markov process model. In I-ERM, the outputs of the component reliability and availability are used as inputs to the system-level safety models, where the production loss scenarios and the safety risk scenarios are constructed and quantified. The financial performance is computed using a cost function, where the direct maintenance and the production loss costs are quantified based on the outputs from the multi-phase Markov process model, the maintenance performance model coupled with the physics-of-failure, as well as the system-level safety and production loss risk models.

Future research is recommended in the following areas:

- Expand the theoretical developments (Section 2.2) to capture deeper intra-organizational mechanisms underlying the unit work process (e.g., safety culture) and their causal paths up to safety and the financial performance of NPPs through the unit work process. In addition, the theoretical development for external factors is another area for future research. One example would

be to extend the causal model to include the legal and regulatory implications on the plant O&M so that the indirect path between safety and financial performance mediated by the impact of regulation can be analyzed explicitly.

- Advance individual I-ERM modules and their interfaces (Chapter 3) by (i) extending the Financial Analysis module to include other cost elements, such as accident damage and regulatory costs; (ii) creating an interface between PRA and Financial Analysis so that the impact of NPP accidents and incidents on the financial performance can be quantified; and (iii) evaluating other types of renewal process models for ERAA such as a semi-Markov process model and a discrete event simulation.

- Address epistemic uncertainties associated with initial and boundary conditions of the FEA-based PPoF Analysis module (Chapter 4),

    - Advance uncertainty analysis, especially characterization and propagation of epistemic uncertainties for the FEA initial and boundary conditions. The PI's team, in their ongoing work [14, 124, 180], is developing a Probabilistic Validation (PV) methodology for systematic uncertainty analysis for simulation models used in PRA. An application of PV to the I-ERM methodological framework should be investigated.

    - Improve the resolution of the PPoF model by focusing on thermal stratification layer modeling. Ongoing research by the PI's team is evaluating coupled Computational Fluid Dynamics (CFD) and FEA, which can solve the temperature distribution in fluid and piping material simultaneously, instead of adopting a separate analytical model for the fluid temperature distribution, e.g., a hyper-tangent function.

- Evaluate how the computational modules and interfaces of I-ERM developed in this project can be added to the Risk Analysis and Virtual Environment (RAVEN) framework. This addition will help further research and developments of RAVEN and practical applications by the nuclear industry.

- Apply the I-ERM framework for advanced reactors to facilitate an integration of safety risk with the financial risk associated with the operation and maintenance of advanced reactors.

    - One of the key methodological challenges for PRA of advanced reactors is that a design-specific experiential database is often limited or not available for advanced reactors, while the applicability and relevancy of the experiential data from the existing fleet to advanced reactors may be questionable due to differences in design principles, physical conditions,

and operation and maintenance procedures. A possible path to alleviate this challenge is to incorporate into PRA the simulation of underlying causality, including the interactions of physics of phenomena with human and organizational factors that drive the performance of structures, systems, and components. The integrated methodological platform generated under this project that couples physics of degradation phenomena with models of maintenance work processes (e.g., in-service inspection and repair) would be valuable for PRA of advanced reactors [13, 14].

5.1 Publication List

The publications generated in this project (as of August 31, 2021) are listed below.

5.1.1 Technical Reports

1) W.-C. Cheng, J. Beal, P. Farshadmanesh, T. Sakurahara, S. Reihani, E. Kee, Z. Mohaghegh, "Data Requirements Document Database Selection, Collection, and Reduction," Technical Report, Project ID: DE-NE0008700, Milestone ID: M3NU-17-IL-UIUC-030401-052, 2020.

2) T. Sakurahara, N. O'Shea, W.-C. Cheng, S. Zhang, S. Reihani, E. Kee, Z. Mohaghegh, "Integrating Renewal Process Modeling with Probabilistic Physics-Of-Failure for Component Reliability and Availability Analysis: Application for Estimation of Loss of Coolant Accident (LOCA) Frequencies in Nuclear Power Plants," Technical Report, Project ID: DE-NE0008700, Milestone ID: M3NU-17-IL-UIUC-030401-053, 2019.

3) J. Beal, T. Sakurahara, P. Farshadmanesh, S. Reihani, E. Kee, A. Rowell, F. Yilmaz, Z. Mohaghegh, "Coupling Probabilistic Risk Assessment with Production Loss and Equipment Availability under an Integrated Enterprise Risk Management (I-ERM) Framework for Nuclear Power Plants," Technical Report, Project ID: DE-NE0008700, Milestone ID: M3NU-17-IL-UIUC-030401-054, 2020.

4) W.-C. Cheng, J. Beal, T. Sakurahara, S. Reihani, E. Kee, Z. Mohaghegh, "Integrated Probabilistic Physics-of-Failure Framework for Incorporating the Coupling of Physical Degradation and Maintenance into Risk-informed Analyses of Nuclear Power Plants," Technical Report, Project ID: DE-NE0008700, Milestone ID: M3NU-17-IL-UIUC-030401-057, 2020.

5) P. Farshadmanesh, J. Beal, T. Sakurahara, S. Reihani, E. Kee, A. Rowell, F. Yilmaz, Z. Mohaghegh, "Financial Analysis for Integrated Enterprise Risk Management (I-ERM) of Nuclear Power Plants,"

Technical Report, Project ID: DE-NE0008700, Milestone ID: M3NU-17-IL-UIUC-030401-058, 2020.

5.1.2 Journal Articles

6) P. Farshadmanesh, J. Beal, T. Sakurahara, S. Reihani, E. Kee, A. Rowell, F. Yilmaz, Z. Mohaghegh, "Modeling Interconnections of Safety and Financial Performance of Nuclear Power Plants, Part 1: Categorical Review and Theoretical Bases," Under Review of Progress in Nuclear Energy, (2021)

7) J. Beal, T. Sakurahara, P. Farshadmanesh, S. Reihani, E. Kee, A. Rowell, F. Yilmaz, Z. Mohaghegh, "Modeling Interconnections of Safety and Financial Performance of Nuclear Power Plants, Part 2: Methodological Developments and Case Study," Under Review of Progress in Nuclear Energy, (2021)

8) W.-C. Cheng, J. Beal, T. Sakurahara, S. Reihani, E. Kee, Z. Mohaghegh, "Modeling Interconnections of Safety and Financial Performance of Nuclear Power Plants, Part 3: Spatiotemporal Probabilistic Physics-of-Failure Analysis and Its Connection to Safety and Financial Performance," Under Review of Progress in Nuclear Energy, (2021)

5.1.3 Conference Papers

9) J. Beal, T. Sakurahara, J. Pence, P. Farshadmanesh, S. Reihani, E. Kee, Z. Mohaghegh, "Coupling Degradation and Maintenance to Model Safety Risk and Financial Risk Under an Integrated Enterprise Risk Management Methodology for Nuclear Power Plants," Proceedings of 25th International Conference on Structural Mechanics in Reactor Technology (SMiRT 25), Charlotte, NC, 2019

10) J. Beal, T. Sakurahara, E. Kee, S. Reihani, Z. Mohaghegh, "Integrated Enterprise Risk Management to Synchronize Safety and Profitability Analysis for Nuclear Power Plants," Proceedings of 2020 American Nuclear Society (ANS) Winter Meeting, Online Virtual Conference, 2020

11) J. Beal, T. Sakurahara, S. Reihani, E. Kee, Z. Mohaghegh, "An Algorithm for Risk-Informed Analysis of Advanced Reactors with a Case Study of Pipe Failure Rate Estimation," Proceedings of 30th European Safety and Reliability Conference & 15th Probabilistic Safety Assessment and Management Conference (ESREL2020 & PSAM15), Venice, Italy, 2020

12) W.-C. Cheng, J. Beal, T. Sakurahara, S. Reihani, E. Kee, Z. Mohaghegh, "Integrated Probabilistic Physics of Failure Methodology to Estimate Pipe Failure Rates for Risk-Informed Analysis of

Advanced Nuclear Reactors," Proceedings of 2020 American Nuclear Society (ANS) Winter Meeting, Online Virtual Conference, 2020

5.1.4 Relevant Publications

13) H. Bui, T. Sakurahara, J. Pence, S. Reihani, E. Kee, Z. Mohaghegh, "An algorithm for enhancing spatiotemporal resolution of probabilistic risk assessment to address emergent safety concerns in nuclear power plants," Reliability Engineering & System Safety, Vol. 185, pp. 405-428, (2019)

14) T. Sakurahara, G. Schumock, S. Reihani, E. Kee, Z. Mohaghegh, "Simulation-Informed Probabilistic Methodology for Common Cause Failure Analysis," Reliability Engineering & System Safety, Vol. 185, pp. 84-99, (2019)

15) T. Sakurahara, N. O'Shea, W.-C. Cheng, S. Zhang, S. Reihani, E. Kee, Z. Mohaghegh, "Integrating renewal process modeling with probabilistic physics-of-failure: Application for estimation of loss of coolant accident (LOCA) frequencies in nuclear power plants," Reliability Engineering and System Safety, Vol. 190, 106479, (2019)

16) W.C. Cheng, T. Sakurahara, S. Zhang, P. Farshadmanesh, S. Reihani, E. Kee, Z. Mohaghegh, K. Heckmann, J. Sievers, B. Lydell, C. Zammali, X.-X. Yuan, X. Duan, R. Alzbutas, G.-G. Lee, T. Jevremovic, C. Takasugi, "Review and Categorization of Existing Studies on the Estimation of Probabilistic Failure Metrics for Reactor Coolant Pressure Boundary Piping and Steam Generator Tubes in Nuclear Power Plants," Progress in Nuclear Energy, Vol. 118, 103105, (2020)

REFERENCES

[1] Nuclear Energy Institute, "Delivering the Nuclear Promise: Advancing Safety, Reliability and Economic Performance," 2016.

[2] J. Pence, M. Abolhelm, Z. Mohaghegh, S. Reihani, M. Ertem, and E. Kee, "Methodology to evaluate the monetary benefit of Probabilistic Risk Assessment by modeling the net value of Risk-Informed Applications at nuclear power plants," *Reliability Engineering & System Safety,* vol. 175, pp. 171-182, 2018.

[3] M. Abolhelm, J. Pence, Z. Mohaghegh, E. Kee, F. Yilmaz, and D. Johnson, "Toward Demonstrating the Monetary Value of Probabilistic Risk Assessment for Nuclear Power Plants," in *Proceedings of 12th International Topical Meeting on Probabilistic Safety Assessment and Analysis (PSAM12)*, 2014.

[4] G. Schumock, S. Zhang, P. Farshadmanesh, J. G. Owens, N. Kasza, J. Stearns, T. Sakurahara, and Z. Mohaghegh, "Integrated Risk-Informed Design (I-RID) methodological framework and computational application for FLEX equipment storage buildings of Nuclear Power Plants," *Progress in Nuclear Energy,* vol. 120, p. 103186, 2020.

[5] J. Beal, T. Sakurahara, J. Pence, P. Farshadmanesh, E. Kee, and Z. Mohaghegh, "Coupling Degradation and Maintenance to Model Safety Risk and Financial Risk under an Integrated Enterprise Risk Management for Nuclear Power Plants," in *Proceedings of the 25th International Conference on Structural Mechanics in Reactor Technology (SMiRT-25)*, Charlotte, NC, 2019.

[6] J. Beal, T. Sakurahara, E. Kee, S. Reihani, and Z. Mohaghegh, "Integrated Enterprise Risk Management to Synchronize Safety and Profitability for Nuclear Power Plants," in *American Nuclear Society Winter Meeting & Expo*, Chicago, IL, 2020.

[7] Z. Mohaghegh and A. Mosleh, "Incorporating Organizational Factors into Probabilistic Risk Assessment of Complex Socio-Technical Systems: Principles and Theoretical Foundations," *Safety Science,* vol. 47, no. 8, pp. 1139-1158, 2009.

[8] Z. Mohaghegh, "On the theoretical foundations and principles of organizational safety risk analysis," Doctoral dissertation, University of Maryland, College Park, MD, 2007.

[9] *Consideration of Economic Consequences within the U.S. Nuclear Regulatory Commission's Regulatory Framework, SECY-12-0110*, August 14, 2012.

[10] J. Beal, T. Sakurahara, P. Farshadmanesh, S. Reihani, E. Kee, A. Rowell, F. Yilmaz, and Z. Mohaghegh, "Modeling Interconnections of Safety and Financial Performance of Nuclear Power Plants, Part 2: Methodological Developments and Case Study," *Under Review of Progress in Nuclear Energy,* 2021.

[11] W.-C. Cheng, J. Beal, T. Sakurahara, S. Reihani, E. Kee, and Z. Mohaghegh, "Modeling Interconnections of Safety and Financial Performance of Nuclear Power Plants, Part 3: Spatiotemporal Probabilistic Physics-of-Failure Analysis and Its Connection to Safety and Financial Performance," *Under Review of Progress in Nuclear Energy,* 2021.

[12] P. Farshadmanesh, J. Beal, T. Sakurahara, S. Reihani, E. Kee, A. Rowell, F. Yilmaz, and Z. Mohaghegh, "Modeling Interconnections of Safety and Financial Performance of Nuclear Power Plants, Part 1: Categorical Review and Theoretical Bases," *Under Review of Progress in Nuclear Energy,* 2021.

[13] W.-C. Cheng, J. Beal, T. Sakurahara, S. Reihani, E. Kee, and Z. Mohaghegh, "Integrated Probabilistic Physics of Failure Methodology to Estimate Pipe Failure Rates for Risk-Informed Analysis of Advanced Nuclear Reactors," in *2020 American Nuclear Society (ANS) Winter Meeting*, Online Virtual Conference, 2020.

[14] J. Beal, T. Sakurahara, S. Reihani, E. Kee, and Z. Mohaghegh, "An Algorithm for Risk-Informed Analysis of Advanced Reactors with a Case Study of Pipe Failure Rate Estimation," in *30th European Safety and Reliability Conference & 15th Probabilistic Safety Assessment and Management Conference (ESREL2020 & PSAM15)*, Venice, Italy, 2020.

[15] J. Beal, T. Sakurahara, E. Kee, S. Reihani, and Z. Mohaghegh, "Integrated Enterprise Risk Management to Synchronize Safety and Profitability Analysis for Nuclear Power Plants," in *2020 American Nuclear Society (ANS) Winter Meeting*, Online Virtual Conference, 2020.

[16] J. Beal, T. Sakurahara, J. Pence, P. Farshadmanesh, S. Reihani, E. Kee, and Z. Mohaghegh, "Coupling Degradation and Maintenance to Model Safety Risk and Financial Risk Under An Integrated Enterprise Risk Management Methodology for Nuclear Power Plants," in *25th International Conference on Structural Mechanics in Reactor Technology (SMiRT 25)*, Charlotte, NC, 2019.

[17] Z. Mohaghegh, R. Kazemi, and A. Mosleh, "Incorporating organizational factors into Probabilistic Risk Assessment (PRA) of complex socio-technical systems: A hybrid technique formalization," *Reliability Engineering and System Safety,* vol. 94, no. 5, pp. 1000-1018, 2009.

[18] Z. Mohaghegh, "Combining system dynamics and Bayesian belief networks for socio-technical risk analysis," in *2010 IEEE International Conference on Intelligence and Security Informatics*, Vancouver, BC, 2010, pp. 196-201: IEEE.

[19] Z. Mohaghegh, "Modeling emergent behavior for socio-technical probabilistic risk assessment," presented at the 6th American Nuclear Society International Topical Meeting on Nuclear Plant Instrumentation, Control, and Human-Machine Interface Technologies, Knoxville, TN, 2009.

[20] Z. Mohaghegh, "Development of an aviation safety causal model using socio-technical risk analysis (SoTeRiA)," in *10th International Conference on Probabilistic Safety Assessment and Management 2010, PSAM 2010*, 2010, pp. 1942-1953.

[21] J. Pence, T. Sakurahara, X. Zhu, Z. Mohaghegh, M. Ertem, C. Ostroff, and E. Kee, "Data-Theoretic Methodology and Computational Platform to Quantify Organizational Factors in Socio-Technical Risk Analysis," *Reliability Engineering & System Safety,* vol. 185, pp. 240-260, 2019.

[22] J. Pence and Z. Mohaghegh, "A Discourse on the Incorporation of Organizational Factors into Probabilistic Risk Assessment: Key Questions and Categorical Review," *Risk Analysis,* 2020.

[23] J. Pence, P. Farshadmanesh, J. Kim, C. Blake, and Z. Mohaghegh, "Data-theoretic approach for socio-technical risk analysis: Text mining Licensee Event Reports of US nuclear power plants," *Safety Science,* vol. 124, p. 104574, 2020.

[24] Z. Mohaghegh and A. Mosleh, "Measurement techniques for organizational safety causal models: Characterization and suggestions for enhancements," *Safety Science,* vol. 47, no. 10, pp. 1398-1409, 2009.

[25] N. Kalemba and F. Campa-Planas, "Safety and the economic and financial performance in the airline industry: is there any relationship?," *Aviation,* vol. 23, no. 1, pp. 7-14, 2019.

[26] P. M. Madsen, "Perils and profits: A reexamination of the link between profitability and safety in U.S. aviation," *Journal of Management,* vol. 39, no. 3, pp. 763-791, 2011.

[27] D. D. Akinleye, L.-A. McNutt, V. Lazariu, and C. C. McLaughlin, "Correlation between hospital finances and quality and safety of patient care," *PloS one,* vol. 14, no. 8, p. e0219124, 2019.

[28] C. C. Blanco, F. Caro, and C. J. Corbett, "Managing Safety-Related Disruptions: Evidence from the US Nuclear Power Industry," *Risk Analysis,* vol. 39, no. 10, 2019.

[29] R. A. Britto, T. M. Corsi, and C. M. Grimm, "The relationship between motor carrier financial performance and safety performance," *Transportation Journal,* vol. 49, no. 4, p. 42, 2010.

[30] J. W. Miller and J. P. Saldanha, "A new look at the longitudinal relationship between motor carrier financial performance and safety," *Journal of Business Logistics,* vol. 37, no. 3, pp. 284-306, 2016.

[31] N. L. Rose, "Profitability and product quality: economic determinants of airline safety performance," *Journal of Political Economy,* vol. 98, no. 5, Part 1, pp. 944-964, 1990.

[32] IAEA, "Risk management: A tool for improving nuclear power plant performance (IAEA-TECDOC-1209)," Vienna, Austria2001.

[33] Y. Feng, S. Zhang, and P. Wu, "Factors influencing workplace accident costs of building projects," *Safety science,* vol. 72, pp. 97-104, 2015.

[34] A. Asfaw, C. Mark, and R. Pana-Cryan, "Profitability and occupational injuries in US underground coal mines," *Accident Analysis & Prevention,* vol. 50, pp. 778-786, 2013.

[35] P. Yakovlev and R. S. Sobel, "Occupational safety and profit maximization: Friends or foes?," *The Journal of Socio-Economics,* vol. 39, no. 3, pp. 429-435, 2010.
[36] B. Fernández-Muñiz, J. M. Montes-Peón, and C. J. Vázquez-Ordás, "Relation between occupational safety management and firm performance," *Safety science,* vol. 47, no. 7, pp. 980-991, 2009.
[37] J. M. Argilés-Bosch, J. Martí, T. Monllau, J. Garcia-Blandón, and T. Urgell, "Empirical analysis of the incidence of accidents in the workplace on firms' financial performance," *Safety science,* vol. 70, pp. 123-132, 2014.
[38] F. J. Forteza, J. M. Carretero-Gomez, and A. Sese, "Occupational risks, accidents on sites and economic performance of construction firms," *Safety science,* vol. 94, pp. 61-76, 2017.
[39] S. Xu, "The relationship between financial performance and safety in the aviation industry: A worldwide perspective," Master of Science, The John Molson School of Business, Concordia University, Quebec, Canada, 2015.
[40] J. Antonakis, S. Bendahan, P. Jacquart, and R. Lalive, "On making causal claims: A review and recommendations," *The leadership quarterly,* vol. 21, no. 6, pp. 1086-1120, 2010.
[41] G. L. Reniers and H. N. Van Erp, *Operational safety economics: a practical approach focused on the chemical and process industries*. John Wiley & Sons, 2016.
[42] A. Gavious, S. Mizrahi, Y. Shani, and Y. Minchuk, "The costs of industrial accidents for the organization: developing methods and tools for evaluation and cost–benefit analysis of investment in safety," *Journal of Loss Prevention in the Process Industries,* vol. 22, no. 4, pp. 434-438, 2009.
[43] R. Jallon, D. Imbeau, and N. de Marcellis-Warin, "Development of an indirect-cost calculation model suitable for workplace use," *Journal of Safety Research,* vol. 42, no. 3, pp. 149-164, 2011.
[44] M. Gerbec and B. Kontić, "Safety related key performance indicators for securing long-term business development–A case study," *Safety science,* vol. 98, pp. 77-88, 2017.
[45] K. Kyaw and N. Paltrinieri, "The cost of reputational damage when a major accident occurs," in *Safety and Reliability of Complex Engineered Systems. Proceedings of the European Safety and Reliability Conference, ESREL*, 2015, pp. 4537-4544.
[46] R. Makino, "Stock market responses to chemical accidents in Japan: An event study," *Journal of loss prevention in the process industries,* vol. 44, pp. 453-458, 2016.
[47] *Economic Risks of Nuclear Power Reactor Accidents, NUREG/CR-3673*, 1984.
[48] U. S. NRC. *International Nuclear and Radiological Event Scale (about emergency preparedness)*.
[49] S. Zhang, Z. Ma, H. Zhang, and C. L. Smith, "Multicriterion benefit evaluation methodology for safety enhancements in nuclear power plants and application for FLEX strategies," *Nuclear Engineering and Design,* vol. 376, pp. 111-135, 2021.
[50] *Economic Risks of Nuclear Power Reactor Accidents- NUREG 3673,* U. S. N. R. Commission, 1984.
[51] R. Bizet and F. Lévêque, "The economic assessment of the cost of nuclear accidents," in *Resilience: A New Paradigm of Nuclear Safety*: Springer, Cham, 2017, pp. 79-96.
[52] R. M. Bowen, R. P. Castanias, and L. A. Daley, "Intra-industry effects of the accident at Three Mile Island," *Journal of Financial and Quantitative Analysis,* vol. 18, no. 1, pp. 87-111, 1983.
[53] S. Kawashima and F. Takeda, "The effect of the Fukushima nuclear accident on stock prices of electric power utilities in Japan," *Energy Economics,* vol. 34, no. 6, pp. 2029-2038, 2012.
[54] E. Kanamori, "'"Economizing" TEPCO's Responsibility for the Fukushima Daiichi Nuclear Power Plant Accident," *Nuclear Technology,* pp. 1-14, 2021.
[55] K. Silva, Y. Ishiwatari, and S. Takahara, "Cost per severe accident as an index for severe accident consequence assessment and its applications," *Reliability Engineering & System Safety,* vol. 123, pp. 110-122, 2014.
[56] K. Silva, K. Okamoto, Y. Ishiwatari, S. Takahara, and J. Promping, "Consideration of decontamination model for severe accident consequence assessment," *Journal of Nuclear Science and Technology,* vol. 52, no. 11, pp. 1402-1416, 2015.

[57] K. Silva and W. Vechgama, "Consideration of change over time in nuclear accident consequence assessment to support optimization of long-term remediation strategy," *Nuclear Engineering and Design,* vol. 373, p. 111022, 2021.
[58] N. E. Bixler, F. Walton, J. E. Leute, L. L. Eubanks, and K. L. McFadden, "MACCS (MELCOR Accident Consequence Code System) User Guide," Sandia National Lab.(SNL-NM), Albuquerque, NM (United States)2021.
[59] P. H. Kobos, T. E.-X. Drennen, A. V. Outkin, E. K. Webb, S. M. Paap, and S. Wiryadinata, "Techno-Economic Analysis: Best Practices and Assessment Tools," Sandia National Lab, Albuquerque, NM2020.
[60] P. Noto, "Regulatory Analysis Guidelines of the U.S. Nuclear Regulatory Commission, NUREG/BR-0058," Office of Nuclear Reactor Regulation2017.
[61] U. S. NRC, "NRC Non-Light Water Reactor (Non-LWR) Vision and Strategy, Volume 3: Computer Code Development Plans for Severe Accident Progression, Source Term, and Consequence Analysis," Technical report, US NRC2019.
[62] A. Nosek, *Fukushima-Informed Recovery and Cost Assessment: A Proposed Approach to Estimating the Cost of Nuclear Disasters*. The University of Wisconsin-Madison, 2018.
[63] I. Karanta, "Seasonal and contextual factors in level 3 PSA," *Espoo: VTT. VTT Technology VTT,* 2018.
[64] V. Bier, M. Corradini, R. Youngblood, C. Roh, and S. Liu, "Development of an Updated Societal-Risk Goal for Nuclear Power Safety," Idaho National Laboratory (INL)2014.
[65] R. Denning and V. Mubayi, "Insights into the societal risk of nuclear power plant accidents," *Risk analysis,* vol. 37, no. 1, pp. 160-172, 2017.
[66] D. Dube, B. Albinson, R. Wolfgang, M. Saunders, and G. Krueger, "Exelon Economic Enterprise Risk Modeling of a BWR," in *International Probabilistic Safety Analysis and Assessment (PSA)*, Pittsburgh, PA, 2017.
[67] NRC, "NRC Fines TVA More Than $900,000 for Watts Bar Nuclear Power Plant Violations; Cites Three Individuals for Their Roles in the 2015 Incident," in *NRC News, No: 20-055*, November 6, 2020.
[68] S. Shavell, "Liability for harm versus regulation of safety," *The Journal of Legal Studies,* vol. 13, no. 2, pp. 357-374, 1984.
[69] J. Bellamy, "Civil liability for nuclear damage in countries developing nuclear new build programmes," *The Journal of World Energy Law & Business,* vol. 12, no. 1, pp. 108-120, 2019.
[70] X. Vásquez-Maignan, "Fukushima: liability and compensation," in *NEA News, No. 29.2*, 2011.
[71] U.S. Department of Labor & U.S. NRC. (2013). *Memorandum of Understanding between the U.S. Nuclear Regulatory Commission and the Occupational Safety and Health Administration, Standard Number: 1903.6*. Available: https://www.osha.gov/laws-regs/mou/2013-09-06
[72] Occupational Safety and Health Administration, "Business Case for Safety and Health," in *Trade News*.
[73] G. Vierendeels, G. L. Reniers, and B. Ale, "Modeling the major accident prevention legislation change process within Europe," *Safety science,* vol. 49, no. 3, pp. 513-521, 2011.
[74] C. R. Sunstein, *Risk and reason: Safety, law, and the environment*. Cambridge University Press, 2002.
[75] J. B. Ruhl and J. Salzman, "Mozart and the Red Queen: The problem of regulatory accretion in the administrative state," *91 Geo. L.J. 757,* 2003.
[76] F. B. Cross, "Paradoxical perils of the precautionary principle," *53 Wash. & Lee L. Rev. 851,* 1996.
[77] C. R. Sunstein, "Risk versus Risk: Tradeoffs in protecting health and the environment. Edited by John D. Graham and Jonathan Baert Wiener," pp. 1-42, 1995.
[78] S. Martorell, I. Martón, A. Sánchez, and S. Carlos, "Harmonisation of surveillance requirements and maintenance in a context of ageing and obsolescence based on reliability, availability and risk information," *Reliability Engineering & System Safety,* vol. 202, p. 106992, 2020.

[79] F. Mohammadhasani and A. Pirouzmand, "Multi-state unavailability analysis of safety system redundant components with aging effect under surveillance testing," *Progress in Nuclear Energy,* vol. 126, p. 103415, 2020.
[80] N. Dupin and E.-G. Talbi, "Matheuristics to optimize refueling and maintenance planning of nuclear power plants," *Journal of Heuristics,* vol. 27, no. 1, pp. 63-105, 2021.
[81] J. Wang, D. Ge, S. Chen, Z. Wang, D. Guo, Z. Xu, J. Wang, and F. Wang, "Maintenance strategy design for nuclear reactors safety systems using a constraint particle swarm evolutionary methodology," *Annals of Nuclear Energy,* vol. 150, p. 107878, 2021.
[82] D. Kančev, M. Čepin, and B. Gjorgiev, "Development and application of a living probabilistic safety assessment tool: Multi-objective multi-dimensional optimization of surveillance requirements in NPPs considering their ageing," *Reliability Engineering & System Safety,* vol. 131, pp. 135-147, 2014.
[83] E. Popova, D. Morton, P. Damien, and T. Hanson, "Bayesian analysis and decisions in nuclear power plant maintenance," *The Oxford Handbook of Applied Bayesian Analysis,* pp. 219-239, 2010.
[84] D. Mandelli, Z. Ma, R. Youngblood, S. S. Germain, C. Smith, P. Talbot, S. Hess, D. Dube, C. Pope, and J. Miller, "Plant Integral Risk-informed System Health Program," INL Technical Report INL-EXT-19-558082019.
[85] D. Mandelli, C. Wang, S. Staples, C. S. Ritter, A. L. Mack, S. W. St Germain, A. Alfonsi, C. Rabiti, and R. Kunz, "Cost Risk Analysis Framework (CRAFT): An Integrated Risk Analysis Tool and Its Application in an Industry Use Case," Idaho National Lab.(INL), Idaho Falls, ID (United States)2018.
[86] S. Zhang, Z. Ma, H. Zhang, and C. L. Smith, "Multicriterion benefit evaluation methodology for safety enhancements in nuclear power plants and application for flex strategies," *Nuclear Engineering and Design,* vol. 376, p. 111135, 2021.
[87] Z. Ma, S. Zhang, H. Zhang, J. Park, J. Yu, C. D. Blakely, T. A. Ulrich, and R. L. Boring PhD, "Risk-Informed ATF and FLEX Analysis for an Enhanced Resilient BWR Under Design-Basis and Beyond-Design-Basis Accidents," Idaho National Lab.(INL), Idaho Falls, ID (United States)2020.
[88] M. Khalaquzzaman, H. G. Kang, M. C. Kim, and P. H. Seong, "Optimization of periodic testing frequency of a reactor protection system based on a risk-cost model and public risk perception," *Nuclear Engineering and Design,* vol. 241, no. 5, pp. 1538-1547, 2011.
[89] EPRI. (2002). *Risk-Informed Asset Management (RIAM) Devlopment Plan*.
[90] J. Xing, Z. Zeng, and E. Zio, "Joint optimization of safety barriers for enhancing business continuity of nuclear power plants against steam generator tube ruptures accidents," *Reliability Engineering & System Safety,* vol. 202, p. 107067, 2020.
[91] G. Heo and J. Park, "A framework for evaluating the effects of maintenance-related human errors in nuclear power plants," *Reliability Engineering & System Safety,* vol. 95, no. 7, pp. 797-805, 2010.
[92] A. Mancuso, M. Compare, A. Salo, and E. Zio, "Portfolio optimization of safety measures for reducing risks in nuclear systems," *Reliability Engineering & System Safety,* vol. 167, pp. 20-29, 2017.
[93] J. Cluever, T. Esselman, and P. Bruck, "Maintenance Optimization: Finding the Best Frequencies of Maintenance Activities," in *Pressure Vessels and Piping Conference*, 2020, vol. 83884, p. V008T08A029: American Society of Mechanical Engineers.
[94] H. Wu, Y.-F. Li, and C. Bérenguer, "Optimal inspection and maintenance for a repairable k-out-of-n: G warm standby system," *Reliability Engineering & System Safety,* vol. 193, p. 106669, 2020.
[95] M. M. Cowing, M. E. Paté-Cornell, and P. W. Glynn, "Dynamic modeling of the tradeoff between productivity and safety in critical engineering systems," *Reliability Engineering & System Safety,* vol. 86, no. 3, pp. 269-284, 2004.
[96] M. Du, C. Zhang, T. Zhou, and Y.-F. Li, "Imperfect Maintenance Scheduling for High Pressure Feedwater Heater System in Nuclear Power Plant," in *2020 Asia-Pacific International Symposium on Advanced Reliability and Maintenance Modeling (APARM)*, 2020, pp. 1-6: IEEE.

[97] H. Terada, H. Nagai, K. Tsuduki, A. Furuno, M. Kadowaki, and T. Kakefuda, "Refinement of source term and atmospheric dispersion simulations of radionuclides during the Fukushima Daiichi Nuclear Power Station accident," *Journal of environmental radioactivity,* vol. 213, p. 106104, 2020.
[98] K. Silva and K. Okamoto, "A simple assessment scheme for severe accident consequences using release parameters," *Nuclear Engineering and Design,* vol. 305, pp. 688-696, 2016.
[99] V. Mubayi, V. Sailor, and G. Anandalingam, "Cost-benefit considerations in regulatory analysis, NUREG/CR-6349, BNL-NUREG-52466," 1995.
[100] *Severe Accident Mitigation Alternatives (SAMA) Analysis, Guidance Document (NEI-05-01)*, 2005.
[101] K. Hiraoka, S. Tateishi, and K. Mori, "Review of health issues of workers engaged in operations related to the accident at the Fukushima Daiichi Nuclear Power Plant," *Journal of Occupational Health,* pp. 15-0084-RA, 2015.
[102] K. Wada, T. Yoshikawa, T. Hayashi, and Y. Aizawa, "Emergency response technical work at Fukushima Dai-ichi nuclear power plant: occupational health challenges posed by the nuclear disaster," *Occupational and environmental medicine,* vol. 69, no. 8, pp. 599-602, 2012.
[103] D. Mandelli, Z. Ma, R. Youngblood, S. S. Germain, C. Smith, P. Talbot, S. Hess, D. Dube, C. Pope, J. Miller, M. Robbins, D. Das, M. Azarian, and J. Coble, "Plant Integral Risk-informed System Health Program," Idaho National Lab, Idaho Falls, Idaho2019, vol. INL-EXT-19-55808.
[104] M. Milczarek, J. Kosk-Bienko, K. Muylaert, R. Op te Beeck, S. Royo, C. Grusenmeyer, G. Owczarek, E. Flaspöler, S. Kaluza, and B. Lafrenz, "Maintenance and Occupational Safety and Health: A statistical picture," *European risk observatory EA-OSHA, Luxembourg,* 2010.
[105] R. Lloyd, *A survey of crane operating experience at US nuclear power plants from 1968 through 2002 - NUREG-1774*. Division of Systems Analysis and Regulatory Effectiveness, Office of Nuclear, 2003.
[106] IAEA, "Industrial Safety Guidelines for Nuclear Facilities," International Atomic Energy Agency, Vienna, Austria2018.
[107] J. H. Johnson Jr, "A model of evacuation--decision making in a nuclear reactor emergency," *Geographical Review,* pp. 405-418, 1985.
[108] World Nuclear Association. (Access date: March 5 2021). *Decommissioning Nuclear Facilities*. Available: https://www.world-nuclear.org/information-library/nuclear-fuel-cycle/nuclear-wastes/decommissioning-nuclear-facilities.aspx#:~:text=For%20US%20reactors%20the%20expected,to%20%241.22%20million%20per%20MWe.
[109] E. S. Murphy and G. M. Holter, "Technology, Safety and Costs of Decommissioning Reference Light-Water Reactors Following Postulated Accidents, NUREG/CR-2601," Pacific Northwest Laboratory, Washington, D.C.1982.
[110] (December 21, 2017). *Summary of Decommissioning and Contaminated Water Management*. Available: https://www.meti.go.jp/english/earthquake/nuclear/decommissioning/pdf/20171221_e.pdf
[111] INPO, "Special Report on the Nuclear Accident at the Fukushima Daiichi Nuclear Power Station, Revision 0," Institute of Nuclear Power Operations, Atlanta, GA2011, vol. INPO 11-005.
[112] U. S. NRC, "Environmental Assessment for Decontamination of the Three Mile Island Unit 2 Reactor Building Atmosphere (NUREG-0662)," TMI Support Staff, Office of Nuclear Reactor Regulation, U.S. Nuclear Regulatory Commission, Washington, D.C.1980.
[113] ANS, "Special Committee on Fukushima. Fukushima Daiichi: ANS Committee Report," American Nuclear Society, La Grange, IL2012.
[114] (2014). *NRC Incident Investigation Program (Management Directive 8.3) - DT-17-158*. Available: https://www.nrc.gov/docs/ML1807/ML18073A200.pdf
[115] IAEA, "Root Cause Analysis Following an Event at a Nuclear Installation: Reference Manual," International Atomic Energy Agency, Vienna2015.

[116] Tokyo Electric Power Company Holdings. (2018). *Overview of FY2017 Financial Results (Released on April 26, 2018)*. Available: https://www.tepco.co.jp/en/wp-content/uploads/hd05-02-01-000-180426_1-e-001.pdf
[117] OECD, "Japan's Compensation System for Nuclear Damage (As Related to the TEPCO Fukushima Daiichi Nuclear Accident)," NEA&OECD2012.
[118] U. S. NRC, "Safety Enhancements After Fukushima."
[119] U.S.NRC. *Backgrounder on Nuclear Insurance and Disaster Relief*. Available: https://www.nrc.gov/reading-rm/doc-collections/fact-sheets/nuclear-insurance.html#act
[120] A. E. Rota, A. Lindner, C. Wolanin, and M. R. DellaCroce, "Risk Management and Insurability Strategies for Power Generation," 2017.
[121] *American Society of Mechanical Engineers Boiler Pressure Vessel Code*, 2019.
[122] (2003). *IAEA-TECDOC-1383 Guidance for Optimizing Nuclear Power Plant Maintenance Programmes*.
[123] T. Sakurahara, S. Reihani, E. Kee, and Z. Mohaghegh, "Global importance measure methodology for integrated probabilistic risk assessment," *Proceedings of the Institution of Mechanical Engineers, Part O: Journal of Risk and Reliability,* vol. 234, no. 2, pp. 377-396, 2020.
[124] T. Sakurahara, G. Schumock, S. Reihani, E. Kee, and Z. Mohaghegh, "Simulation-Informed Probabilistic Methodology for Common Cause Failure Analysis," *Reliability Engineering & System Safety,* vol. 185, pp. 84-99, 2019.
[125] K. Canavan and G. Hannaman, "Introduction to Simplified Generation Risk Assessment Modeling," *EPRI Report, EPRI,* vol. 1007386, 2004.
[126] J. Liming, E. Kee, C. Grantom, and A. Richards, "Risk-informed profitability-based analysis support of nuclear power station balance-of-plant change management," 2001.
[127] D. Blanchard, Brinsfield, W., Szetu, P., "Generation Risk Assessment (GRA) Plant Implementation Guide, EPRI, Palo Alto, CA: 1008121.," 2004.
[128] E. Kee, F. Yilmaz, and P. Nelson, "A Comparative Study of Methodologies for Determining Plant Availabilities and Initiator Frequencies," in *International Conference on Nuclear Engineering*, 2009, vol. 43529, pp. 983-992.
[129] E. Kee, F. Yilmaz, D. Wakefield, and S. Epstein, "STP balance of plant model update experience and results," in *International Conference on Nuclear Engineering*, 2009, vol. 43529, pp. 945-953.
[130] S. Wu, L. Zhang, A. Barros, W. Zheng, and Y. Liu, "Performance analysis for subsea blind shear ram preventers subject to testing strategies," *Reliability Engineering & System Safety,* vol. 169, pp. 281-298, 2018.
[131] E. Kee, A. Sun, S. Rodgers, E. Popova, P. Nelson, V. Moiseytseva, and E. Wang, "A Method to Quantify Plant Availability and Initiating Event Frequency Using a Large Event Tree, Small Fault Tree Model," in *14th International Conference on Nuclear Engineering*, 2006, pp. 149-157: American Society of Mechanical Engineers.
[132] (2007). *Industry-Average Performance for Components and Initiating Events at U.S. Commercial Nuclear Power Plants, NUREG/CR-6928*.
[133] ABS Consulting, "Riskman for Windows, Version 15.0," ABS Consulting, Irvine, CA2014.
[134] D. Berg, Campbell, J., "Main Feedwater Pump Maintenance Guide, EPRI: TR-105933," 1995.
[135] M. Khalaquzzaman, H. G. Kang, M. C. Kim, and P. H. Seong, "Quantification of unavailability caused by random failures and maintenance human errors in nuclear power plants," *Nuclear engineering and design,* vol. 240, no. 6, pp. 1606-1613, 2010.
[136] J. Xing, G. Parry, M. Presley, J. Forester, S. Hendrickson, and V. Dang, "An Integrated Human Event Analysis System (IDHEAS) for Nuclear Power Plant Internal Events At-Power Application (NUREG-2199), vol. 1," *US Nuclear Regulatory Commission,* 2017.
[137] M. Wald. (2020). *Why Refuel a Nuclear Reactor Now?* Available: https://www.nei.org/news/2020/why-refuel-plant-during-pandemic
[138] U.S. Energy Information Administration. (April 2021). *U.S. nuclear capacity outages were 35% higher in summer 2020 than 2019*.

[139] D. Blanchard, W. Brinsfield, and P. Szetu, "Generation Risk Assessment (GRA) at Cooper Nuclear Station," Palo Alto, CA1011924, 2005.
[140] T. Sakurahara, N. O'Shea, W.-C. Cheng, S. Zhang, S. Reihani, E. Kee, and Z. Mohaghegh, "Integrating renewal process modeling with probabilistic physics-of-failure: Application for estimation of loss of coolant accident (LOCA) frequencies in nuclear power plants," *Reliability Engineering and System Safety,* vol. 190, p. 106479, 2019.
[141] G. Vinod, S. Bidhar, H. Kushwaha, A. K. Verma, and A. Srividya, "A comprehensive framework for evaluation of piping reliability due to erosion–corrosion for risk-informed inservice inspection," *Reliability Engineering & System Safety,* vol. 82, no. 2, pp. 187-193, 2003.
[142] S. D. Unwin, P. P. Lowry, R. F. Layton, P. G. Heasler, and M. B. Toloczko, "Multi-State Physics Models of Aging Passive Components in Probabilistic Risk Assessment," in *2011 International Topical Meeting on Probabilistic Safety Assessment and Analysis (PSA2011)*, Wilmington, NC, 2011: American Nuclear Society (ANS).
[143] O. Cronvall and I. Männistö, "Combining Discrete-Time Markov Processes and Probabilistic Fracture Mechanics in RI-ISI Risk Estimates," *International Journal of Pressure Vessels and Piping,* vol. 86, no. 11, pp. 732-737, 2009.
[144] Y.-F. Li, E. Zio, and Y.-H. Lin, "A multistate physics model of component degradation based on stochastic petri nets and simulation," *IEEE Transactions on Reliability,* vol. 61, no. 4, pp. 921-931, 2012.
[145] O. Cronvall, K. Simola, I. Männistö, J. Gunnars, L. Alverlind, P. Dillström, and L. Gandossi, "A Study on the Effect of Flaw Detection Probability Assumptions on Risk Reduction Achieved by Non-Destructive Inspection," *Reliability Engineering & System Safety,* vol. 105, pp. 90-96, 2012.
[146] A. Guler, T. Aldemir, and R. Denning, "Multi-State Physics Based Aging Assessment of Passive Components," in *2013 International Topical Meeting on Probabilistic Safety Assessment and Analysis (PSA2013)*, Columbia, SC, 2013: American Nuclear Society (ANS).
[147] A. Guler, T. Aldemir, and R. Denning, "Uncertainty Evaluation in Multi-State Physics Based Aging Assessment of Passive Components," in *12th Probabilistic Safety Assessment and Management Conference (PSAM12)*, Honolulu, HI, 2014.
[148] F. Di Maio, D. Colli, E. Zio, L. Tao, and J. Tong, "A Multi-State Physics Modeling approach for the reliability assessment of Nuclear Power Plants piping systems," *Annals of Nuclear Energy,* vol. 80, pp. 151-165, 2015.
[149] F. Di Maio, D. Colli, E. Zio, T. Liu, and J. Tong, "A Multi-State Physics Modeling for Estimating the Size-and Location-Dependent Loss of Coolant Accident Initiating Event Probability," in *2017 International Topical Meeting on Probabilistic Safety Assessment and Analysis (PSA2017)*, Pittsburgh, PA, 2017: American Nuclear Society (ANS).
[150] OECD NEA, "Operating Experience Insights into Pressure Boundary Component Reliability and Integrity Management," in "Topical Report by the Component Operational Experience, Degradation and Ageing Programme (CODAP) Group," 2017.
[151] T. Lu, X. G. Zhu, and H. T. Li, "Large-Eddy Simulation of Thermal Stratification in a Straight Branch of a Tee Junction with or without Leakage," *Progress in Nuclear Energy,* vol. 64, pp. 41-46, 2013.
[152] B. Cai, Y. Weng, Y. Wang, X. Qin, F. Cao, H. Gu, and H. Wang, "Experimental Investigation on Thermal Stratification in a Pressurizer Surge Line with Different Arrangements," *Progress in Nuclear Energy,* vol. 98, pp. 239-247, 2017.
[153] Z. Guo, J. Zou, Y. Chen, K. Xu, T. Lu, and B. Liu, "Monitoring of Wall Temperature Fluctuations for Thermal Fatigue in a Horizontal Mixing T-Junction Pipe," *Progress in Nuclear Energy,* vol. 104, pp. 298-305, 2018.
[154] T. Feng, M. Wang, P. Song, L. Liu, W. Tian, G. H. Su, and S. Qiu, "Numerical research on thermal mixing characteristics in a 45-degree T-junction for two-phase stratified flow during the emergency core cooling safety injection," *Progress in Nuclear Energy,* vol. 114, pp. 91-104, 2019.

[155] M. Jin, Y. Chai, S. Xue, G. Wang, and Z. Chen, "Thermal and stress analysis of window target for accelerator-driven sub-critical system during beam trip transients," *Progress in Nuclear Energy,* vol. 85, pp. 325-332, 2015.
[156] W. Wang, P. Buhl, A. Klenk, and Y. Liu, "The effect of in-service steam temperature transients on the damage behavior of a steam turbine rotor," *International Journal of Fatigue,* vol. 87, pp. 471-483, 2016.
[157] M. A. Khaleel and F. A. Simonen, "Effect of Through-Wall Stress Gradients on Piping Failure Probabilities," *Nuclear engineering and design,* vol. 197, no. 1-2, pp. 89-106, 2000.
[158] W.-C. Cheng, T. Sakurahara, S. Zhang, P. Farshadmanesh, S. Reihani, E. Kee, Z. Mohaghegh, K. Heckmann, J. Sievers, B. Lydell, C. Zammali, X.-X. Yuan, X. Duan, R. Alzbutas, G.-G. Lee, J. A. Karim, V. Morozov, C. Takasugi, and T. Jevremovic, "Review and Categorization of Existing Studies on the Estimation of Probabilistic Failure Metrics for Reactor Coolant Pressure Boundary Piping and Steam Generator Tubes in Nuclear Power Plants," *Progress in Nuclear Energy,* vol. 118, pp. 1-51, 2020.
[159] S. Li, H. Zhang, S. Li, Y. Wang, F. Xue, and X. Wang, "Probabilistic fracture mechanics analysis of thermally aged nuclear piping in a pressurized water reactor," *Nuclear Engineering and Design,* vol. 265, pp. 611-618, 2013.
[160] H. Machida, "Effect of Dispersion of Seismic Load on Integrity of Nuclear Power Plant Piping," in *16th International Conference on Structural Mechanics in Reactor Technology (SMiRT 16)*, Washington, DC, 2001.
[161] H. Machida and S. Yoshimura, "Probabilistic Fracture Mechanics Analysis of Nuclear Piping Considering an Embedded Crack," in *2002 Pressure Vessels and Piping Conference (PVP2002)*, Vancouver, BC, Canada, 2002: American Society of Mechanical Engineers (ASME).
[162] H. Machida, N. Yamashita, S. Yoshimura, and G. Yagawa, "Reliability Assessment of Piping in a Nuclear Power Plant Considering Flaw Detection Probability," in *2004 Pressure Vessels and Piping Conference (PVP2004)*, San Diego, CA, 2004: American Society of Mechanical Engineers (ASME).
[163] T. Schimpfke, H. Grebner, and J. Sievers, "Analysis Methods for Structure Reliability of Piping Components," in *30th MPA-Seminar in Conjunction with 9th German-Japanese Seminar* Stuttgat, Germany, 2004.
[164] H. Machida, "Study on Reliability of Nuclear Power Plant Piping Considering Defect Sizing Accuracy," in *2006 Pressure Vessels and Piping Conference (PVP2006)*, Vancoucer, BC, Canada, 2006: American Society of Mechanical Engineers (ASME).
[165] D. Datta and C. Jang, "Failure Probability Assessment of A PWR Primary System Piping Subcomponents under Different Loading Conditions," in *IAEA Second International Symposium on Nuclear Power Plant Life Management*, Shanghai, China, 2007.
[166] H. Machida, "Reliability Assessment of PLR Piping Based on Domestic SCC Data," in *2007 Pressure Vessels and Piping Conference (PVP2007)*, San Antonio, TX, 2007: American Society of Mechanical Engineers (ASME).
[167] D. Datta and C. Jang, "Failure Assessment of Nuclear Piping Components due to Combined Degradation Mechanisms by An Advanced Probabilistic Fracture Mechanics Code," in *2009 Pressure Vessels and Piping Conference (PVP2009)*, Prague, Czech Republic, 2009: American Society of Mechanical Engineers (ASME).
[168] D. Datta and C. Jang, "Incorporation of Materials' Sensitive Simulation Technique into the PINTIN-CAM Code for Integrity of Nuclear Piping System," in *2010 Pressure Vessels and Piping Conference (PVP2010)*, Bellevue, WA, 2010: American Society of Mechanical Engineers (ASME).
[169] O. Cronvall, M. Ilkka, and A. Jouni, "On Assessment of Initial Cracks for RI-ISI Analysis Purposes," *Journal of Materials Science and Engineering,* pp. 296-307, 2011.
[170] O. K. Chopra and J. Smith, "Crack initiation in smooth fatigue specimens of austenitic stainless steel in light water reactor environments," Argonne National Lab., IL (US)1999.

[171] T. Schimpfke, H. Grebner, J. Peschke, and J. Sievers, "Development on Methods for Evaluating Structure Reliability of Piping Components," in *17th International Conference on Structural Mechanics in Reactor Technology (SMiRT17)*, Prague, Czech Republic, 2003.
[172] A. Zahoor, *Ductile Fracture Handbook*. Electric Power Research Institute, 1989.
[173] J. C. Newman Jr and I. S. Raju, "Stress-Intensity Factor Equations for Cracks in Three-Dimensional Finite Bodies Subjected to Tension and Bending Loads," National Aeronautics and Space Administration (NASA), Langley Research Center, Hampton, VA, NASA Technical Memorandom N84-23925, 1984.
[174] American Petroleum Institute & American Society of Mechanical Engineers, "Fitness-For-Service," Washington, DC, API 579-1/ASME FFS-1, 2016.
[175] T. L. Anderson, G. V. Thorwald, D. J. Revelle, and C. Lanaud, "Stress Intensity Solutions for Surface Cracks and Buried Cracks in Cylinders, Spheres, and Flat Plates," *Service Experience and Fitness-For-Service in Power and Petroleum Processing,* vol. 411, pp. 105-120, 2000.
[176] American Society of Mechanical Engineers, "ASME BPVC.CC.NC.XI 2019 — Section XI, Rules for Inservice Inspection of Nuclear Power Plant Components," New York, NY2019.
[177] D. O. Harris, D. Dedhia, and S. C. Lu, "Theoretical and Users Manual for pc-PRAISE: A Probabilistic Fracture Mechanics Computer Code For Piping Reliability Analysis," US Nuclear Regulatory Commission, Washington, DC, NUREG/CR-5864 (UCRL-ID-109798), 1992.
[178] L. Burgazzi, "Addressing the Uncertainties Related to Passive System Reliability," *Progress in Nuclear Energy,* vol. 49, no. 1, pp. 93-102, 2007.
[179] (2017). *Guidance on the Treatment of Uncertainties Associated with PRAs in Risk-Informed Decisionmaking (NUREG-1855, Revision 1)*.
[180] H. Bui, T. Sakurahara, S. Reihani, J. Biersdorf, and Z. Mohaghegh, "I-PRA Uncertainty Importance Ranking to Enhance Fire PRA Realism for Nuclear Power Plants," in *2020 American Nuclear Society (ANS) Winter Meeting*, Virtual Conference, 2020.
[181] Electric Power Research Institute, "Thermal Stratification, Cycling, and Striping (TASCS)," in "Section 3.2," 1994.
[182] G. BECKER, L. CAMARINOPOULOS, and W. OHLMEYER, "Discontinuities in Homogeneous Markov Processes and Their Use in Modelling Technical Systems under Inspection," *Microelectron. Reliab.,* vol. 34, no. 5, pp. 771-788, 1994.
[183] US Nuclear Regulatory Commission, "Standard Technical Specifications: Westinghouse Plants," 2011, vol. 2.
[184] I. Boros, G. Petoefi, and A. Aszody, "CFD Analysis of Thermal Stratification in the Primary Circuit," in *Fifteenth Symposium of Atomic Energy Research*, Hungary, 2005.
[185] T. Lu, H. Li, and X. Zhu, "Numerical Simulation of Thermal Stratification in an Elbow Branch Pipe of a Tee Junction with and without Leakage," *Annals of Nuclear Energy,* vol. 60, pp. 432-438, 2013.
[186] M. Kamaya, "Assessment of Thermal Fatigue Damage Caused by Local Fluid Temperature Fluctuation (Part I: Characteristics Of Constraint And Stress Caused By Thermal Striation And Stratification)," *Nuclear Engineering and Design,* vol. 268, pp. 121-138, 2014.
[187] Electric Power Research Institute, "Mitigation of Thermal Fatigue in Unisolable Piping Connected to PWR Reactor Coolant Systems (MRP-29)," Palo Alto, CA1001017, 2000.
[188] Abaqus GUI, "Abaqus 6.14 Users Manual 6.14," Dassault Systèmes Simulia Corp Providence, RI, USA, 2014.
[189] American Society of Mechanical Engineers, "ASME BPVC.II.D.M 2019 — Section II, Materials, Part D, Properties (Metric)," New York, NY, 2019.
[190] J. Broussard, "Material Reliability program: welding residual stress dissimilar Metal butt-weld finite element modeling handbook (MRP-317, Revision 1)," *EPRI, Palo Alto, CA,* 2015.
[191] M. A. Khaleel, F. A. Simonen, H. K. Phan, D. O. Harris, and D. Dedhia, "Fatigue Analysis of Components for 60-Year Plant Life," Pacific Northwest National Laboratory (PNNL), Richland, WA, NUREG/CR-6674 (PNNL-13227), 2000.

[192] American Society of Mechanical Engineers, "ASME BPVC.XI.1 2019 — Section XI, Rules for Inservice Inspection of Nuclear Power Plant Components, Division 1, Rules for Inspection and Testing of Components of Light-Water-Cooled Plants," New York, NY: American Society of Mechanical Engineers (ASME), 2019.
[193] P. Scott, R. Kurth, A. Cox, R. Olson, and D. Rudland, "Development of the PRO-LOCA Probabilistic Fracture Mechanics Code," Swedish Radiation Safety Authority (SSM), Stockholm, Sweden, MERIT Final Report 2010:46, 2010.
[194] Y.-J. Kim, N.-S. Huh, Y.-J. Park, and Y.-J. Kim, "Elastic–plastic J and COD estimates for axial through-wall cracked pipes," *International journal of pressure vessels and piping,* vol. 79, no. 6, pp. 451-464, 2002.
[195] R. E. Henry, "The two-phase critical discharge of initially saturated or subcooled liquid," *Nuclear Science and Engineering,* vol. 41, no. 3, pp. 336-342, 1970.
[196] R. E. Henry, H. K. Fauske, and S. T. McComas, "Two-phase critical flow at low qualities Part I: Experimental," *Nuclear Science and Engineering,* vol. 41, no. 1, pp. 79-91, 1970.
[197] R. E. Henry, H. K. Fauske, and S. T. McComas, "Two-phase critical flow at low qualities Part II: Analysis," *Nuclear Science and Engineering,* vol. 41, no. 1, pp. 92-98, 1970.
[198] C. Priya, K. B. Rao, M. B. Anoop, N. Lakshmanan, V. Gopika, H. S. Kushwaha, and R. K. Saraf, "Probabilistic Failure Analysis of Austenitic Nuclear Pipelines Against Stress Corrosion Cracking," (in English), *Proceedings of the Institution of Mechanical Engineers Part C: Journal of Mechanical Engineering Science,* vol. 219, no. 7, pp. 607-626, 2005.
[199] A. Guedri, "Reliability Analysis of Stainless Steel Piping Using A Single Stress Corrosion Cracking Damage Parameter," *International Journal of Pressure Vessels and Piping,* vol. 111-112, pp. 1-11, 2013.
[200] A. Guedri, "Effects of Remedial Actions on Small Piping Reliability," *Journal of Risk and Reliability,* vol. 227, no. 2, pp. 144-161, 2013.
[201] Q. Wang and W. Zhou, "A New Burst Pressure Model for Thin-Walled Pipe Elbows Containing Metal-Loss Corrosion Defects," *Engineering Structures,* vol. 200, p. 109720, 2019.
[202] S. R. Gosselin, F. A. Simonen, P. G. Heasler, and S. R. Doctor, "Fatigue Crack Flaw Tolerance in Nuclear Power Plant Piping: A Basis for Improvements to ASME Code Section XI Appendix L," US Nuclear Regulatory Commission, Washington, DC, NUREG/CR-6934 (PNNL-16192), 2007.
[203] D. Harris, E. Lim, and D. Dedhia, "Probability of pipe fracture in the primary coolant loop of a PWR plant. Volume 5. Probabilistic fracture mechanics analysis. Load Combination Program Project I final report," Lawrence Livermore National Lab., CA (USA); Science Applications1981.
[204] A. M. Law, *Simulation Modeling and Analysis (Fifth edition)*. McGraw-Hill New York, 2014.
[205] L. Spain, J. Keller, and A. Deardorff, "Thermal Fatigue Management Guideline for Normally Stagnant Non-Isolable Branch Lines," Electric Power Research Institute (EPRI), Presentation package PRS-04-086/1, 2005.